TECHNICAL AND VOCATIONAL TRAINING INSTITUTE (TVTI)

School of Graduate Studies

FACULTY OF ELECTRICAL AND ELECTRONICS TECHNOLOGY AND INFORMATION AND COMMUNICATION TECHNOLOGY

(DEPARTMENT OF ELECTRICAL AND ELECTRONICS TECHNOLOGY)

Design of Multivariable PID Control Scheme for Humidity and Temperature Control of Neonatal Incubator

MSc Thesis for the Partial Fulfilment of

Master of Science in Electrical Automation and Control Technology Management

By,

Lamrot H/Michael (MTR/623/13)

Supervisor,

Dr. Arun Ramaveerapathiran

August, 2022

Addis Ababa, Ethiopia

Design of Multivariable PID Control Scheme for Humidity and Temperature Control of Neonatal Incubator

A Thesis submitted to

TECHNICAL AND VOCATIONAL TRAINING INSTITUTE (TVTI)

FACULTY OF ELECTRICAL AND ELECTRONICS TECHNOLOGY AND INFORMATION AND COMMUNICATION TECHNOLOGY

(DEPARTMENT OF ELECTRICAL AND ELECTRONICS TECHNOLOGY)

In partial fulfilment for the Degree

MASTER OF SCIENCE *in* ELECTRICAL AUTOMATION AND CONTROL TECHNOLOGY MANAGEMENT

By,

Lamrot H/Michael (MTR/623/13)

Supervisor,

Dr. Arun Ramaveerapathiran

August, 2022

Addis Ababa, Ethiopia

DECLARATION

I hereby declare that the work which is being presented in this thesis entitled "Design of Multivariable PID Control Scheme for Humidity and Temperature Control of Neonatal Incubator" is the original work of my own, has not been presented for a master's thesis in this or other universities and all sources of materials used for this thesis work have been fully acknowledged.

Name: Lamrot H/Michael (MTR/623/13)

Signature: _____

Place: Addis Ababa

Date of Submission: _____

his thesis work has been submitted for examination with my approval as a TVTI advisor.

Dr. Arun Ramaveerapathiran _____ _____

Advisor Name Signature Date

TECHNICAL AND VOCATIONAL TRAINING INSTITUTE (TVTI)

FACULTY OF ELECTRICAL AND ELECTRONICS TECHNOLOGY AND INFORMATION AND COMMUNICATION TECHNOLOGY

(DEPARTMENT OF ELECTRICAL AND ELECTRONICS TECHNOLOGY)

Thesis on

Design of Multivariable PID Control Scheme for Humidity and Temperature Control of Neonatal Incubator

By,

Lamrot H/Michael (MTR/623/13)

APPROVED BY THESIS ADVISOR COMMITTEE

Name of the Advisor	Signature	Date
Dr. Arun Ramaveerapathiran	_____	_____
Name of Examiner, Internal	Signature	Date
Dr. Yohans G/Meskel	_____	_____
Name of Examiner, Internal	Signature	Date
_____	_____	_____
Name of Examiner, External	Signature	Date
Dr. Menegesha Mamo	_____	_____
Name of Chairperson	Signature	Date
_____	_____	_____

Acknowledgement

First and foremost, I would like to thank God. He has given me strength and encouragement throughout all the challenging moments of completing this thesis.

I would like to express my deepest gratitude to my advisor, Dr. Arun Ramaveerapathiran, for his critical and valuable comments, suggestions, and advice. And also, I would like to thank Addis Lema and Ermiyas Tegene (staff members at Debre Berhan Referral Hospital) for their valuable support. I have to give great thanks to Bekele Shete, who works at the Juniper Glass factory.

Finally, I would like to thank my husband, who always helps me by giving comments, technical support, and sharing his ideas. He has made a great contribution to the preparation of this study in the desired way.

Lamrot H/Michael

Addis Ababa, Ethiopia

Abstract

One among the most essential and delicate concerns in the world is preterm neonatal care. To cope with the external environment, a preterm baby requires an environment that is identical to that of the womb. Therefore, a neonatal incubator can be utilized to offer a comparable environment to neonates in the womb. The progress in neonatal incubator technology is utilized to prevent neonates' mortality cases caused by infection and inadequate facility equipment management.

In this thesis work, the overall system is designed using mathematical analysis. The neonate's shape is modelled as a cylinder. The neonate is shown as a single lump with two layers: core and skin. The model includes every component of the neonatal incubator system, including the core, mattress, air circulation fan, heater, incubator walls, and humidification container.

The neonatal incubator system is fully simulated in MATLAB/Simulink to investigate the heat exchange interactions, elements, and influences on the overall system. Both skin and air mode have a closed loop simulation model that is controlled by a multivariable PID controller. The multivariable PID controller is tuned automatically using PID tuner to determine the controller parameters. Using a step input allows for the system's overall stability. The simulation results show that for the skin temperature (T_s), the overshoot is reduced from 23.1096% to 6.117% and the settling time is also reduced from 4066.8 seconds to 755.8 seconds using decoupling and sequential loop closing tuning method with PID controller. On the other hand, using decoupling and sequential loop closing tuning method with PID controller for air mode operation, the simulation results show that for air temperature (T_a), the overshoot is reduced from 59.65% to 7.2456%, and the settling time is also reduced from 2302.1 seconds to 530.48 seconds. For both skin mode and air mode operation, using decoupling and sequential loop closing tuning method with PID controller, the relative humidity has an improved settling time with an overshoot of 8.559% and 9.43%, respectively. In general, the PID controller improves the overall system performances as observed from the simulation results. The PID controller also makes the system to become robust and make the system faster by reducing the time constant.

Keywords: Neonatal Incubator, Temperature, Humidity, PID Controller, MATLAB /Simulink

Table of Contents

List of Tables

List of Figures

Abbreviations

A_{al1}	Finned aluminum block exposed part area (m^2)
A_{al2}	Finned aluminum block submerged part area (m^2)
A_c	Area of the Incubator (m^2)
A_{cv}	Skin surface area (m^2)
Age	Age of the Neonate (day)
A_{mat}	Mattress total area (m^2)
A_{net}	Mattress area which is uncovered by the neonate (m^2)
A_r	Neonate surface area normal to the incubator walls (m^2)
A_s	Surface area of skin in contact normal to the incubator walls (m^2)
A_w	Incubator normal surface area (m^2)
A_{wi}	Incubator wall surface area ($m^{2)}$
bf	Parameter for the flow rate of the blood (sec^{-1})
C_{pa}	Air specific heat ($J.kg^{-1}\ ^oC^{-1}$)
C_{pal}	Aluminum specific heat ($J.kg^{-1}\ ^oC^{-1}$)
C_{pb}	Blood specific heat ($J.kg^{-1}\ ^oC^{-1}$)
C_{pc}	Core specific heat ($J.kg^{-1}\ ^oC^{-1}$)
C_{pm}	Mattress specific heat ($J.kg^{-1}\ ^oC^{-1}$)
C_{pm}	Moist air specific heat ($J.kg^{-1}\ ^oC^{-1}$)
C_{pN}	Nitrogen specific heat ($J.kg^{-1}\ ^oC^{-1}$)
C_{po2}	Oxygen specific heat ($J.kg^{-1}\ ^oC^{-1}$)
C_{ps}	Vapor specific heat ($J.kg^{-1}\ ^oC^{-1}$)
C_{psk}	Skin specific heat ($J.kg^{-1}\ ^oC^{-1}$)
C_{pw}	Specific heat of the wall ($J.kg^{-1}\ ^oC^{-1}$)
C_{pwa}	Water specific heat ($J.kg^{-1}\ ^oC^{-1}$)
D_{sph}	Diameter of the neonate (m)
GA	Gestational age (week)
h_{acv}	Coefficient of heat transfer for forced convection ($W.m^{-2}.^oC^{-1}$)
h_{al1}	Aluminum block exposed part heat transfer coefficient ($W.m^{-2}.^oC^{-1}$)
h_{al2}	Aluminum block submerged part heat transfer coefficient ($W.m^{-2}.^oC^{-1}$)
hfg	Water latent heat at 35 ^oC ($J.kg^{-1}$)
$hfg1$	Water latent heat at 50 ^oC ($J.kg^{-1}$)
h_{scv}	Neonate skin heat transfer coefficient ($W.m^{-2}.^oC^{-1}$)
h_{wa}	Water heat transfer coefficient ($W.m^{-2}.^oC^{-1}$)
IV	Inspired volume ($mL.kg^{-1}$)
K_a	Air thermal conductivity ($W.m^{-1}.^oC^{-1}$)
K_c	Core thermal conductivity ($W.m^{-1}.^oC^{-1}$)
K_{mat}	Mattress thermal conductivity ($W.m^{-1}.^oC^{-1}$)
L_{con}	Water container length (m)
L_f	Fin Length of the fin (m)
INC	Incubator
m	Neonate mass (kg)

M_a	Incubator air mass (kg)
M_{al}	Aluminum block mass (kg)
MATLAB	Matrix Laboratory
m_c	Core mass (kg)
MIMO	Multiple Input Multiple Output
M_m	Mattress mass (kg)
M_{ri}	Each segment percentage heat production
M_{rst}	Metabolic rate at rest (W/m^2)
m_s	Skin mass (kg)
M_w	Wall mass (kg)
N_2	Nitrogen
N_f	Aluminum block fins number
n_g	Aluminum block fins gap
Nu	Nusselt number
O_2	Oxygen
P	Perimeter of the incubator (m)
PID	Proportional Integral Derivative
P_{H2O}	Water vapor partial pressure (torr)
P_{sat}	Saturation pressure (torr)
P_t	Atmospheric pressure (torr)
Q_{acv}	Convection between incubator air wall (Watt)
Q_{bc}	Convection between core and skin (Watt)
Q_{cd}	Conduction between core and skin (Watt)
Q_{cvo}	Convection between walls and environment (Watt)
Q_{heater}	Power rating of the heater (Watt)
Q_{ht}	Heat energy supplied by convection to the hood (Watt)
Q_{ic}	Conduction between mattress and incubator (Watt)
Q_{lat}	Latent heat energy (Watt)
Q_{mat}	Convection between walls and environment (Watt)
Q_{mc}	Conduction between skin and mattress (Watt)
Q_{met}	Heat production due to metabolic process (Watt)
Q_{ro}	Radiation between walls and environment (Watt)
Q_{scv}	Convection between skin and air (Watt)
Q_{se}	Evaporation between skin and air (Watt)
Q_{sen}	Sensible heat energy (Watt)
Q_{sr}	Radiation between skin and wall (Watt)
Re	Reynolds number
RH	Relative humidity (%)
R_r	Respiratory rate (sec^{-1})
S_a	Body segment surface area (m^2)
T_a	Temperature of the air (^oC)
T_{al}	Temperature of the aluminum block (^oC)
T_c	Temperature of the core (^oC)

T_e	Ambient temperature (°C)
T_{ex}	Exhaled air temperature (°C)
T_{ha}	Temperature of the heater air (°C)
th_f	Thickness of the fin (m)
th_m	Thickness of the mattress (m)
th_s	Thickness of the skin (m)
th_w	Thickness of the wall (m)
T_m	Temperature of the mattress (°C)
T_{mx}	Temperature of the mixed air (°C)
T_s	Temperature of the skin (°C)
T_{sply}	Temperature of the supplied air (°C)
T_w	Temperature of the wall (°C)
T_{wa}	Temperature of the water air (°C)
T_{wet}	Temperature of the wetted air (°C)
V	Air viscosity (m^2/sec)
V_a	Velocity of the air (m/sec)
V_{cb}	Volume of the blood (mL)
V_t	Volume of the tidal (mL)
W_a	Inhaled air humidity ratio
W_{con}	Water container width (m)
W_{ex}	Exhaled air humidity ration
W_g	Aluminum block fins width (m)
w_l	Fin height above the water (m)
w_{lw}	Fin height inside the water (m)
ε_s	Skin radiant emissivity
ε_w	Wall radiant emissivity
μ_a	Air absolute viscosity (kg/m*sec)
ρ_a	Density of the air (kg/mL)
ρ_{bl}	Density of the blood (kg/mL)
ρ_c	Density of the core (kg/m^3)
ρ_{H2O}	Density of the water (kg/mL)
ρ_{ha}	Density of the heated air (kg/ m^3)
ρ_s	Density of the skin (kg/ m^3)
ρ_w	Density of the wall (kg/ m^3)
ρ_{wet}	Density of the wetted air (kg/ m^3)
σ	Stefan-Boltzmann constant

CHAPTER ONE

1. INTRODUCTION

1.1 Background

Since about 160 years, the incubators were used to produce and maintain a safe and comfortable hydrothermal atmosphere for low-birth weight, sick, or preterm new-borns. The conception of these devices has evolved in the time. Currently, most of them have to keep humidity and temperature in optimal ranges set by medical staff [1], [2], [3].

The capabilities of a preterm baby are identical to those of a mature homeotherm, but the temperature range in which a neonate may successfully operate is strictly limited. In reaction to thermal stress, the neonates cannot be able to preserve heat by shifting position. And also, the neonates cannot adjust clothing. The suitable thermal environment can reduce the rate of neonates' morbidity and mortality.

Neonatal nursing in carefully air-controlled temperature incubators was found to reduce mortality rates by at least 22%. Finding out which variables, or stimuli, can be used to influence the generation of heat is an intriguing topic to research when researching a control system. In contrast to absolute values of either deep body temperature or surface temperature, Adamsons, Gandy, and James find that the rate of oxygen consumption of the neonate is primarily a function of the temperature gradient between the body surface and the surroundings. A flow sensor would be required, or a sensor to assess the temperature difference between skin and surroundings, if heat generation were controlled by heat flow [4], [5], [6].

Professor Mildred Stahlman founded the first recognized neonatal intensive-care unit (NICU) for neonates at Vanderbilt University in 1961. Premature or exceptionally small babies are placed in an incubator, which provides a regulated and protected environment for their care [7], [8].

In the developing world, more than 1 million neonates die due to heat loss and dehydration that could have been prevented with the use of a neonatal Incubator. Thus, Incubators provide a comfortable environment for neonates, which aids in temperature and Humidity regulation. The incubator is a specially designed air-conditioned room where we can monitor the baby's condition.

Incubators are specially developed to provide the best possible environment for new-borns with growth issues (premature babies) or illnesses [9], [10].

The incubator is a dust and bacteria-free environment with the ability to maintain optimum levels of humidity, oxygen, and temperature by regulating them. Heat losses from the new-born should be reduced by temperature and humidity management. Temperature, humidity, oxygen saturation, and light are the key physical elements that determine the incubator environment [11], [12] .

In this thesis work, the mathematical model is designed for the overall system of neonatal incubator. If the plant has a mathematical model, it is possible to use a variety of design strategies to choose controller parameters that satisfy the plant's transient and steady-state requirements. On the other hand, if the plant has no a mathematical model and the plant is too complex, a multivariable PID controller cannot be designed analytically or computationally [13], [14].

The Controller tuning is the process of choosing the controller parameters to satisfy stated performance requirements. In order to select values for K_p, T_i, and T_d based on experimental step responses, Ziegler and Nichols proposed certain guidelines for tuning PID controllers. Instead of providing the final settings for all at once, the Ziegler-tuning Nichol's rules offer the appropriate prediction that serve as an initial point for fine tuning [13], [15].

This research mainly focuses on designing a neonatal incubator system using a multivariable PID controller to monitor and adjust temperature and humidity. PID (Proportional, Integral, and Derivative) is one method of regulating a plant automatically. It is one of the most well-known and widely used techniques.

1.2 Statement of the Problem

In developing countries, thousands of neonates die each year because of premature birth [16]. The normal pregnancy weeks are 36 or 37. However, for preterm neonates, the period of pregnancy is less than the normal period. During this period, the neonates are not physiologically developed and the neonate body cannot regulate their temperature. Therefore, the neonates are exposed to a variety of health problems. As a result, the neonate is at danger of suffering hypoxia, hypothermia, dehydration and a variety of other problems. Both of these will ultimately result in death due to an

underdeveloped nervous system response to cold and overheating. Evaporation, conduction, convection, and radiation are the four ways in which a baby loses heat [16], [17].

The neonatal incubator is an extremely complicated system. because of nonlinearity in the systems and many inputs and outputs. Previous research on the subject investigated neonate heat losses, humidity and temperature monitoring, and heat flow analysis between the neonate and the external environment. However, since the system is complicated because of nonlinearity, those studies didn't achieve well [18], [19].

This research shows the multivariable PID control schemes for neonatal incubators by considering multiple inputs and multiple outputs. The previous studies were done by considering single input and single output systems by using many other controllers as well as multiple input and multiple output systems using the PI controller. The benefits of utilizing a PID controller in this system over other control algorithms are that they improve the stability of the system, make it more robust to tuning mismatches, make the system faster by reducing the time constant feasibility, and use fewer resources.

1.3 Objectives

1.3.1 General Objective

The main objective of this study is to design the multivariable PID control scheme for humidity and temperature control of neonatal incubator.

1.3.2 Specific Objectives

- To develop and analyze the mathematical model of neonatal incubator systems.
- To validate the modelled system using the available data.
- To design multivariable PID controller for the neonatal incubator system.
- To evaluate system performance using MATLAB/Simulink software.

1.4 Significance of the Thesis

The multivariable PID control scheme for relative humidity and temperature control of neonatal incubator is designed in this thesis.

Nowadays, the majority of medical equipment in our country is imported from other developed countries in the world. Neonatal incubators are among the most expensive medical devices imported from developed countries. Since the cost of the imported neonatal incubators is high, it is difficult to get easy access to neonatal incubators in many health centres in Ethiopia. This research shows the multivariable PID control schemes for neonatal incubators by considering multiple inputs and multiple outputs. The previous studies were done by considering single input and single output. Therefore, this thesis contributes to maintaining the preterm neonate thermal conditions by managing skin temperature, relative humidity and air temperature of the incubator based on the appropriate values. The result of this research can also be used by other researchers for further studies.

1.5 Limitations and Scope of the Study

This study is limited to studying the most important parameters to be monitored in a neonatal incubator. These are levels of relative humidity and temperature. In the incubator, other parameters such as light and oxygen level are not measured. The multivariable PID was selected for this thesis work. Then, the designed system is simulated using MATLAB and Simulink software. Based on the results of the simulations, the performance of the controller for regulating humidity and temperature is analyzed.

CHAPTER TWO

2. LITERATURE REVIEW

In 2015, Felipe C. Freitas, Francisco V. Andrade, Bismark C. Torrico, and Jose C. T. Campos published an article entitled “Temperature Control of a Neonate Intensive Care Unit Using Kalman Filter”. A Kalman Filter was used as a controller design method. In this article, the Kalman Filter was employed as a controller design method. Simulation was used to compare the Kalman Filter and another state observer controller. Both controls were utilized to keep the temperature in a neonatal unit under control. For tuning purposes, the State Space Controller used the Pole Placement approach [20].

Another work by M. A. Zermani, E. Feki, and A. Mami was released in 2012 titled “Multivariable Control Applied to Temperature and Humidity Case Study: Neonate Incubator”. In a neonatal incubator, multivariable control mechanisms for humidity and temperature were described. There are two inputs and two outputs in this operation. The experiment approach was used to determine the transfer function matrix. The discrete-time system transfer matrix parameters were determined in real time using the least squares method. The outputs are then coupled, and a generalized predictive decoupled control system is created. The simulation results were used to evaluate the proposed strategy’s effectiveness [21].

P. Subha Hency Jims, S. Dharmalingam, and G. Jims John Wessley published “An Improved Method to Control the Critical Parameters of a Multivariable Control System” in 2017. This paper looked at a utility boiler with a multivariable system. This study uses a classical tuning technique by calculating the controller parameters. These controller parameters are found during fuel switching disturbances and they are used to control the boiler parameters. The proposed approach was used to regulate crucial parameters in aviation systems [22].

In 2019, J. El Hadj Ali1, E. Feki, and A. Mami was published a paper entitled “Dynamic Matrix Control DMC for Neonate Incubator using the Tuning Procedure based on First Order Plus Dead Time”. The aim of this paper was to observe the effect of temperature within a neonatal incubator for premature new-borns. The Dynamic Matrix Control (DMC) was proposed as a control mechanism in this work. The multi-input multi-output (MIMO) systems were the most unique

applications of this method. Its goal was to compare distinct coupled transfer functions obtained by two earlier identification approaches. Inside the machine, a simulation of the atmospheric temperature and humidity was also achieved [23].

In the year 2019, Liheng Wang and Zhifeng Zhu published “Research on Temperature and Humidity Decoupling Control of Constant Temperature and Humidity Test Chamber”. In this study, temperature and humidity were controlled by using the decupling methods of feed forward compensation. This method provided an effective result for system modelling. As it was observed from the simulation result, the feed forward decupling controller provided an excellent result under various experimental settings [24].

M. S. Mardianto, A.I. Saputra, C. Sukma, and A. Nasrulloh published “Neonatal Incubator Temperature Controlled and Body Temperature Monitor using Arduino Mega2560 and ADS1232” in 2019. The Arduino programming language was used to construct a neonatal incubator with temperature and humidity control, a seven-segment display, and button settings controlled by a microcontroller running the ATMega2560. Along with an optocoupler sensor to make sure the airflow fan is operating, a solid-state relay to regulate the heating element's AC supply current, an electric current sensor, and an LM35 sensor to monitor feedback current consumption and temperature measurement of the heating component, the incubator’s DS18B20 sensor module measures humidity and temperature. When the temperature inside the incubator rises or falls, the component acting as a heater and the fan acting as a heat spreader will function in accordance with the microcontroller ATMega2560’s instructions to normalize the temperature inside the incubator as needed. In addition, a thermistor sensor from the RTD YSI 400 series and a 24-bit ADC ADS1232 have been used to measure the body temperature of neonates. Temperature and humidity incubator monitoring devices, as well as monitoring the baby’s body temperature, are all part of the suggested strategy [25].

Another paper entitled “Design of an Enhanced Temperature Control System for Neonatal Incubator” was published by Tamanna Afrin Tisa, Zinat Ara Nisha, and Md. Adnan Kiber in 2012. They created and developed an improved temperature management system that uses thermistors as temperature sensors and incorporates both Pulse Width Modulation (PWM) and switch mechanism. The temperature range of fluctuation versus the specified temperature (37 ^{o}C) was

found to be 1 ^{o}C, which is acceptable. The temperature output (voltage) monitor has been constructed to be linearly proportional to the temperature using a circuit network integrating a thermistor. This enabled it to simply show the temperature using a straightforward millivoltmeter by using the right scale. An alarm circuit was created to safeguard the baby's safety, and it produces audible alarms for staff attention if the temperature exceeds a defined safe range, in this case 26 ^{o}C – 38 ^{o}C [26].

Abdul Latif, Hendro Agus Widodo, Rachmad Andri Atmoko, Thanh Nguyen Phong, and Elsayed T. Helmy published a paper entitled as "Temperature and Humidity Controlling System for Baby Incubator" in 2021. The incubator in this work has a length of 60 cm, a width of 40 cm, and a height of 30 cm. The fan and/or heating in the baby incubator will automatically turn on or off on the basis of the typical incubator temperature and humidity range. Temperatures ranges from 33°C to 35°C are commonly used. While the normal range for air humidity in the incubator is 40 to 60%, The data collection system includes a temperature and humidity sensor, an ATmega8535 microprocessor, a fan, a heater, and an LCD to manage the temperature in the incubator [27].

Sheetal A. Pangarkar and S. R. Deshpande released a paper in 2014 titled "Artificial Neural Network based Temperature Controllers for Incubators". This research intends to apply an Artificial Neural Network (ANN)-based control mechanism to replicate the temperature-controlling action in neonates, and so begins the process of attempting to maintain body temperature in accordance with the surrounding environment. A linear semiconductor temperature sensor could be used to compute the temperature of the baby's body. The sensor's amplified output will then be translated into digital representation and sent to the microcontroller to be processed. With the use of an external membrane keypad, the desired set point can be set. The heater will be powered by the microcontroller's PWM output. The detected body temperature and needed set point, as well as the percentage of power delivered to the heater, will be shown on the LCD and sent to the central station via RS485 protocol. The heater's power is determined by ANN. This central monitoring station is situated some distance away from the bed as a result, the set temperature and the actual temperature of the baby can be monitored remotely [28].

In 2018, M Alzgool and H Nouri released another study titled "PID controller design for a new multi-input multi-output boost converter hub", according to the title. A novel multi-input multi-

output boost converter topology was designed, controlled, and modelled in this research. For the provision of multiple output voltage levels, renewable energy sources can be combined by the converter hub. These renewable energy sources include fuel cells, solar arrays, and wind turbines, Classic PID controllers that use the concept of closed-loop voltage mode control are used to obtain the regulated output voltage levels. Software simulation is used to show the converter's control performance [29].

In 2019, "A review on industrial MIMO decoupling control" was published by Lu Liu, Siyuan Tian, Dingyu Xue, Tao Zhang, Yang Quan Chen, and Shuo Zhang. Multi-Input and Multi-Output systems are becoming increasingly popular in industrial applications. In the literature, a variety of decoupling control techniques have been investigated. The scattered coupling interaction analysis and decoupling algorithms are gathered in this work and split into distinct groups, each with its own set of characteristics, application fields, and helpful comments for selection. Furthermore, some of the most commonly discussed decoupling control issues are highlighted [30].

In 2012, R. Hanuma Naik, D.V. Ashok Kumar, and K.S.R. Anjaneyulu published a paper titled "Controller for Multivariable Processes Based on Interaction Approach". This paper argues that designing a control strategy for multivariable processes is extremely difficult due to their innately nonlinear character and the interconnections that exist within the loops. It is too difficult to tune a conventional PID controller for a multivariable operation. The notion of IMC is used in this research to find a multivariable PID controller parameter [31].

"Design of Multivariable PID Controllers: A Comparative Study" by Shabeena Memon and Arbab Nighat Kalhoro was published in 2021. A comparison of DS (Direct Synthesis), IMC (Internal Model Control), and ETF (Effective Transfer Function) PID controller design methodologies were done in this paper. MIMO PID controllers are developed for a variety of process models with multiple delays. Simulation studies in the MATLAB/Simulink software were used to assess the performance of the three techniques [32].

The study "Effective temperature under radiant infant warmer: Does the device make a difference?" was written by Daniele Trevisanuto, Ivano Coretti, Nicoletta Doglioni, Angelo Udilano, Francesco Cavallin, and Vincenzo Zanardo. Temperatures under RIWs (radiant infant warmers) ranged from 21.5 to 44.7 degrees Celsius, with one RIW never reaching 37 degrees Celsius. Based on the measurement period and preselected power output, thermal exposure varied

widely across the three devices. The temperature in RIWs was not affected by room temperature in a meaningful way [33].

S. Thulasi dharan, K. Kavyarasan, and V. Bagyaveereswaran submitted a paper in 2017 titled "Tuning of PID controller utilizing optimization techniques for a MIMO process". The Continuous Stirred Tank Reactor and quadruple tank process were studied in this paper. These processes are applicable in chemical facilities. Due to the MIMO process, the mathematical model of both processes must be completed first, followed by the system's linearization. In this paper, two optimization strategies were used for tuning parameters and the results of these strategies were compared [34].

"Inverted Decoupling PID Controller Design for a MIMO System", by Mehmet Ali Ustuner and Sezai Taskin, was published in 2019. The inverted decoupling PID approach is used to remove loop interactions in multiple input and multiple output system. First, the system is modelled for this purpose. The loop interactions are then eliminated using decoupler blocks. Finally, a simulation of the modelling system and actual experiments are carried out. On system performance, the impact of inverted decoupling PID control and the impact of conventional PID control are examined [35].

2.1 Summary of Literature Review

In general, various kinds of work have been done from the research papers that are presented above. When summarizing the work done, temperature-regulating action in neonates and thus starts trying to maintain the body temperature according to the environment. Controlling the temperature in the incubator was done by using the micro controllers and different programming languages to control the temperature, as well as the humidity of the baby incubator, were done by using an ON-OFF control system. What they reviewed about related work is that they can control temperature and humidity using a PI (Proportional Integral) controller, but the derivative (D) controller was not included. The capabilities of a preterm baby are identical to those of a mature homeotherm, but the temperature range in which a neonate may successfully operate is strictly limited. In reaction to thermal stress, the neonates cannot be able to preserve heat by shifting position. And also, the neonates cannot adjust clothing. The suitable thermal environment can reduce the rate of neonates' morbidity and mortality.

Previous research on the topic used a variety of computational and experimental approaches to explore and analyze the numerous physical dynamic processes of neonatal incubators. These research studies' main contributions included analysis of neonate heat losses; heat transfer and control; air circulation; control of humidity; and understanding of the heat interactions between both the neonate and its environment. However, achieving these goals is challenging because neonatal incubator system controlled-parameters have time-varying and non-linear properties, as well as thermal design issues.

In addition to these studies, some articles that contains the researches on multivariable PID control are reviewed. Although the studies were not designed for neonatal incubators, the multivariable PID controller with coupling and decoupling methods are included. Due to their innately nonlinear character and the interconnections that exist within the loops, designing a control strategy for multivariable processes is extremely difficult. Indeed, it is too difficult to tune a conventional PID controller for a multivariable operation. Because of the MIMO process, the mathematical model of both processes must be completed first, followed by the system's linearization. Controller tuning has a greater significance for controlling the entire process. Therefore, the controller should be designed appropriately based on their applications.

In general, based on these reviewed studies, every component using for neonatal incubator has an effect on relative humidity and temperature. So, the components should be conditioned. The mathematical model of each component of the neonatal incubator is designed and monitor the relative humidity and temperature in the neonatal incubator by using decoupling and sequential loop closing tuning method with PID controller.

CHAPTER THREE

3. MATHEMATICAL MODELLING OF NEONATAL INCUBATOR

3.1 Introduction

Providing suitable thermo-neutral conditions for new-born neonates, particularly preterm neonates, is a crucial concern while feeding them shortly after birth. This allows the neonates to have a standard temperature of between 36.5 and 37.5 °C [9], [26]. Only by placing new-born neonates within thermoregulation equipment, commonly known as “neonate warmers”, can this be accomplished. The neonatal incubators are used to deliver an appropriate temperature and relative humidity for preterm neonates. The mathematical model is developed in this chapter.

3.2 Neonatal Incubator Components

The neonatal incubator consists of many components such as the core layer, skin layer, air inside the incubator, walls, mattress, heater, and fan. Those components have their own heat interactions among each other, as depicted in Figure 3.1. Radiation, conduction, evaporation, and convection are the four ways in which a baby loses heat [27].

To simplify the modelling, appropriate assumptions are made where necessary. Various empirical relationships are implemented during the process of modelling in order to further simplify the equations [16], [36].

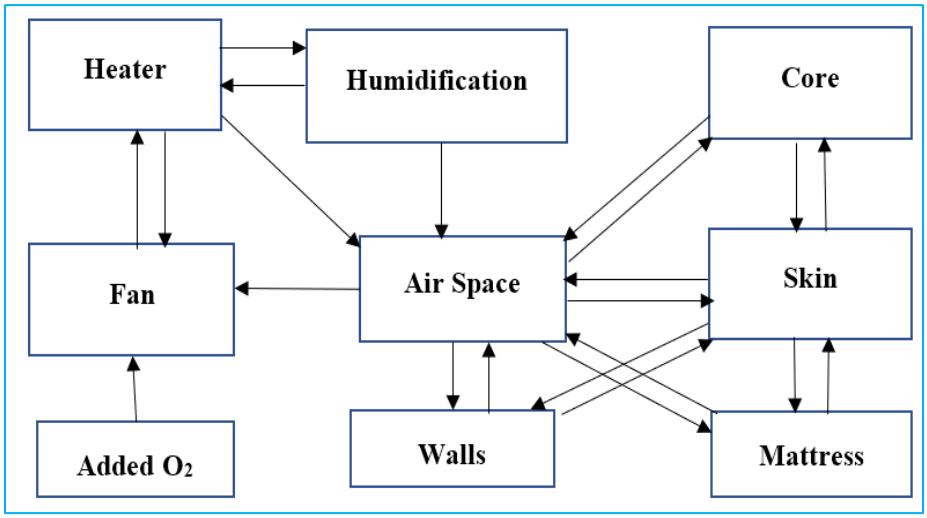

Figure 3. 1 Neonatal incubator component interactions

The type of incubator model selected for this study is the ATOM V-850. This type of neonatal incubator is most commonly used [16]. The components of the selected neonatal incubator are illustrated in Figure 3.2. The heat flow between the components of the neonatal incubator is shown in Figure 3.3.

Figure 3. 2 Neonatal incubator (Model: ATOM V-850)

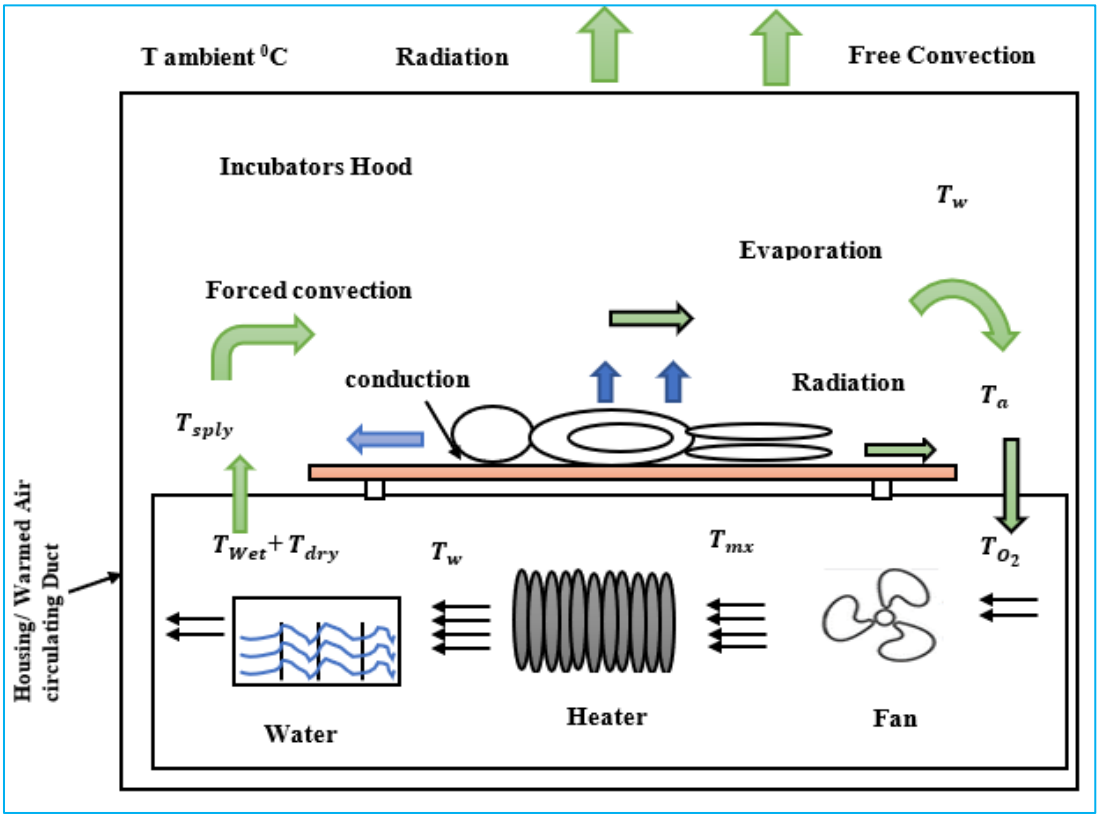

Figure 3. 3 Heat flow diagram

3.3 Neonate Modelling

The modelling of the neonate can be done by considering the neonate as one lumped or four lumped. For the four lumped together, the parts of the neonates are considered limbs (upper and lower), head and trunk. The neonate is divided into core and skin layers in each of the formulated models, as shown in Figure 3.4 [16], [37].

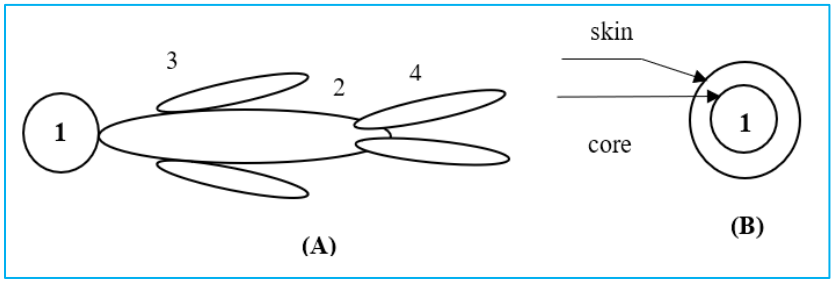

Figure 3. 4 (A) Neonate modelling, (B) Layers of the neonate

In this thesis work, the neonate is considered as one lump. Many assumptions are made to simplify the neonate model. For instance, the neonate is modelled as a black cylinder, the neonate is considered at rest, and the incubator is placed in the room with the air that has a minimum velocity.

The components of the neonatal incubator have temperature changes over time. This change in temperature is called instantaneous temperature. In order to model each component using mathematical analysis, the first law of thermodynamics is applicable. The heat storage (Q_{str}) is the difference between heat in (Q_{in}) and heat out (Q_{out}), and it can be computed using the energy conversion law of the heat balance in a period of dt as follows [38]:

$$Q_{str} = [Q_{in} - Q_{out}]dt \tag{3.1}$$

3.3.1 Modelling of the Core Layer

When the core layer is modelled, the mathematical equation (3.2) can be used by considering the neonate mass as one lump. Therefore, the heat balance over a period of time is calculated as [38]:

$$dT_c m_c C_{pc} = -[Q_{bc} + Q_{lat} + Q_{sen} + Q_{cd} - Q_{met}]dt \tag{3.2}$$

Where: Q_{met} denotes the neonate's core ability to generate heat, Q_{sen} denotes sensible heat, and Q_{lat} denotes latent heat. Q_{cd} stands for skin layer conduction. Q_{bc} = Convection skin-blood, mc = the neonate's core mass, C_{pc} = Core specific heat, T_c = Core temperature.

The core instantaneous temperature is calculated as:

$$\frac{dT_c}{dt} = \frac{-[Q_{bc} + Q_{lat} + Q_{sen} + Q_{cd} - Q_{met}]}{C_{pc} m_c} \tag{3.3}$$

Equation (3.3) can be rewritten using the differential operator *D*= *dt* as follows:

$$T_c = \frac{-[Q_{bc} + Q_{lat} + Q_{sen} + Q_{cd} - Q_{met}]}{C_{pc} m_c D} \tag{3.4}$$

The core temperature can be determined using equation (3.4) using the heat flow rates which has influences on the neonate's body. The terms used in equation (3.4) cab be determined as follows.

3.3.1.1 Neonate Core Heat Production

The neonate's core can generate heat (Q_{met}) and it can be calculated as:

$$Q_{met} = S_a \, x \;\; M_{rst} \tag{3.5}$$

Where: M_{rst} = metabolic rate at rest (M_{rst} is 24.80 W/m^2 [16]), and S_a is the neonate's surface area.

3.3.1.2 Neonate Core Heat Loss

The neonate's heat loss occurs during breathing as a convective heat form. This convective heat consists of sensitive loss of heat (Q_{sen}) attributable to the warming of breathed air and latent heat loss (Q_{lat}) because-of inhaled and expelled air difference in water-vapour pressure.

The respiration loss can be computed using the respiratory rate and tidal volume as follows [16], [39]:

$$Q_{sen} = rr \times C_{pa} \times v_t \times (T_{ex} - T_a) \times \rho_a \tag{3.6}$$

$$Q_{lat} = hfg \times rr \times v_t \times (W_{ex} - W_a) \times \rho_a \tag{3.7}$$

Equations (3.6) and (3.7) modified for inspired minute volume 200 mL/kg of neonate mass [16].

$$Q_{sen} = m \times IV \times \rho_a \times (T_{ex} - T_a) \times C_{pa} \tag{3.8}$$

$$Q_{lat} = IV \times m \times hfg \times (W_{ex} - W_a) \times \rho_a \tag{3.9}$$

Where: Inspired air volume (*IV*) = 3.333 mL/kg/sec.

As a result, the inhaled air and exhaled air humidity ratio can be computed as follows [38].

$$W_{ex} = -\frac{0.622 \times P_{H_2o}}{P_{H_2o} - P_t} \tag{3.10}$$

$$W_a = -\frac{0.622 \times P_{H_2o}}{P_{H_2o} - P_t} \tag{3.11}$$

To calculate the water-vapour partial pressure at T_a and T_{ex}, apply the following equation [38].

$$P_{H_2o} = RH \times P_{sat} \tag{3.12}$$

Thus, T and P_{sat} relationships are represented as:

$$\mathrm{P}_{sat} = -[18.104 - 2.2347T] \tag{3.13}$$

The value of temperature in equation (3.13), which is used to estimate the saturation pressure, ranges from 0.01-60 °C. At an exhaled temperature of 37 °C, the humidity is considered to be 100% [9], [16].

Conduction via the core layer also causes the core to lose heat. Hence, the conduction rate is computed as:

$$\mathrm{Q_{cd}} = \frac{K_c \times (T_c - T_s) \times {S_a}^2 \times \rho_c}{m} \tag{3.14}$$

The convective heat losses by the blood-core are also calculated as:

$$\mathrm{Q_{bc}} = \mathrm{V}_{cb} \times (\mathrm{T}_c - \mathrm{T_s}) \times bf \times \mathrm{C}_{p_b} \times \rho_{bl} \tag{3.15}$$

The mass of the neonate body layer is used to calculate the blood volume [37]:

$$V_{cb} = 80 \times m \tag{3.16}$$

Equation (3.17) is used to determine the blood flow rate (*bf)* [16].

$$bf = q_c \times \rho_{bl} \tag{3.17}$$

The neonate's core mass m_c is computed by:

$$m_c = m_s \times m \tag{3.18}$$

The neonate skin mass (m_s) is computed as:

$$m_s = s_a \times th_s \times \rho_s \tag{3.19}$$

The empirical formula, given in equation (3.20), can be utilized to determine the total surface area (S_a) of the neonate body [16]:

$$S_a = \frac{m^{3/4}}{10.8} \tag{3.20}$$

3.3.2 Modelling of the Skin Layer

When the skin layer is modelled, the mathematical equation (3.21) can be used by considering the neonate mass as one lump. Therefore, the heat balance in a period of time is calculated by [38]:

$$dT_s\, m_s C_{p_{sk}} = -[Q_{sr} + Q_{se} - Q_{bc} - Q_{cd} + Q_{scv} + Q_{mc}]dt \tag{3.21}$$

Where: Q_{scv} = skin-incubator airspace convection, Q_{mc} = skin-mattress conduction, Q_{se} stands for skin evaporative loss. Q_{sr} stands for skin-wall radiation. Q_{cd} = Skin layer conduction Q_{bc} = Convection skin-blood, m_s = neonatal skin mass C_{psk} = skin specific heat, T_s = skin temperature.

The core instantaneous temperature can be determined as:

$$\frac{dT_s}{dt} = \frac{-[Q_{sr} + Q_{se} - Q_{bc} - Q_{cd} + Q_{scv} + Q_{mc}]}{C_{p_{sk}} m_s} \tag{3.22}$$

Equation (3.23) can be rewritten using the differential operator $D = dt$ as follows:

$$T_s = \frac{-[Q_{sr} + Q_{se} - Q_{bc} - Q_{cd} + Q_{scv} + Q_{mc}]}{C_{p_{sk}} m_s D} \tag{3.23}$$

When the skin and the mattress are in contact, heat loss due to conduction (Q_{mc}) will occur, and it is computed as:

$$Q_{mc} = \frac{K_{mat} \times (T_s - T_m) \times A_s}{th_m} \tag{3.24}$$

The middle of the mattress's specified thickness is where the average mattress temperature is measured. The thickness of the mattress (th_m) is taken by considering half of the total thickness. It is believed that 10% of the whole neonate surface area (m^2) is in contact with the mattress[16].

$$A_s = \frac{S_a}{10} \tag{3.25}$$

The convective heat loss by the incubator air space (Q_{scv}) and neonate skin is computed as:

$$Q_{scv} = A_{cv} \times (T_s - T_a) \times h_{scv} \tag{3.26}$$

About 10% of the neonate's skin is contact to the mattress and 90% is exposed to the air (A_{cv}).

$$A_{cv} = \frac{9 \times S_a}{10} \tag{3.27}$$

The forced convection heat transfer convective value can be computed based on the Reynolds and Nusselt numbers.

$$Nu_{sph} = \frac{h_{scv} \times D_{sph}}{K_a} \tag{3.28}$$

Where: the Reynolds number can be determined as:

$$Re_D = \frac{\rho_a \times V_a \times D_{sph}}{\mu_a} \tag{3.29}$$

Modelling the neonate body is challenging because it has an irregular shape. Therefore, the neonate body is assumed to have a cylindrical shape for this thesis study. Figure 3.5 depicts this assumption.

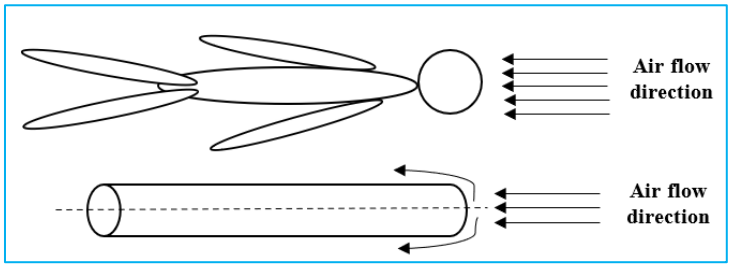

Figure 3. 5 Assumption for the shape of the neonate

The Nusselt number for cylindrical shapes and spherical air flow directions can be determined by the succeeding approximate formula [38].

$$Nu_{sph} = [0.06Re^{0.67} + 0.4Re^{0.5}]\left(\frac{\mu_a}{\mu_s}\right)Pr^{\frac{2}{5}} + 2 \tag{3.30}$$

In equation (3.30), the Prandtl number (P_r) can be determined as [38]:

$$Pr = \frac{C_{p_a} \times \mu_a}{K_a} \tag{3.31}$$

The skin evaporation heat loss (Q_{se}) is computed by the following equation [16]:

$$Q_{se} = \frac{hfg \times m \times Evap. \times \rho_{h_2o}}{86400} \tag{3.32}$$

Where: the term *Evap*. refers to the amount of water that evaporates from a neonate's skin into the environment in millilitres per kilogram per day [16], [40].

$$Evap. = \left[6.5 \exp\left(\frac{168}{age + 11.8}\right) \times \exp\left(\frac{-5.2\text{GA}}{age + 12.2}\right) + 4.8\right] * \left[2 - \left(\frac{P_{H_2o}}{23}\right)\right] \tag{3.33}$$

Where: GA is the gestational age.

The skin-wall radiation (Q_{sr}) can be calculated by [16], [41]:

$$Q_{sr} = \sigma \times A_r \times \varepsilon_s \times [-(T_w + 273.15)^4 + (T_s + 273.15)^4] \tag{3.34}$$

If the neonate is modelled as four lumps, equation (3.5) can be rewritten as:

$$Q_{met} = mr_i \times S_{ai} \times M_{rst} \tag{3.35}$$

Where: The subscript *i* shows the number of segments on the body of the neonate.

3.4 Modelling of the Incubator

Incubator modelling has three parts. These are:

1. Modelling of the Air Inside the Incubator
2. Modelling of the Incubator Walls, and
3. Modelling of the Mattress.

3.4.1 Modelling of the Air space

The neonatal incubator system components heat transfer with the incubator air space, mostly by convection. The processes of evaporation and respiration also include the transfer of mass and heat.

The air temperature in the incubator (T_a) is computed as follows:

$$dT_a C_{p_a} M_a = -(Q_{mat} - Q_{acv} - Q_{se} - Q_{scv} - Q_{sen} - Q_{ht} - Q_{lat})dt \tag{3.36}$$

Equation (3.37) can be used to compute the air space instantaneous temperature.

$$\frac{dT_a}{dt} = \frac{-(Q_{mat} + Q_{acv} - Q_{se} - Q_{scv} - Q_{sen} - Q_{ht} - Q_{lat})dt}{C_{p_a} M_a} \tag{3.37}$$

By using the D-operator ($D = dt$), equation (3.37) is rewritten as follows:

$$T_a = \frac{-[Q_{mat} + Q_{acv} - Q_{se} - Q_{scv} - Q_{sen} - Q_{ht} - Q_{lat}]dt]}{C_{p_a} M_a D} \tag{3.38}$$

The convective heat loss between incubator air and the wall (Q_{acv}) can be computed by:

$$Q_{acv} = A_{wi} \times (T_a - T_w) \times h_{acv} \tag{3.39}$$

The air velocity inside the incubator wall is assumed to be 10 cm/sec. The Reynolds number for this air velocity is 4970.6 [38].

Equation (3.40) can be used in order to determine the equivalent incubator hydraulic diameter, D_h:

$$D_h = \frac{A_c}{0.25 \times p} \tag{3.40}$$

For this situation, the Nusselt number can be calculated as [38]:

$$N_{u_1} = \frac{f \times (Re - 1000) \times Pr}{8 + 101.6 \times (0.125 \times f)^{\frac{1}{2}} \times (Pr^{0.67} - 1)} \tag{3.41}$$

Where: f refers the friction factor, and is computed as [38]:

$$\frac{1}{\sqrt{f}} = -2 \times \log\left(\frac{2.51}{Re \times \sqrt{f}} + \frac{\varepsilon}{3.7 \times D_h}\right) \tag{3.42}$$

Where: ε refers the roughness of the plexiglass, and is zero, f is around 0.0119 [38].

The convective incubator air between loss of heat and mattress (Q_{mat}) is calculated:

$$Q_{mat} = A_{net} \times (T_a - T_m) \times h_{acv} \tag{3.43}$$

Where: A_{net} is the mattress net area which is not covered by the neonate.

$$A_{net} = A_{mat} - A_s \tag{3.44}$$

3.4.2 Modelling of the Incubator Walls

Plexiglass is used to construct the incubator walls. The wall has a 6 mm thickness. The wall temperature (T_w) is calculated by the heat balance equation.

$$dT_w C_{pw} M_w = -[Q_{ro} + Q_{cvo} - Q_{sr} - Q_{acv}]dt \tag{3.45}$$

The wall instantaneous temperature is computed by:

$$\frac{dT_w}{dt} = \frac{-[Q_{ro} + Q_{cvo} - Q_{sr} - Q_{acv}]}{C_{pw} M_w} \tag{3.46}$$

The wall temperature can be rewritten using $D=dt$:

$$T_w = \frac{-[Q_{ro} + Q_{cvo} - Q_{sr} - Q_{acv}]}{C_{pw} M_w D} \tag{3.47}$$

Where: Q_{sr} = heat transfer by radiation, Q_{cvo} = transfer heat by convection between the environment and the incubator wall, Q_{ro} = transfer heat by radiation between the incubator wall and environment, M_w = the wall mass, C_{pw} = wall specific heat, T_w = wall temperature.

The convective heat losses are calculated using Prandtl and Nusselt numbers as follows [38], [42]:

$$Nu_{inc} = \frac{h_{cvo} \times L_c}{K_a} = C \times (Gr_L \times Pr)^n = C \times Ra_L^n \tag{3.48}$$

Where: G_{rL} refers to the Grashof number is calculated as follows [38]:

$$Gr_L = \frac{g \times \beta \times (T_w - T_e) \times L_c^3}{v^2} \tag{3.49}$$

The Rayleigh number (R_{aL}) and average temperature are also computed as [38] [43]:

$$Ra_L = Gr_L = \frac{g \times \beta \times (T_w - T_e) \times L_c^3}{v^2} Pr \tag{3.50}$$

$$T_{avg} = 0.5 \times (T_w + T_e) \tag{3.51}$$

The Nusselt numbers for both the horizontal surface and vertical surface of the incubator wall are computed by using equations (3.52) and (3.53).

$$Nu_{hzt} = \frac{27 \times Ra_L^{0.25}}{10} \tag{3.52}$$

$$Nu_{vrt} = \left[0.825 + \frac{0.387 \times Ra_L^{0.167}}{[1 + (\frac{0.492}{Pr})^{0.56}]^{0.296}}\right]^2 \quad (3.53)$$

Where: L_c is defined by [38]:

$$L_c = \frac{A_c}{P} \quad (2.54)$$

The heat transfer by convection between the incubator environment and wall (Q_{cvo}), the heat loss by convection from the four vertical sides, and the loss of heat as a consequence of radiation from the wall to the environment are expressed in equations (3.55), (3.56) and 3.57, respectively [38].

$$Q_{cvo} = A_{wi} \times (T_w - T_e) \times h_{cvo} \quad (3.55)$$

$$Q_{cvt} = Q_{C_{hzt}} + 2 \times [Q_{c_{vrt}}]_{long} + 2 \times [Q_{c_{vrt}}]_{short} \quad (3.56)$$

$$Q_{ro} = \sigma \times \varepsilon_w \times A_w \times [(T_w + 273.15)^4 - (T_e + 273.15)^4] \quad (3.57)$$

The incubator wall mass (M_w) is computed as:

$$M_w = A_{wi} \times \rho_w \times th_w \quad (3.58)$$

3.4.3 Modelling of the Mattress

The neonatal skin conducts heat through the mattress by conduction, and the incubator airspace convection heats the mattress. The mattress temperature (T_m) can be computed using the heat balance equation.

$$dT_m C_{p_m} M_m = -[Q_{ic} - Q_{mat} - Q_{mc}]dt \quad (3.59)$$

The mattress temperature is expressed by the following equation:

$$\frac{dT_m}{dt} = \frac{-[Q_{ic} - Q_{mat} - Q_{mc}]dt}{C_{pm} M_m} \quad (3.60)$$

The temperature of the mattress, T_m, can be represented mathematically using D =*dt*:

$$T_m = \frac{-[Q_{ic} - Q_{mat} - Q_{mc}]dt}{C_{pm} M_m D} \quad (3.61)$$

3.5 Modelling of the Heating Element

The temperature of mixed air is determined by utilizing the heat balance equation.

$$T_{mx} \times C_{p_{mx}} \times \dot{m}_{mx} = \dot{m}_a \times C_{p_a} \times T_a + \dot{m}_{O_2} \times C_{p_{O_2}} \times T_{O_2} \quad (3.62)$$

$$T_{mx} = \frac{\dot{m}_a \times C_{p_a} \times T_a + \dot{m}_{O_2} \times C_{p_{O_2}} \times T_{O_2}}{C_{p_{mx}} \times \dot{m}_{mx}} \quad (3.63)$$

Where: $\dot{m}_{mx}$ = the mass flow rate of the mixed air, $\dot{m}_{O_2}$ = added oxygen mass flow rate and $\dot{m}_a$ = incubator mass flow rate.

The mixed air temperature can be modified using the volumetric air and oxygen flow rates as:

$$T_{mx} = \frac{T_a \times q_{air} \times C_{p_a} \times \rho_a + T_{O_2} \times q_{O_2} \times C_{p_{O2}} \times \rho_{O_2}}{C_{p_{mx}} \times (q_{air} \times \rho_a + q_{O_2} \times \rho_{O_2})} \quad (3.64)$$

Where: C_{pmx} is considered to be equal to C_{Pa} (1007 J/kg.^{o}C) [38].

The incubator is considered to be filled with an air composition of 21% oxygen and 79% nitrogen, and their concentrations can be calculated as follows.

$$Y_{N_2} = 0.79 - O_2 \quad (3.65)$$

$$Y_{O_2} = 0.21 + O_2 \quad (3.66)$$

The perfect gas law is used for determining the density of both nitrogen and oxygen [38].

$$P_t \times V_{inc} = T_a \times N_t \times R_u \quad (3.67)$$

Where: R_u refers to the constant of molar gas and N_t refers to the total number of moles.

Using the concentration percentage of each gas (Y_{gas}%), the equation of density can be rewritten as follows [38]:

$$Y_{gas\%} = \frac{P_{gas}}{P_t} = \frac{N_{gas}}{N_t} \quad (3.68)$$

The molar concentration (C), (kmol/m^3), can be computed using [38]:

$$C = \frac{N_{gas}}{V_{inc}} \quad (3.69)$$

Hence, each gas density can be determined as [38]:

$$\rho = M \times C \quad (3.70)$$

Where: M denotes molar weights of oxygen (32 kg/kmol) and nitrogen (28 kg/kmol) [38].

The ideal gas law's general form can be applied to each gas (N_2 and O_2) [38]:

$$P_{gas} \times V_{inc} = T_a \times M_a \times R_{gas} \quad (3.71)$$

R_{gas} refer constant of the gas in kJ/kg. K and for N_2: 0.2968, for O_2: 0.2598 [38].

$$P_{gas} = P_t \times Y_{gas\%} \quad (3.72)$$

$$M_a = \left[\left\{\frac{P_t \times Y_{N_2}}{R_{N_2}}\right\} + \left\{\frac{P_t \times Y_{O_2}}{R_{O_2}}\right\}\right] \frac{V_{inv}}{T_a} \quad (3.73)$$

The temperature of the heated air (T_{ha}) can be calculated using the heat balance equation as [38]:

$$\dot{m}_a \times T_{mx} \times C_{p_a} + Q_{heater} = T_{ha} \times \dot{m}_a \times C_{p_a} \tag{3.74}$$

$$T_{ha} = T_{mx} + \frac{Q_{heater}}{C_{p_a} \times \dot{m}_a} \tag{3.75}$$

3.6 Modelling of the Humidification System

The humidifier adds water vapor to the humidification system. This system is made up of plastic containers and finned aluminium blocks. The exchange of air is conducted using 80×50 mm openings. The air flow rate through these openings can be calculated as follows:

$$Q_{ah} = A_{op} \times \mathrm{V}_a \tag{3.76}$$

Where: V_a = 0.1 m/sec and A_{op} = 0.004 m^2. Hence, the air flow rate is 0.0004 m^3/sec.

The heat is stored in the aluminium block. This stored heat is exchanged through the water and air by means of convection. By conduction, some heat is transferred to the unshielded components of the aluminium block[16].

The water tank air temperature is calculated using the heat balance equation as expressed below.

$$\begin{aligned} dT_{wet} C_{p_a} M_{ah} = {} & \left[\dot{m}_a C_{p_a} T_{ha}\right]dt + \left[A_{wa} \frac{h_{wa}}{C_{p_m}} (W_{wet} - W_{ha}) hfg_1\right] dt \\ & - [A_{wa} h_{wa} (T_{wet} - T_{wa})]dt - [h_{al1} A_{al1} (T_{wet} - T_{al})]dt \\ & - \left[\dot{m}_a C_{p_a} T_{wet}\right]dt \end{aligned} \tag{3.77}$$

$$\frac{dT_{wet}}{dt} = \frac{\begin{array}{c}\left[T_{ha} \dot{m}_a C_{p_a}\right]dt + \left[A_{wa} \frac{h_{wa}}{C_{p_m}} (W_{wet} - W_{ha}) hfg_1\right] dt - [A_{wa} h_{wa} (T_{wet} - T_{wa})] \\ -[A_{al1} h_{al1} (T_{wet} - T_{al})] - \left[T_{wet} \dot{m}_a C_{p_a}\right]\end{array}}{C_{P_a} M_{ah}} \tag{3.78}$$

$$T_{wet} = \frac{\begin{array}{c}\left[T_{ha} \dot{m}_a C_{p_a}\right]dt + \left[A_{wa} \frac{h_{wa}}{C_{p_m}} (W_{wet} - W_{ha}) hfg_1\right] dt - [A_{wa} h_{wa} (T_{wet} - T_{wa})] \\ -[A_{al1} h_{al1} (T_{wet} - T_{al})] - \left[T_{wet} \dot{m}_a C_{p_a}\right]\end{array}}{C_{P_a} M_{ah} D} \tag{3.79}$$

Where: $\dot{m}_a$ can be computed as:

$$\dot{m}_a = V_a \times A_{i/o} \times \rho_{ha} \tag{3.80}$$

Where: $A_{i/o}$ refers to the opening area for air flow and equals to 0.004 m^2. The water surface area (A_{wa}), aluminium block exposed parts area (A_{al1}), the mass of the air (M_{ah}), and the moist air specific heat (C_{Pm}) can be calculated as follows [16].

$$A_{wa} = W_{con} \times L_{con} - N_f \times l_f \times th_f \tag{3.81}$$

$$A_{al1} = 2(N_f l_f w_l) \tag{3.82}$$

$$M_{ah} = w_l \times W_{con} \times L_{con} \times \rho_{wet} \tag{3.83}$$

$$C_{p_m} = C_{ps} \times W_{wet} + C_p \tag{3.84}$$

The aluminium Reynolds number is 1112.6 and the water surface is 1863.6. Therefore, the aluminium and water Nusselt numbers are computed as [38]:

$$Nu = 0.664 \times Pr^{\frac{1}{3}} \times Re_L^{\frac{1}{2}} \tag{3.85}$$

$$Nu = \frac{h_{L_c}}{K_a} \tag{3.86}$$

Where:

$$Re = \frac{L_c \times \rho_a \times V_a}{\mu_a} \tag{3.87}$$

$$Pr = \frac{C_{p_a} \times \mu_a}{K_a} \tag{3.88}$$

The water mass temperature (T_{wa}) is calculated by using the heat balance equation as follows:

$$dT_{wa} C_{P_{wa}} M_{wa} = [A_{wa} h_{wa} (T_{wet} - T_{wa})]dt + \left[A_{al_2} h_{al_2} (T_{al} - T_{wa})\right]dt - \left[A_{wa} \frac{h_{wa}}{C_{p_m}} hfg_1 (W_{wet} - W_{ha})\right] dt \tag{3.89}$$

$$\frac{dT_{wa}}{dt} = \frac{[A_{wa} h_{wa} (T_{wet} - T_{wa})] + \left[A_{al_2} h_{al_2} (T_{al} - T_{wa})\right] - \left[A_{wa} \frac{h_{wa}}{C_{p_m}} hfg_1 (W_{wet} - W_{ha})\right]}{C_{p_{wa}} M_{wa}} \tag{3.90}$$

Then,

$$T_{wa} = \frac{[A_{wa}h_{wa}(T_{wet} - T_{wa})] + \left[A_{al_2}h_{al_2}(T_{al} - T_{wa})\right] - \left[A_{wa}\frac{h_{wa}}{C_{p_m}}hfg_1(W_{wet} - W_{ha})\right]}{C_{p_{wa}}M_{wa}D} \quad (3.91)$$

Where:

$$A_{al_2} = 2l_f[N_f \times w_{lw} + 0.5 \times n_g \times W_g] \quad (3.92)$$

The heat transfer coefficient for the convection process (h_{al2}) can be computed as [38]:

$$h_{al_2} = \frac{k_{wa} \times Nu}{S} \quad (3.93)$$

Where: k_{wa} refers to water thermal conductivity, and S refers to adjacent fin spacing (21.63 mm).

The Raleigh number (R_a) can be used to drive Nusselt number (N_u) as follow [38]:

$$Nu = \left(\sqrt{\frac{576}{(Ra_sS/L)^2} + \frac{2.873}{(Ra_sS/L)^{0.5}}}\right)^{-1} \quad (3.94)$$

Where:

$$Ra_s = \frac{\beta \times g \times (T_s - T_\infty)S^3}{V^2}Pr \quad (3.95)$$

The aluminium block temperature (T_{al}) is also derived from the heat balance equation as follows:

$$dT_{al}C_{p_{al}}M_{al} = \left[A_{al_1}h_{al_1}(T_{wet} - T_{al})\right]dt + \left[A_{al_2}h_{al_2}(T_{wa} - T_{al})\right]dt \quad (3.96)$$

$$\frac{dT_{al}}{dt} = \frac{\left[A_{al_1}h_{al_1}(T_{wet} - T_{al})\right]dt + \left[A_{al_2}h_{al_2}(T_{wa} - T_{al})\right]}{C_{p_{al}}M_{al}} \quad (3.97)$$

Then,

$$T_{al} = \frac{\left[A_{al_1}h_{al_1}(T_{wet} - T_{al})\right]dt + \left[A_{al_2}h_{al_2}(T_{wa} - T_{al})\right]}{C_{p_{al}}M_{al}D} \quad (3.98)$$

The moist air and dry air areas can be computed as follows:

$$A_{wet} = -0.0009 + 5 \times 10^{-5} \times RH \quad (3.99)$$

$$A_{dry} = 0.0044 - 5 \times 10^{-5} \times RH \quad (3.100)$$

The temperature of the supplied air (T_{sply}) is calculated below.

$$T_{sply}(\dot{m}_{wet} + \dot{m}_{dry})C_{p_a} = T_{wet}\dot{m}_{wet}C_{p_a} + T_{ha}\,\dot{m}_{dry}C_{p_a} \quad (3.101)$$

$$T_{sply} = \frac{T_{wet} \times \dot{m}_{wet} + T_{ha} \times \dot{m}_{dry}}{\dot{m}_{wet} + \dot{m}_{dry}} \quad (3.102)$$

Where: C_{Pa} = 1007 J/kg. ^{o}C

And, $\dot{m}_{wet}$ and $\dot{m}_{dry}$ can be calculated as:

$$\dot{m}_{wet} = V_a \times A_{wet} \times \rho_{wet} \quad (3.103)$$

$$\dot{m}_{dry} = V_a \times A_{dry} \times \rho_{ha} \quad (3.104)$$

The relative humidity (RH) can be determined using the dew point temperature (t_d) and air temperature (t) as follows [44], [45]:

$$RH = 100 - 5 \times (t - t_d) \quad (3.105)$$

The heat energy transfer to the incubator wall due to convection (Q_{ht}) is computed by the following equation.

$$Q_{ht} = \dot{m}_a \times (T_{sply} - T_a) \times C_{P_a} \quad (3.106)$$

In general, equations (3.1) to (3.106) are used to design the neonatal incubator's overall system magmatically. Therefore, the overall system is simulated using MATLAB/Simulink software by creating subsystems from the mathematical equations of each component.

CHAPTER FOUR

4. MULTIVARIABLE PID CONTROLLER DESIGN USING MATLAB/SIMULINK

4.1 Introduction

The neonatal incubator system model, which was mathematically modelled in chapter three, is transformed into computer simulations in this chapter for each component. a model is being constructed for each component of the plant in the MATLAB/Simulink software. Then, in a single block known as the Plant, these Simulink models are linked together via internal loops. To put it another way, the input to one component serves as the output to another.

The temperature and the relative humidity level are essentially the plant's two variable inputs. The plant is then connected to the multivariable PID controller. The general concept of the simulation model is shown in Figure 4.1.

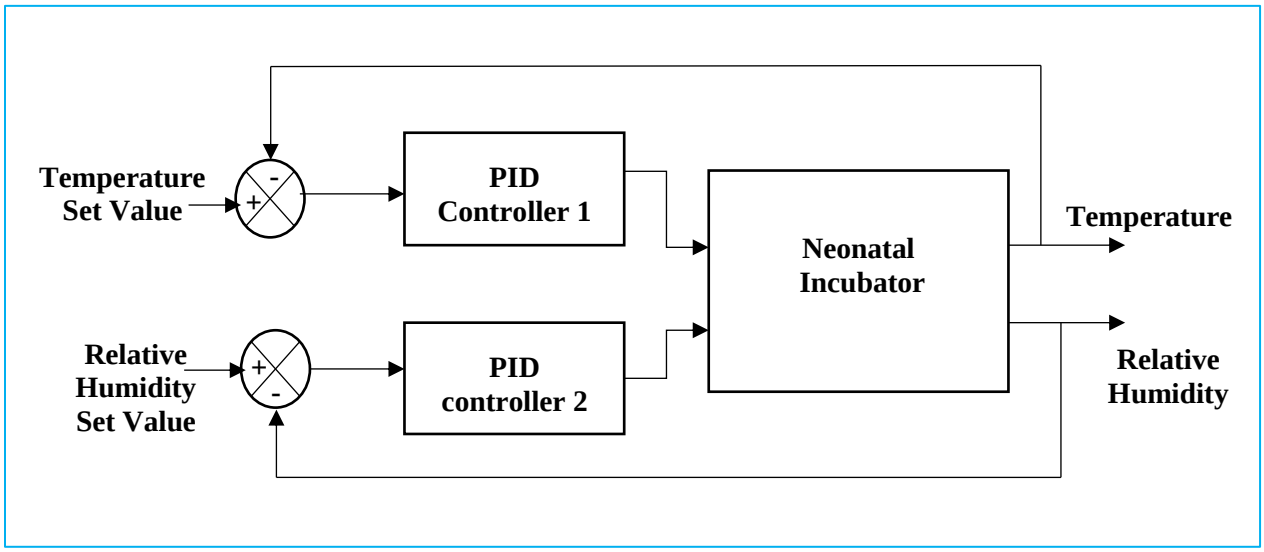

Figure 4. 1 MIMO block diagram

The simulation model's findings are expressed in terms of varying temperature for both the incubator components and the temperature of the neonate's core and skin, the temperature of the incubator wall, the mattress temperature and the temperature of the incubator air space. The humidification tank modelling is also included in the simulation. Figure 4.2 depicts the neonatal incubator system's entire simulation model.

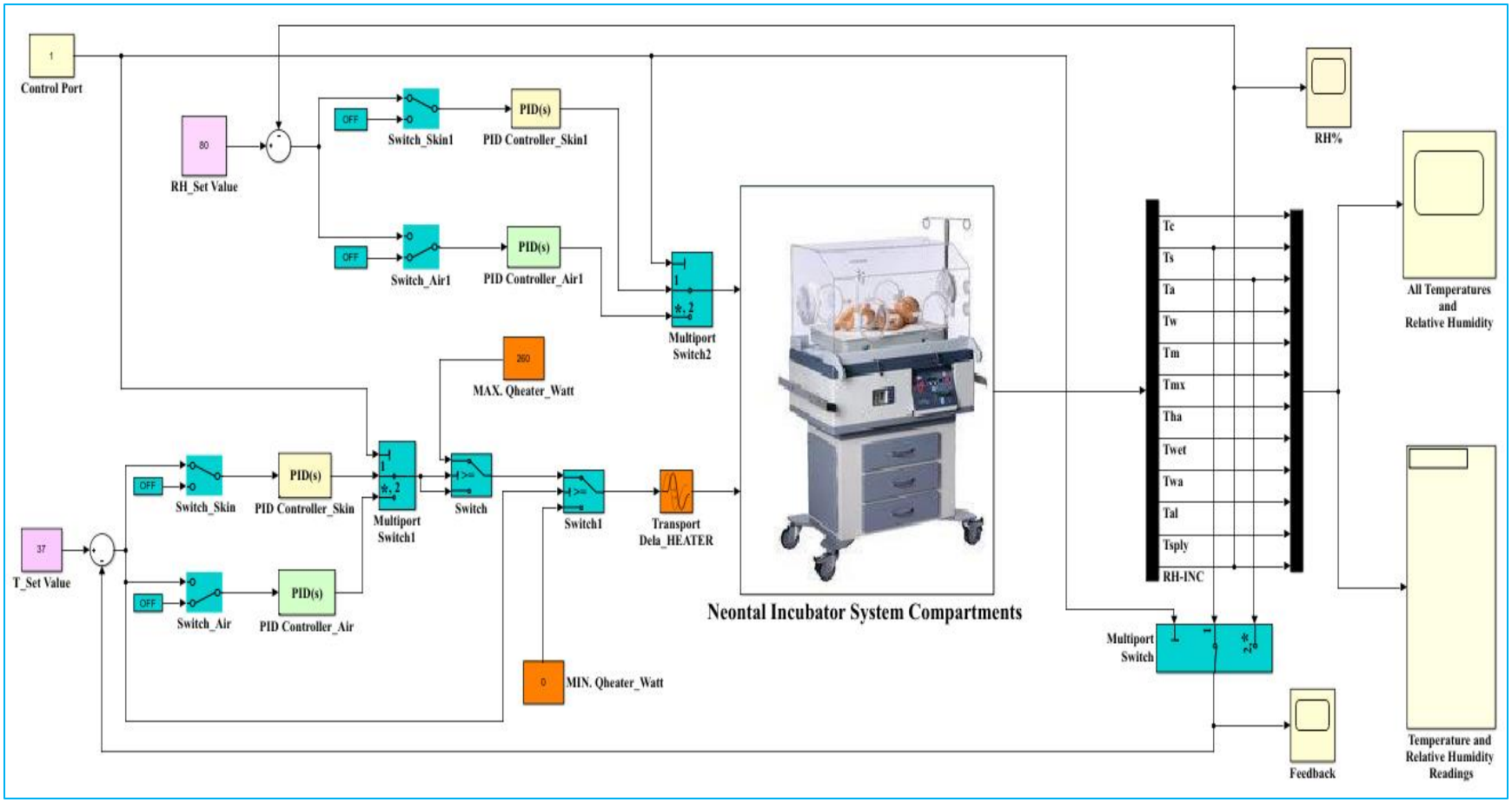

Figure 4. 2 Overall simulation model

4.2 Components of the Neonatal Incubator System

The neonatal incubator system has 12 components. These components are divided into two parts. These are neonate parts and incubator parts, as illustrated in Table 4.1.

Table 4. 1 Overall System Components

Components of Neonate and Incubator	
Neonate Parts	**Incubator Parts**
1. Skin Layer, and 2. Core Layer.	1. Mattress, 2. Heater, 3. Walls, 4. Blowing Fan, 5. Air Space inside the Incubator, 6. Air Space (above Water Surface), 7. Heat Sink (Aluminum), 8. Supplied Air Temperature, 9. Water Surface, and 10. Relative Humidity.

Figure 4.3 illustrates the comprehensive Simulink model for the system component. A Simulink model constructed for every component indicated in Table 4.1 separately.

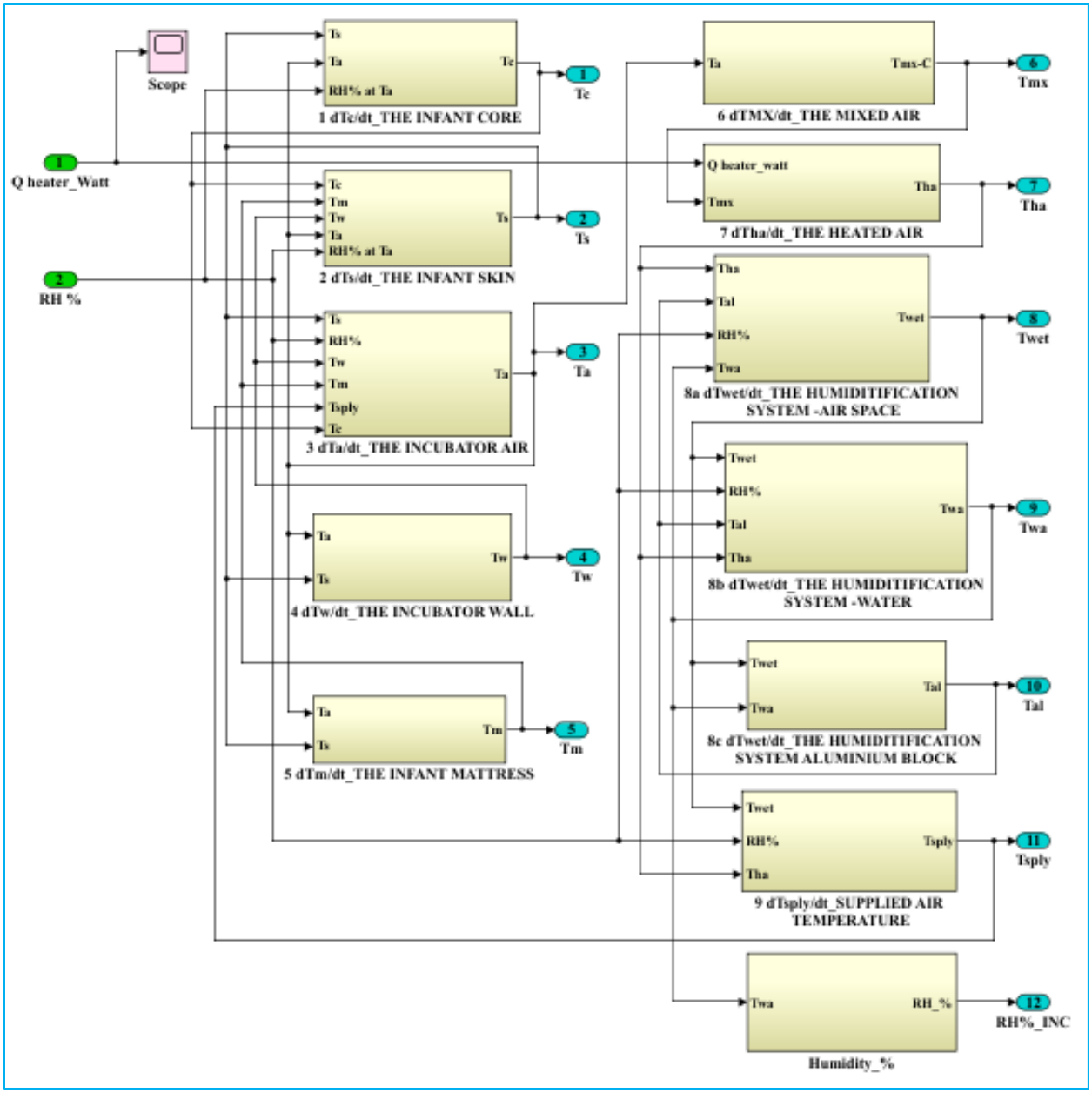

Figure 4. 3 Overall system components

4.2.1 Components of Neonate Core

The transfer of heat in the component of core over time is depicted by each of the subsystems in this figure and is stated in equation (3.3). Each sub-system will receive its own Simulink model. Figure 4.4 depicts the Simulink model for this component.

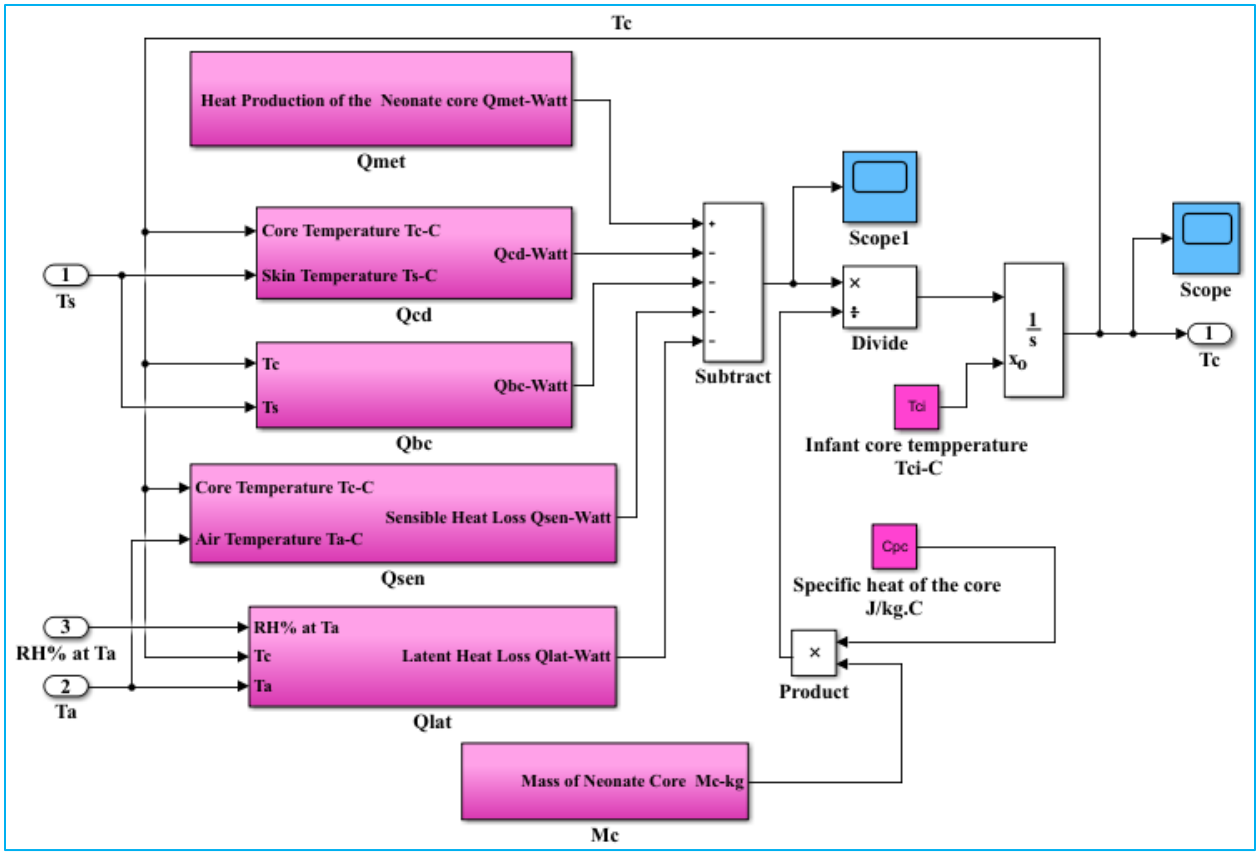

Figure 4. 4 Components of neonate core

4.2.1.1 Neonate Core Heat Production

Figure 4.5 shows the Simulink model for the neonate core heat production that was represented in equation (3.5).

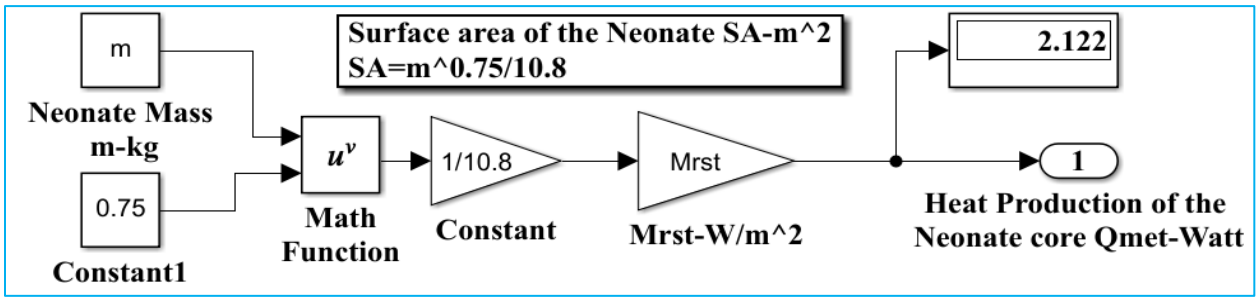

Figure 4. 5 Neonate core heat production

4.2.1.2 Conduction between Core and Skin

The Simulink model that represents the heat transferred by conduction between core and skin is depicted in Figure 4.6. The Simulink model is derived from the mathematical formula that is stated in equation (3.14).

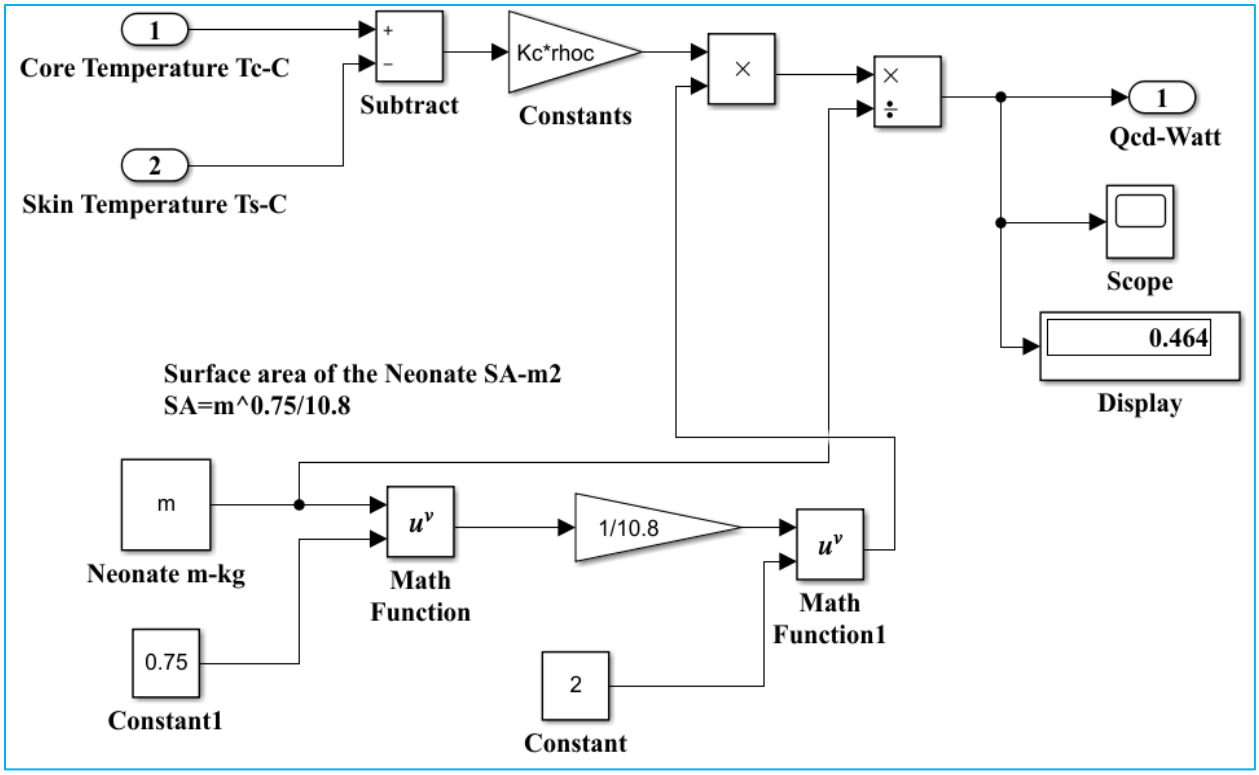

Figure 4. 6 Conduction between core and skin

4.2.1.3 Convection between Core and Skin

The convection transfer of heat between core and skin layer through the blood is shown in Figure 4.7 and is stated in equation (3.15).

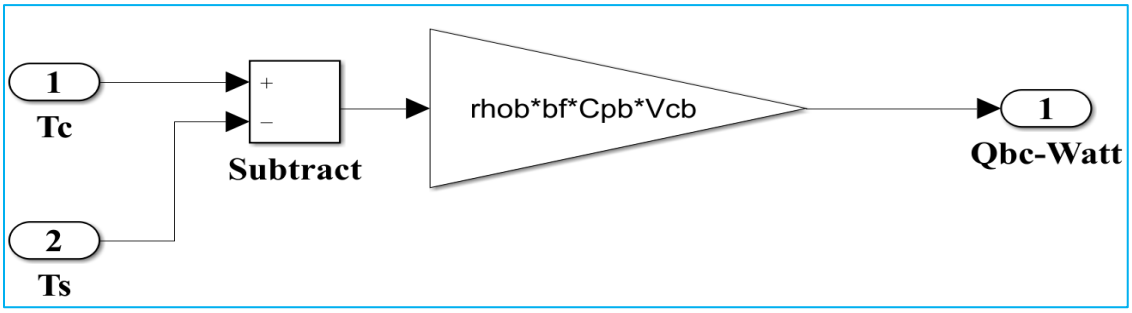

Figure 4. 7 Convection between core and skin

4.2.1.4 Sensible Loss of Heat

Equation (3.8), which describes the temperature differential between the inhaled and exhaled air, is used to model the rate of sensible loss of heat shown in Figure 4.8.

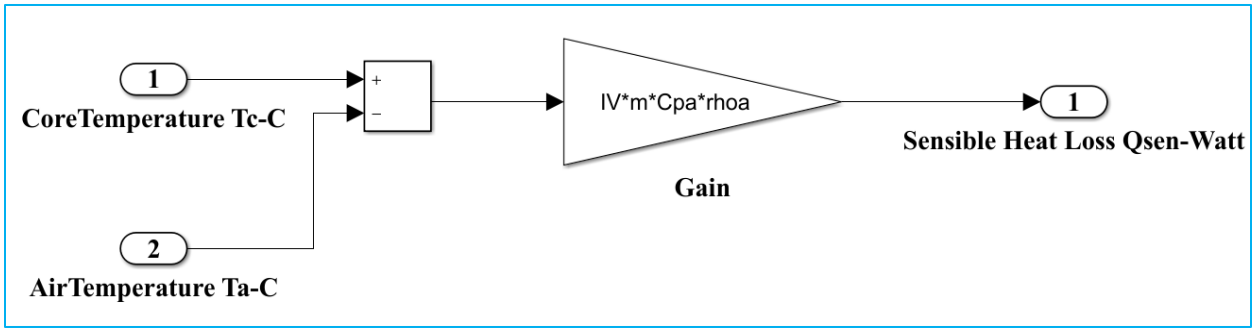

Figure 4. 8 Sensible loss of heat

4.2.1.5 Latent Loss of Heat

Figure 4.9 shows the Simulink model for this particular subsystem.

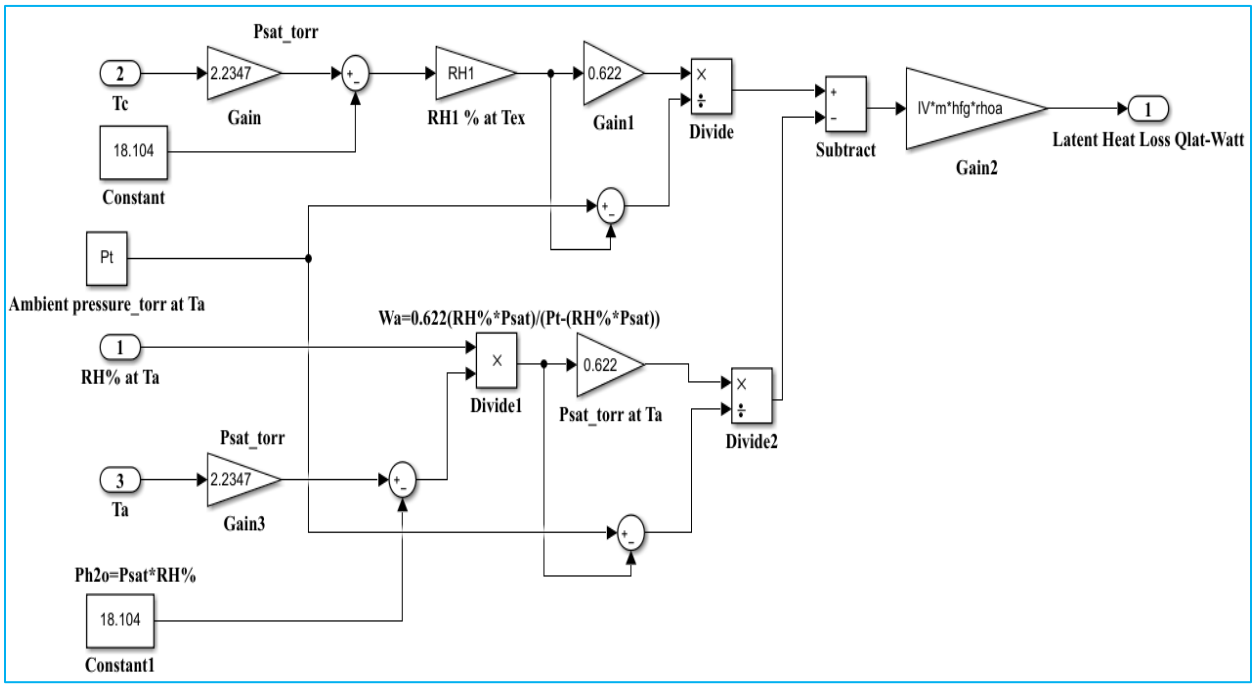

Figure 4. 9 Latent loss of heat

4.2.1.6 Neonate Core Mass

Equation (3.18), which describes the neonate core mass, is used to model the neonate core mass shown in Figure 4.10.

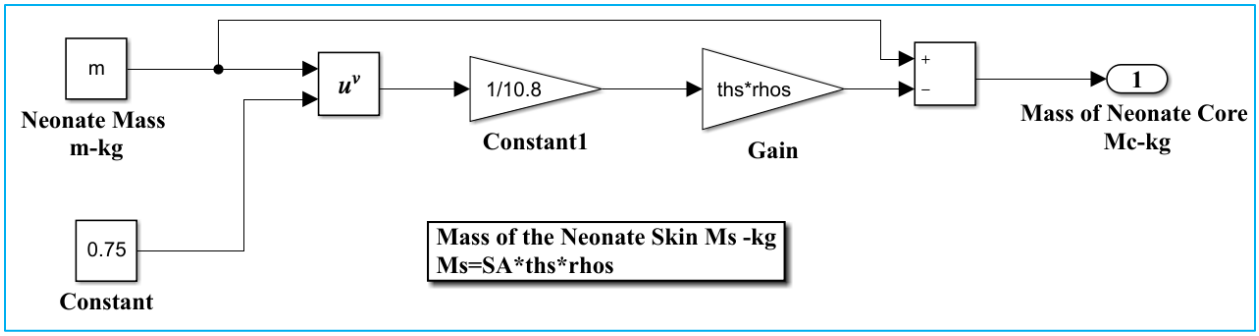

Figure 4. 10 Neonate core mass

4.2.2 Components of Neonate Skin

Equation (3.22) shows the variation of skin temperature over time and is represented by a Simulink model that has been created. An illustration of the Simulink model of the neonate core components is shown in Figure 4.11.

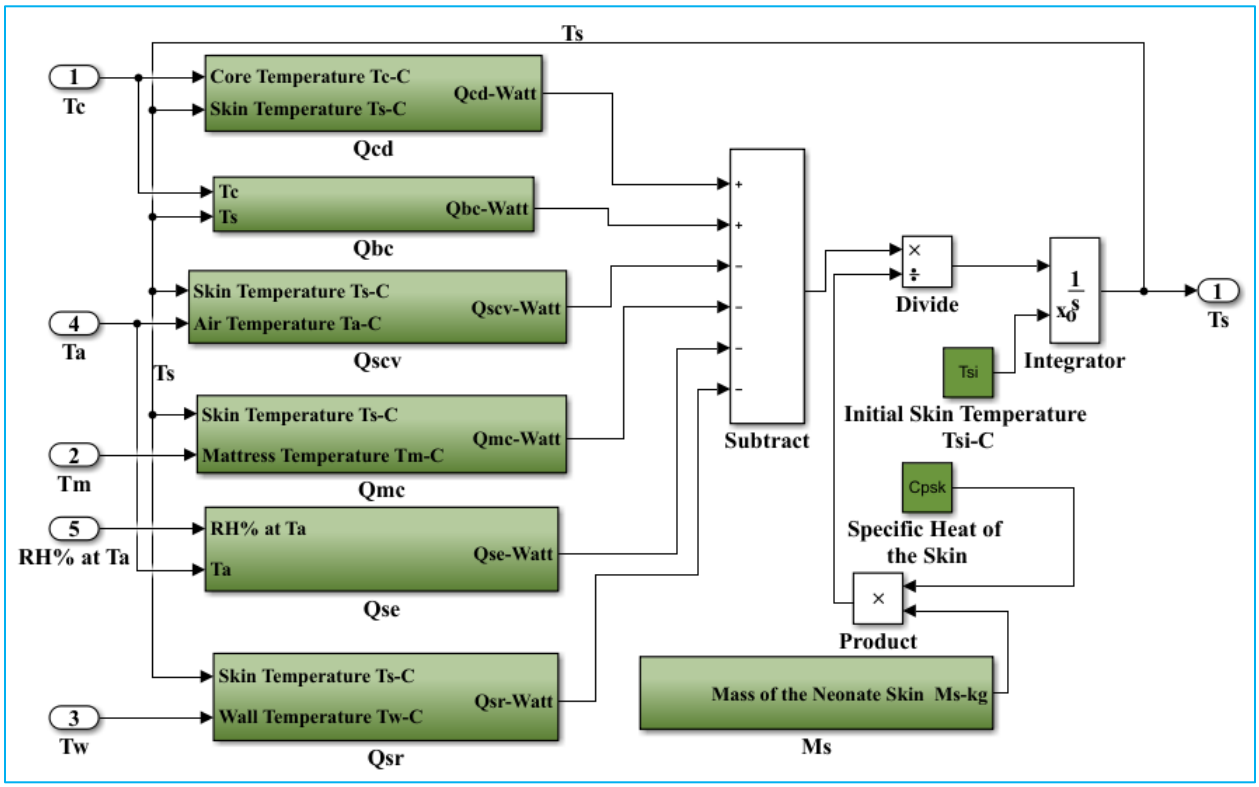

Figure 4. 11 Components of neonate skin

4.2.2.1 Convection between Skin and Air Space

As stated in equation (3.26), the transfer of heat by convection between the air space and skin inside the incubator is modelled using MATLAB/Simulink as shown in Figure 4.12.

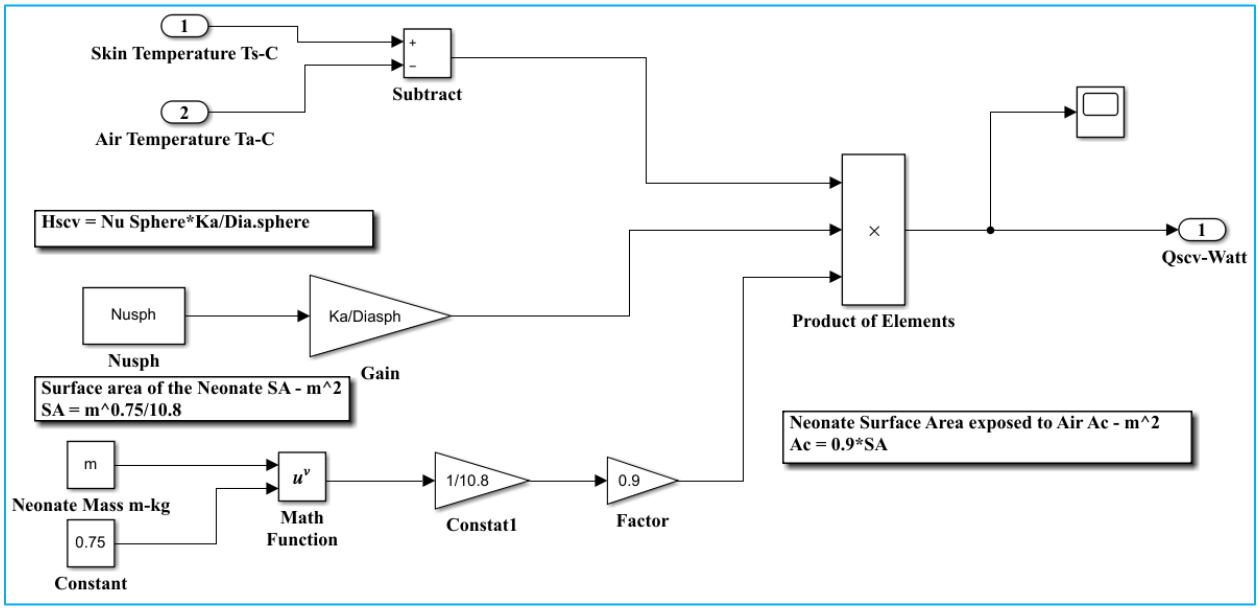

Figure 4. 12 Convection between skin and air space

4.2.2.2 Conduction between Skin and Mattress

The Simulink model of conduction between skin and mattress is illustrated in Figure 4.13 and discussed in equation (3.24).

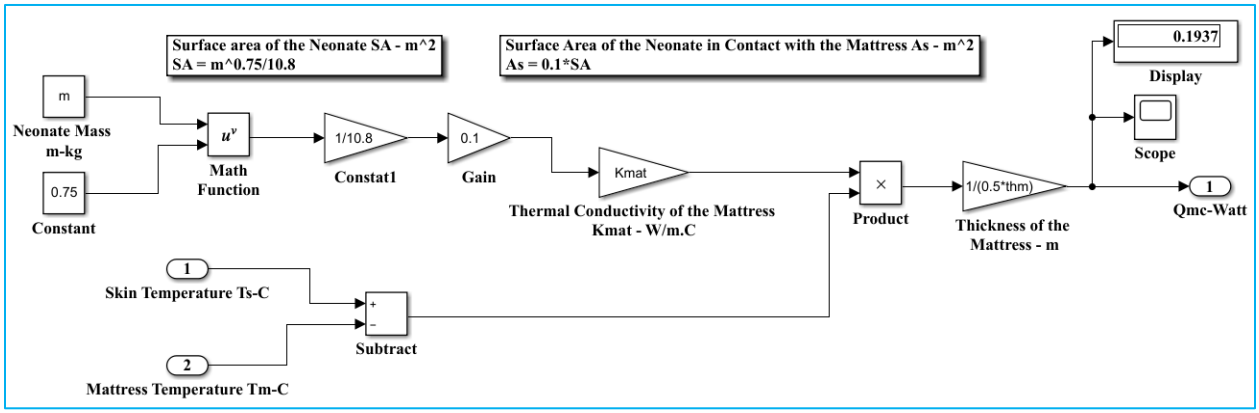

Figure 4. 13 Conduction between skin and mattress

4.2.2.3 Skin Evaporative Loss

The Simulink model of skin evaporative loss is shown in Figure 4.14. It appears in equation (3.32). Figure 4.30 illustrates that the other parameters are also taken from equation (3.33).

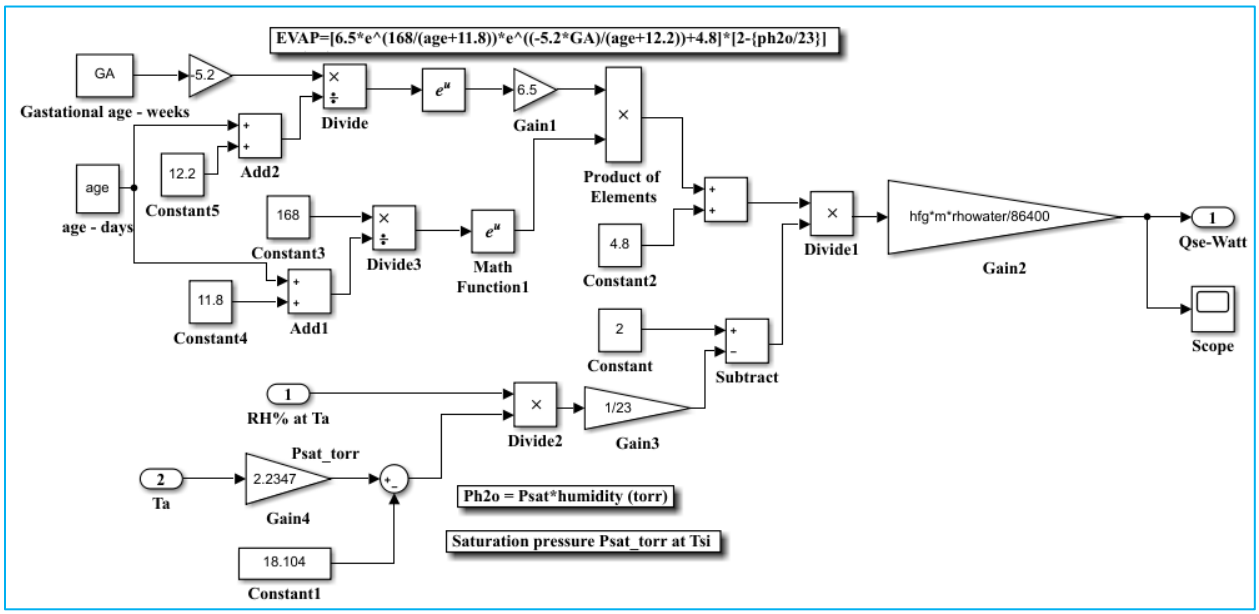

Figure 4. 14 Skin evaporative loss

4.2.2.4 Radiation between Skin and Wall

In Figure 4.15, the radiant transfer of heat between the skin of the neonate and the incubator wall is simulated in accordance with equation (3.34). Note that of the total skin surface area, 5.5% is exposed to the air and is normally in contact with the walls of the incubator.

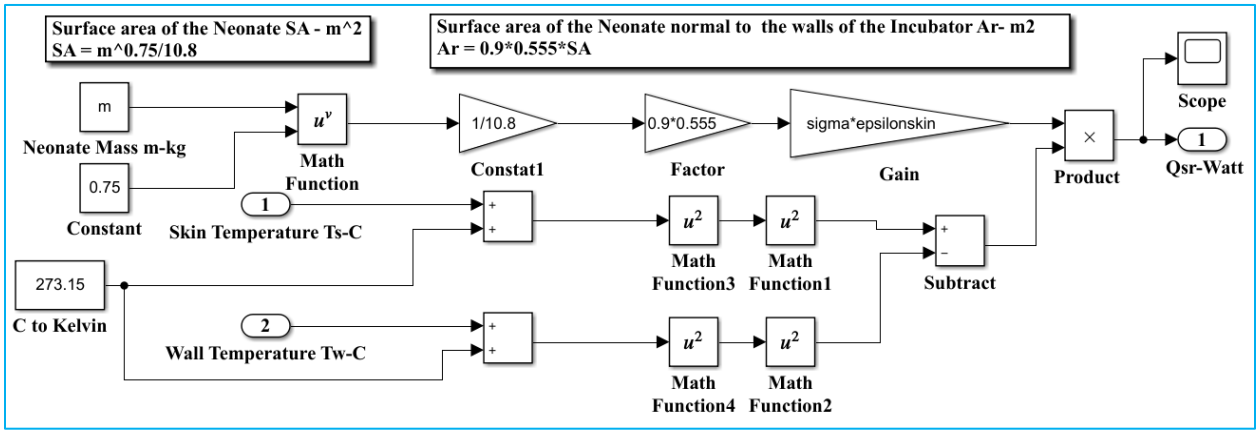

Figure 4. 15 Radiation between skin and wall

4.2.2.5 Neonate Skin Mass

The Simulink model of the neonate skin mass shown in Figure 4.16 corresponds to equation (3.19). The neonate's skin thickness, density, and total surface area are used to calculate the skin mass.

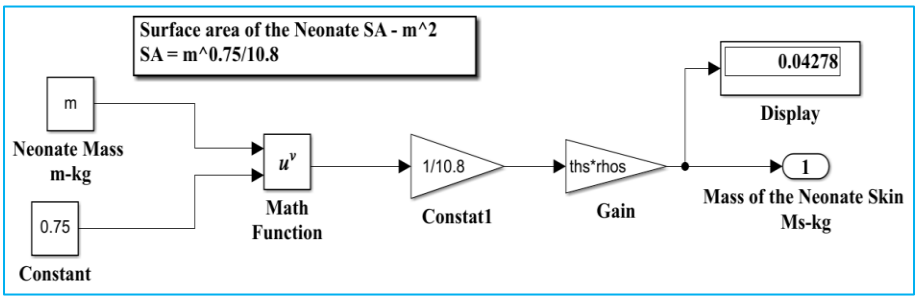

Figure 4. 16 Neonate skin mass

4.2.3 Components of Incubator Air Space

Figure 4.17 shows the Simulink model for these components. As stated in equation (3.38), it indicates the varying temperature of the incubator's air space through time.

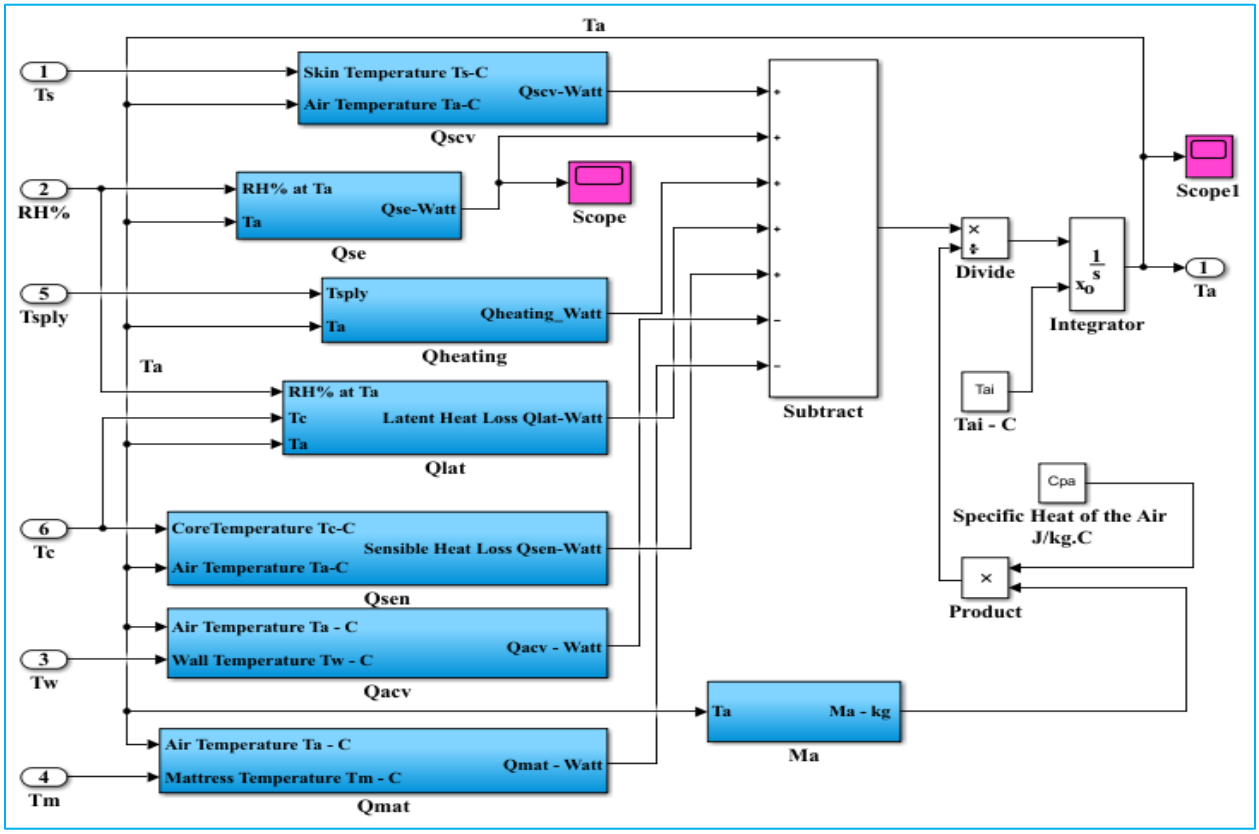

Figure 4. 17 Components of incubator air space

4.2.3.1 Supply of Heat Energy

Figure 4.18 depicts the Simulink model that shows the amount of thermal energy delivered inside the incubator. In which heat transfers between the neonate, the walls of the incubator, and the surrounding air in accordance with equation (3.106).

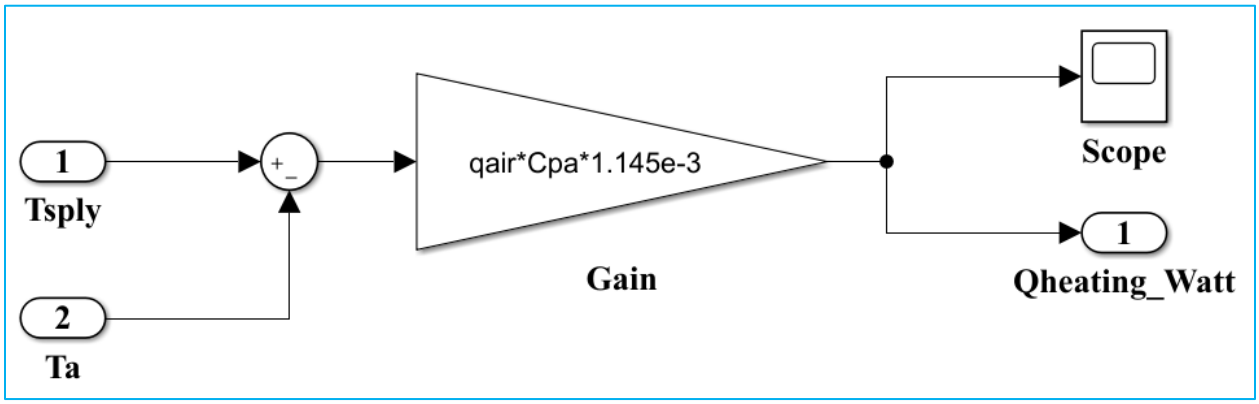

Figure 4. 18 Supply of heat energy

4.2.3.2 Convection between the Air and the Incubator Wall

Figure 4.19 illustrates this sub-system. According to equation (3.39), there is a convective transfer of heat that occurs between the air space and the incubator wall. Because of circulated-air fan, the air flow pattern is forced convection.

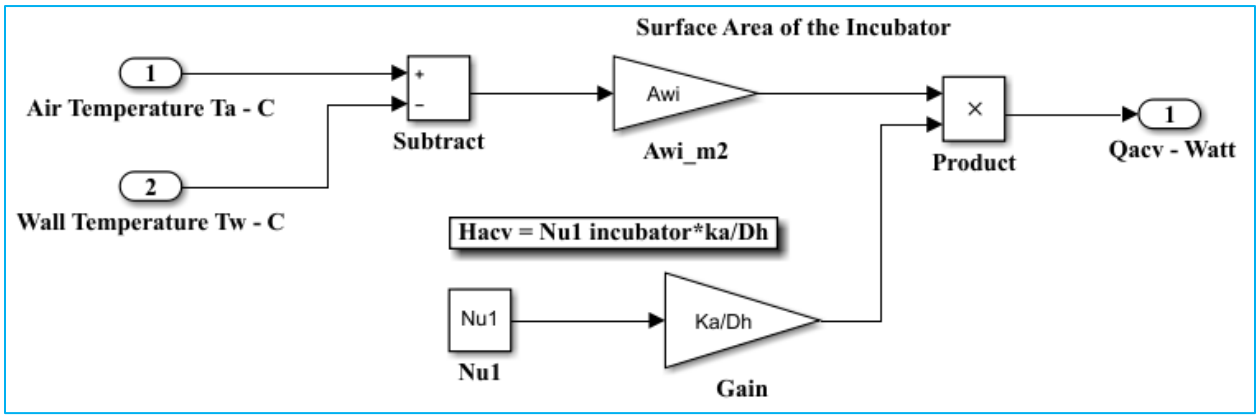

Figure 4. 19 Convection between the air and incubator wall

4.2.3.3 Convection between the Air and the Mattress

Figure 4.20 depicts the convective heat transfer between the air space and the mattress due to their different temperatures, as shown in equation (3.43). About 10% of the neonate's skin is contacted by the mattress, and 90% is exposed to the air. The mattress total area is approximately 0.21 m2.

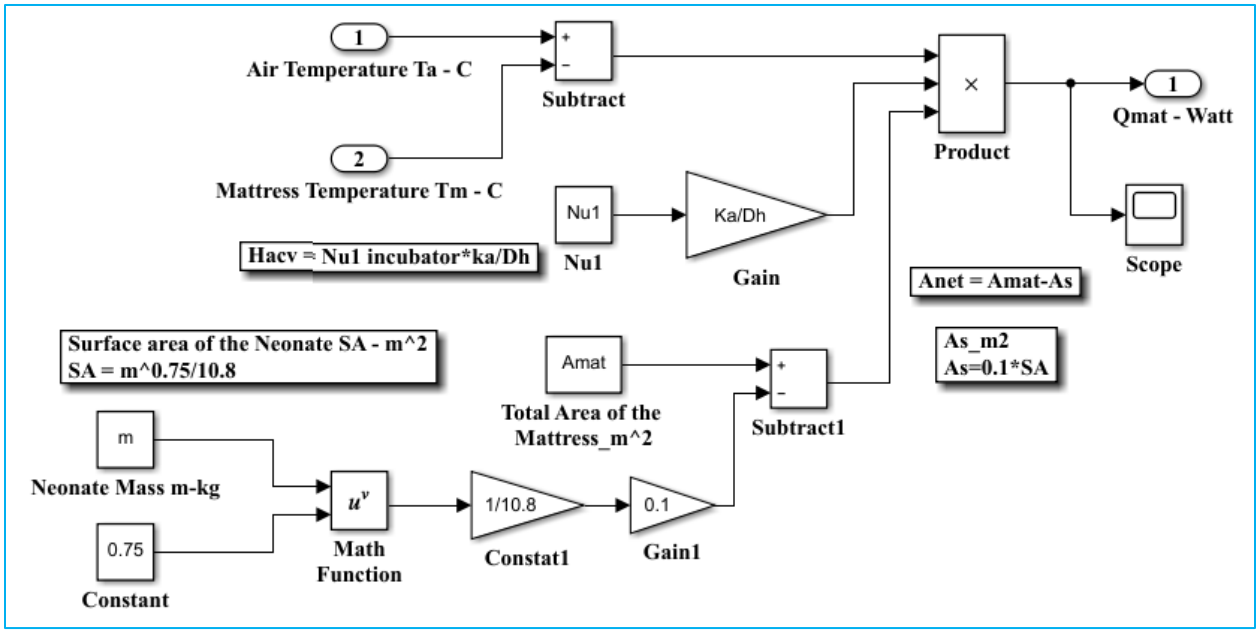

Figure 4. 20 Convection by air and mattress interaction

4.2.3.4 Incubator Air Space Mass

Figure 4.21, which depicts in equation (3.73), provides an illustration of the Simulink model for this subsystem. The mass of the incubator air changes depending on the N_2 and O_2 concentrations and the internal air temperature (also known as the return air temperature).

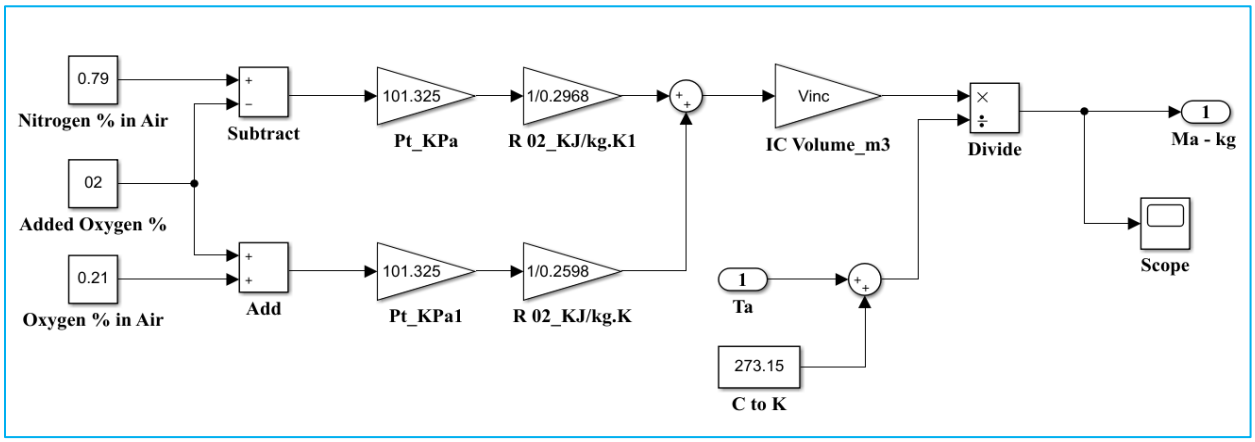

Figure 4. 21 Incubator air space mass

4.2.4 Components of Incubator Wall

Figure 4.22 shows the Simulink model for these components. Equation (3.47) depicts the temperature change of the walls through time. The components of the incubator wall represent the

radiation, forced convection, and free convection interactions between the neonate's skin and the incubator's interior walls as well as the external walls with regard to the surrounding space.

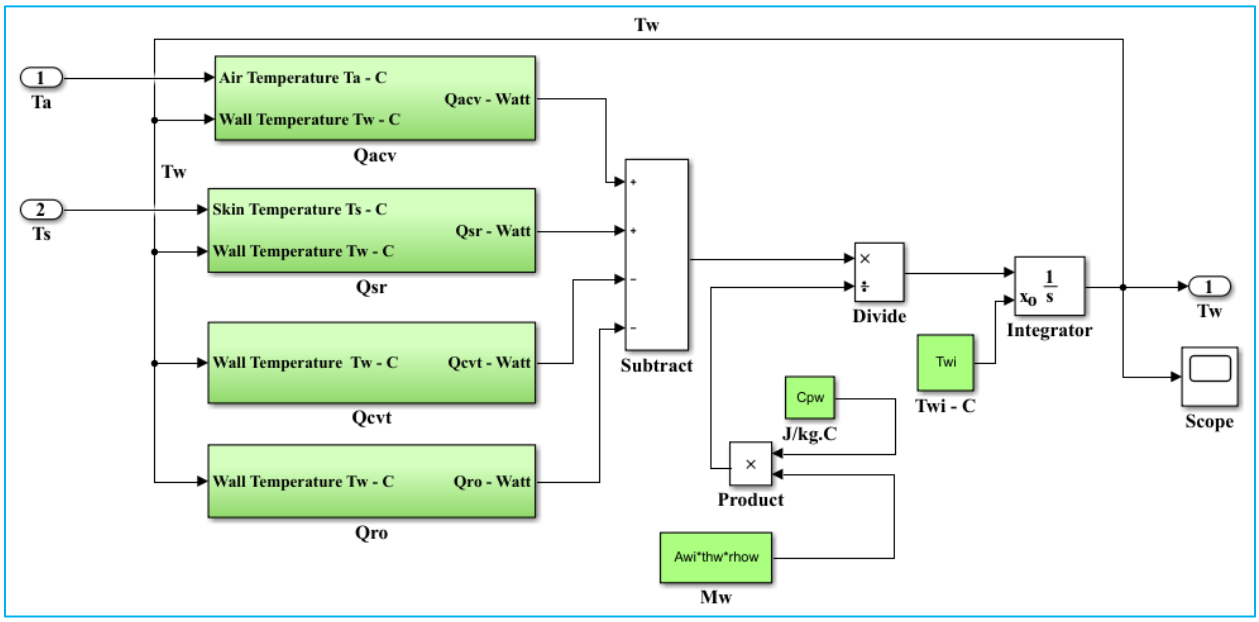

Figure 4. 22 Components of incubator wall

4.2.4.1 Free Convection between Walls and the Environment of the Room

Figure 4.23 depicts the Simulink model for the heat exchange due to free convection that takes place between the walls and the room environment. This subsystem consists of two long side surfaces and two short side surfaces, which together make up three internal subsystems of the free convection. The Simulink models for these three internal free convection subsystems are described in the next sections.

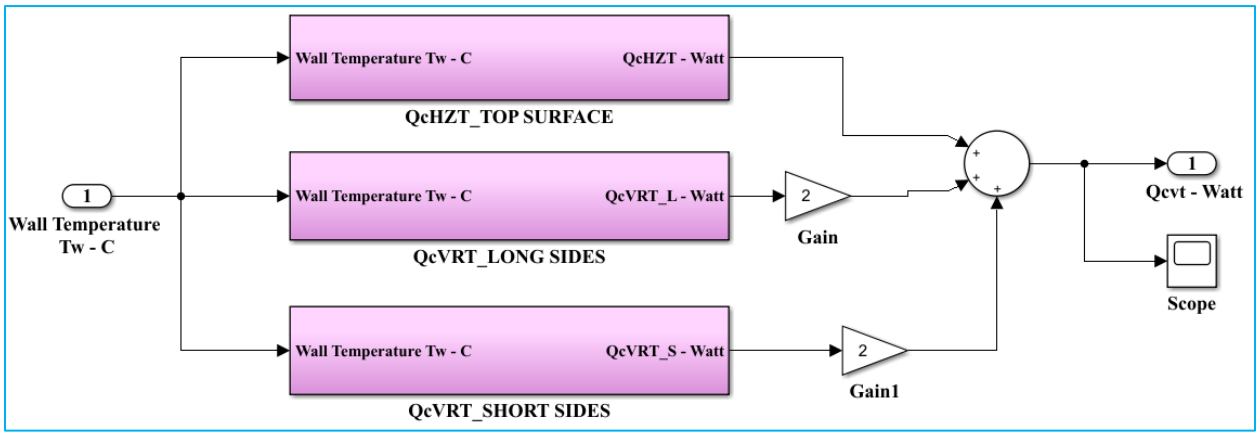

Figure 4. 23 Free convection between walls and the environment of the room

4.2.4.1.1 Free Convection of Hood Horizontal Surface

Figure 4.24 shows the Simulink model for this subsystem. It details how equation (3.52) is applied. The horizontal surface of the incubator hood is the defined and associated reference point for all parameters shown.

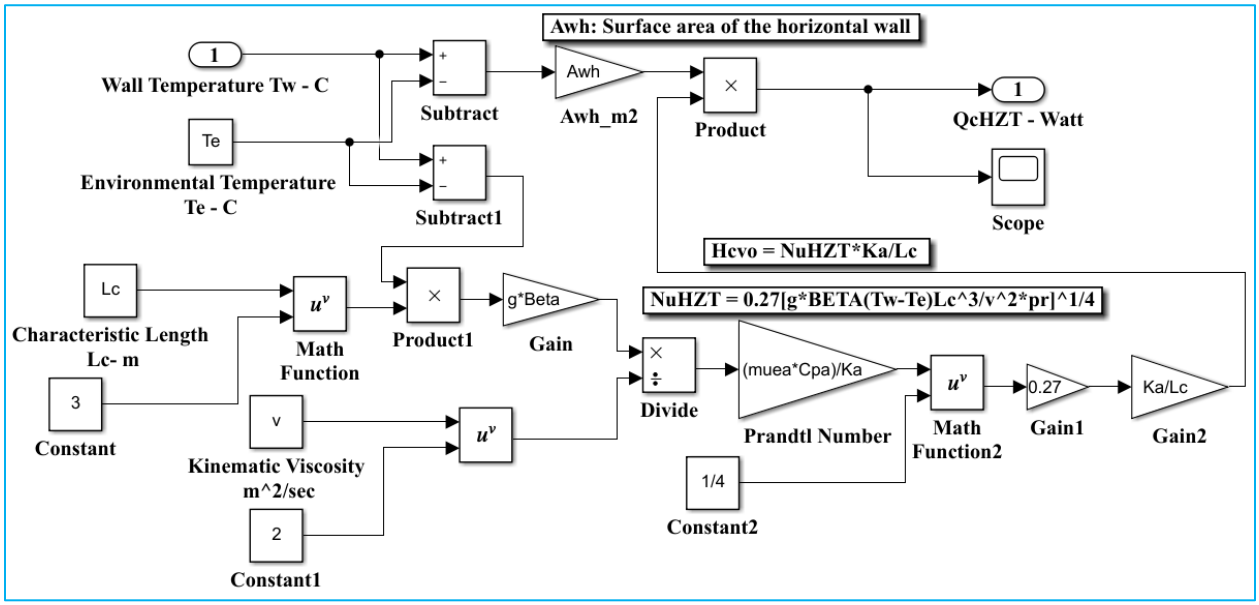

Figure 4. 24 Free convection of hood horizontal surface

4.2.4.1.2 Free Convection of Hood Vertical Surfaces

Figures 4.25 and 4.26 depict the simulation of free conviction of hood vertical surfaces for the long side and short sides, respectively. The only difference between the parameters depicted in these two pictures is the surface area assigned to each side.

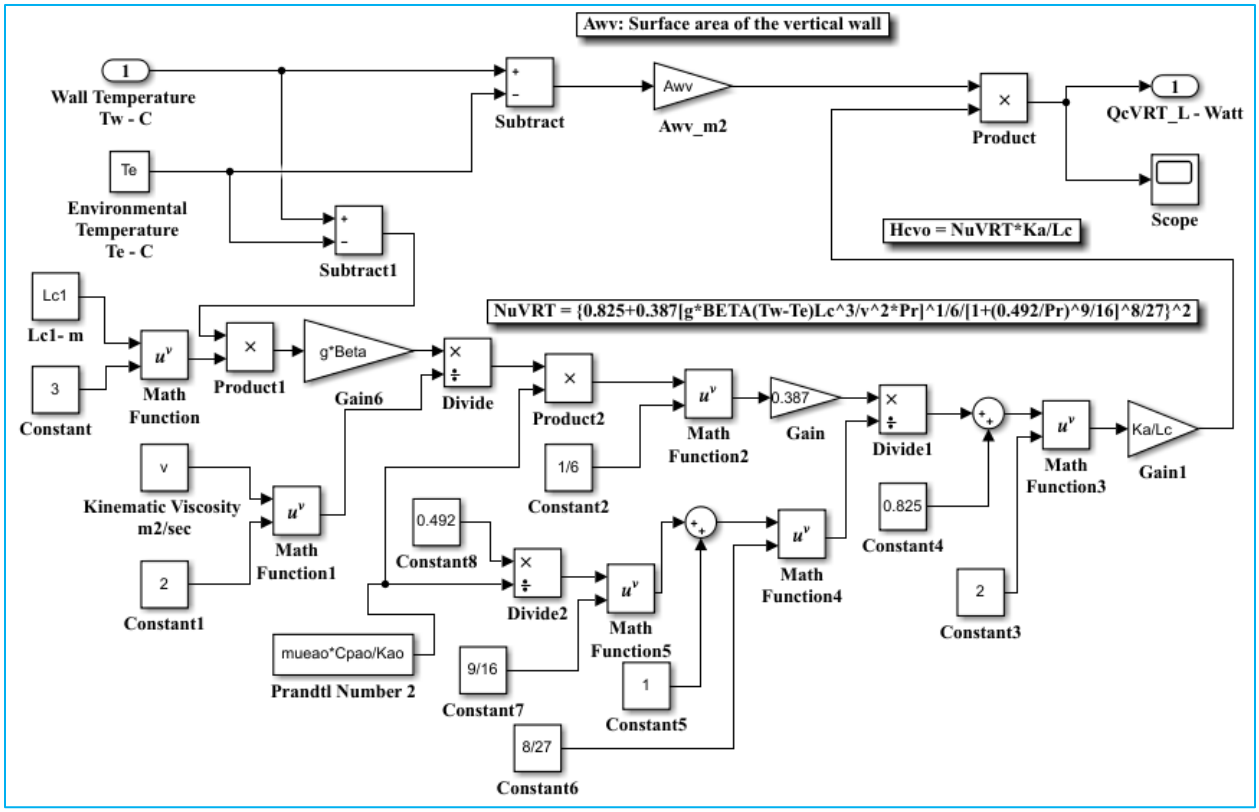

Figure 4. 25 Free convection of hood vertical surfaces (long side)

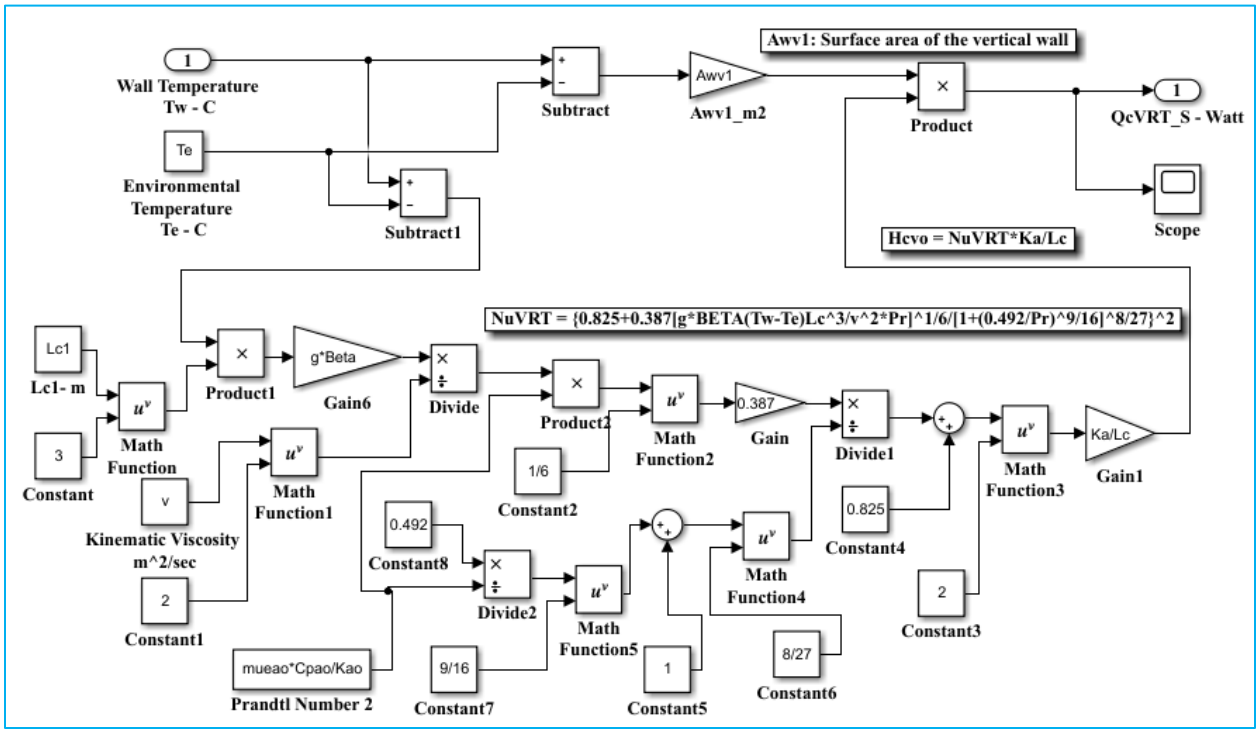

Figure 4. 26 Free convection of hood vertical surfaces (short side)

4.2.4.2 Radiation from the Incubator Walls into Room Environment

In Figure 4.27, which depicts equation (3.57), the Simulink model for the radiation of the incubator wall in the room environment is shown.

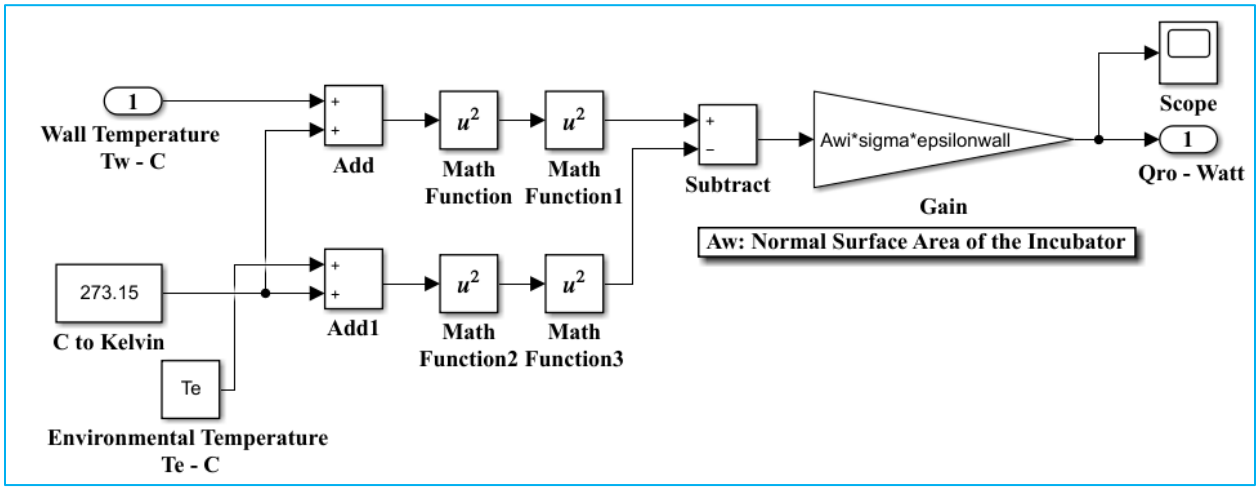

Figure 4. 27 Radiation from the incubator walls into room environment

4.2.5 Components of Incubator Mattress

Equation (3.60) is illustrated by the Simulink model of these components in Figure 4.28. These subsystems consist of the convection by wall and environmental interactions and the conduction by skin and mattress interactions.

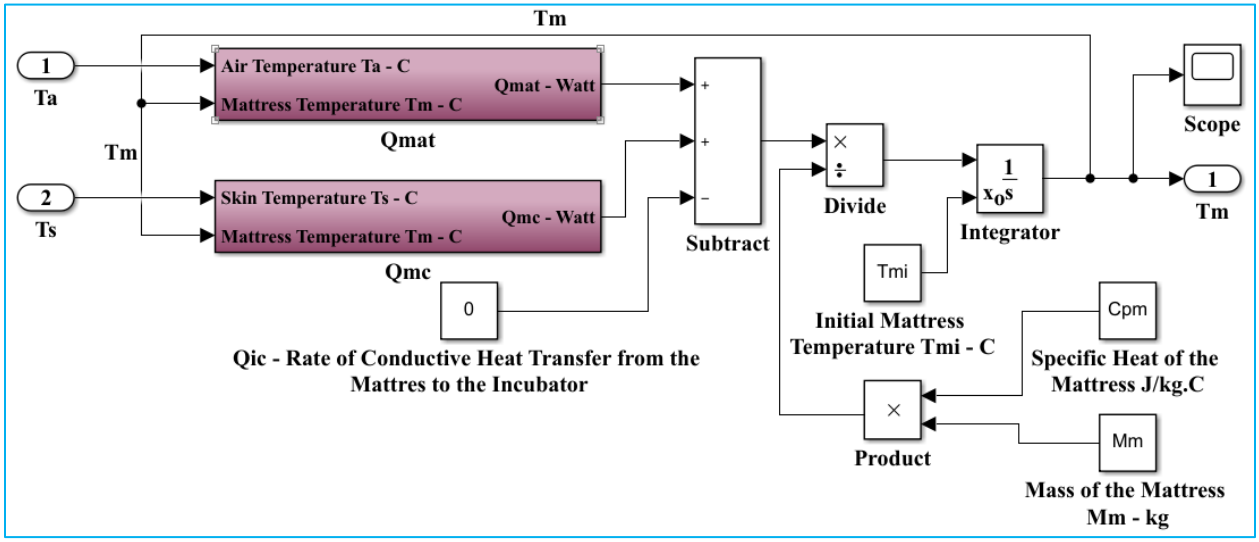

Figure 4. 28 Components of incubator mattress

4.2.6 Circulated-Air Fan Component

Figure 4.29 shows the Simulink model of the components of a circulating fan. According to equation (3.63), it represents the temperature of the mixed air.

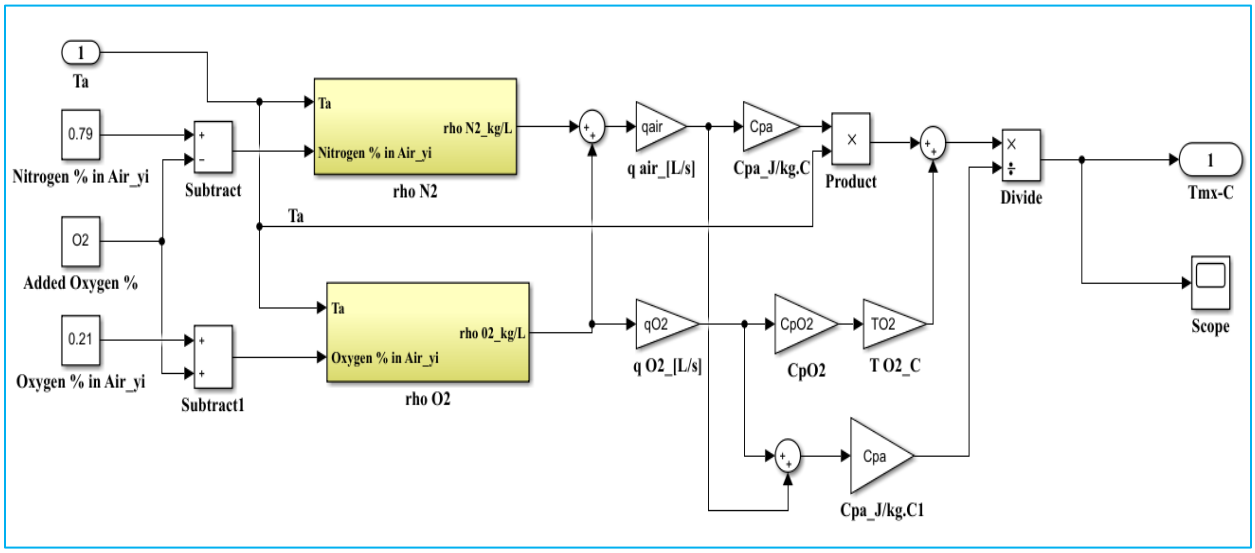

Figure 4. 29 Circulated-air fan component

4.2.6.1 Density of Nitrogen

The Simulink model of how density changes in response to variations in incubator air temperature is shown in Figure 4.30. The density is the output and is expressed in kg/L. The particular equations (3.62) and (3.63) are applied to this Simulink model (3.67).

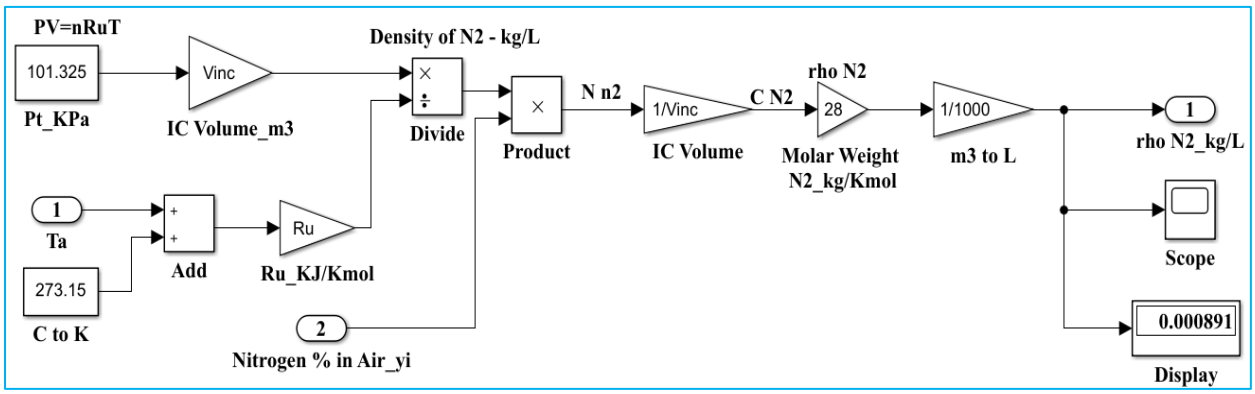

Figure 4. 30 Density of nitrogen

4.2.6.2 Density of Oxygen

Figure 4.31 shows the density of oxygen in the Simulink system model. This Simulink model is similar to Figure 4.30 except that the nitrogen density is replaced by oxygen density in this model.

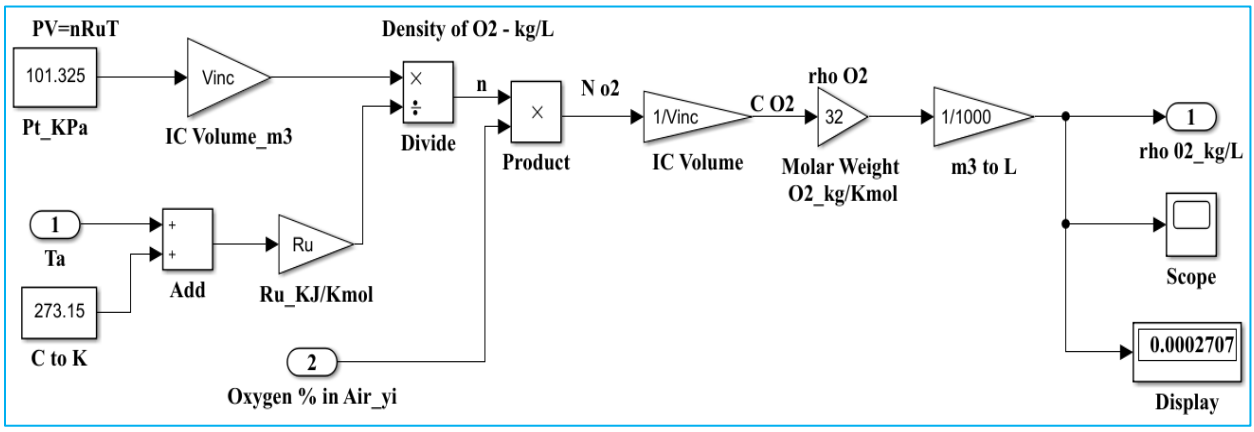

Figure 4. 31 Density of oxygen

4.2.7 Components of Heating Element

It is an equation (3.75). In this Simulink model, the density of the circulated air and the heated air temperature both depend on the mixed air, the amount of supplied oxygen, which alters the density of N_2 and O_2. Additionally, it modifies the heating element's power rating, which for this element ranges from 0-260 Watts.

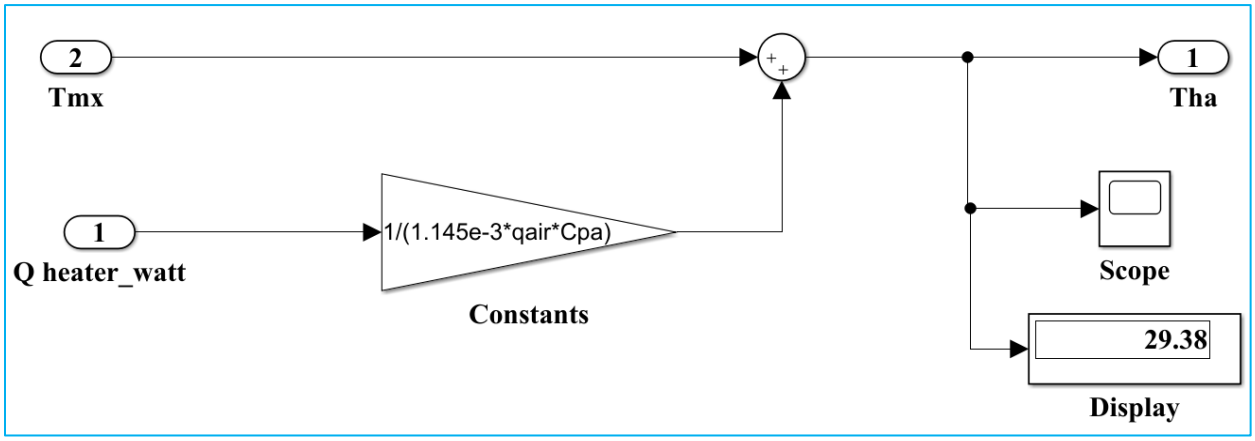

Figure 4. 32 Components of the heating element

4.2.8 Components of Humidification System

The water tank, which houses the humidification system, is made up of three components: an aluminium block, air in the tank, and water. In the sections that follow, a Simulink model is created for each of these components. These three components work in concert to produce the humidification process, which significantly affects the neonatal incubator's overall thermo-neutrality environment.

4.2.8.1 Air Space Components inside the Water Tank

Figure 38 illustrates the air space components inside the water tank, and they are represented by equation (3.78).

The temperature of heated air, aluminium, and water, and relative humidity, are the four external inputs fed from other system components.

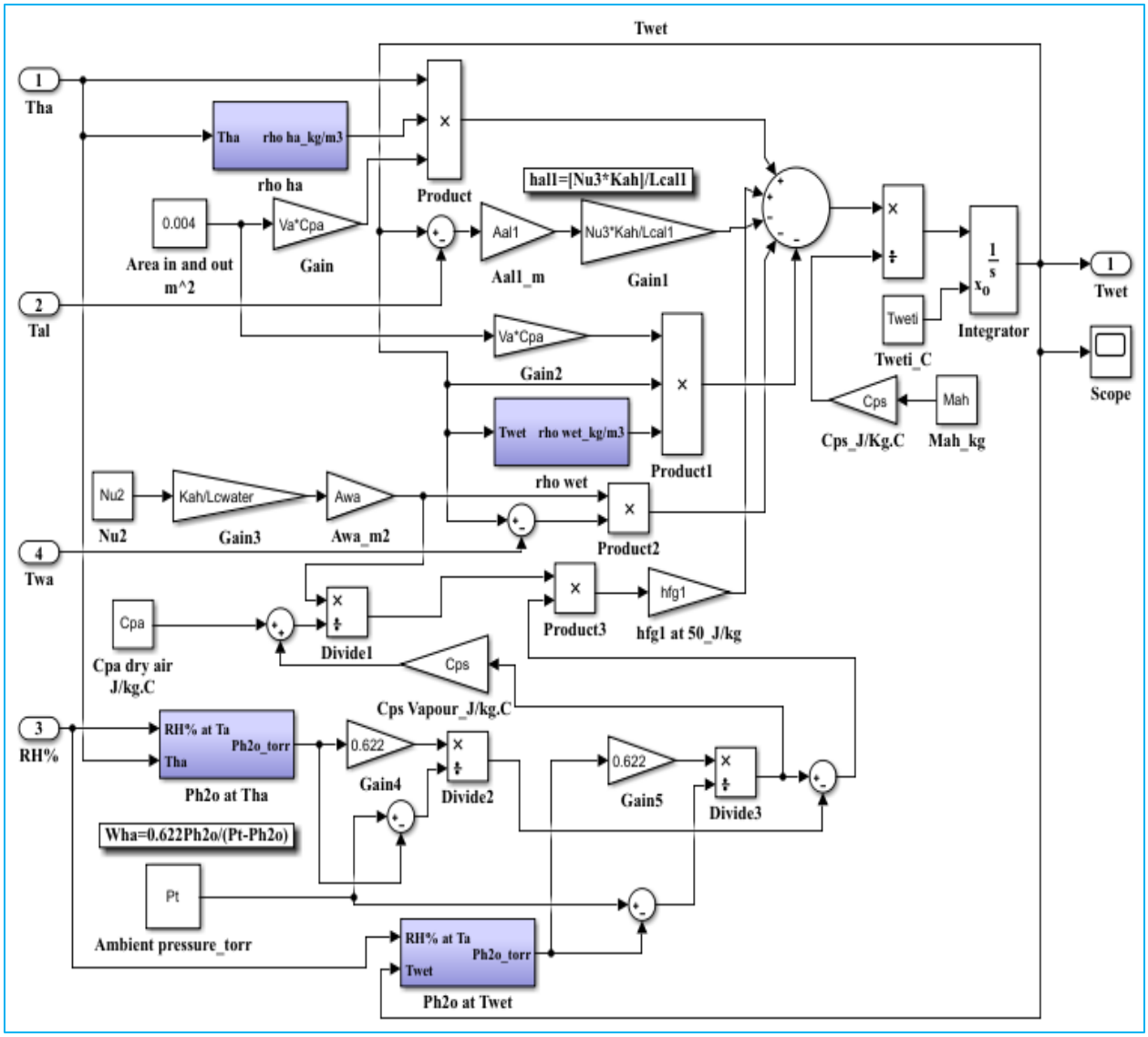

Figure 4. 33 Air space components inside the water tank

Figure 4.33 shows the air space components inside the water tank by considering the air density because of the temperature of wet and heated air.

Figure 4.34 represents the model for the heated air density, while Figure 4.35 represents the model for the density of wet air.

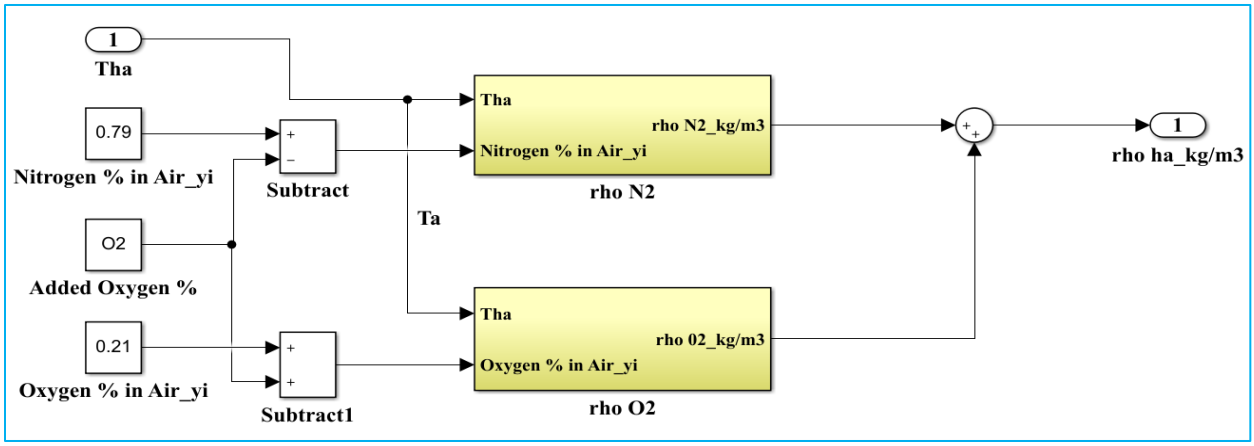

Figure 4. 34 Density of heated air

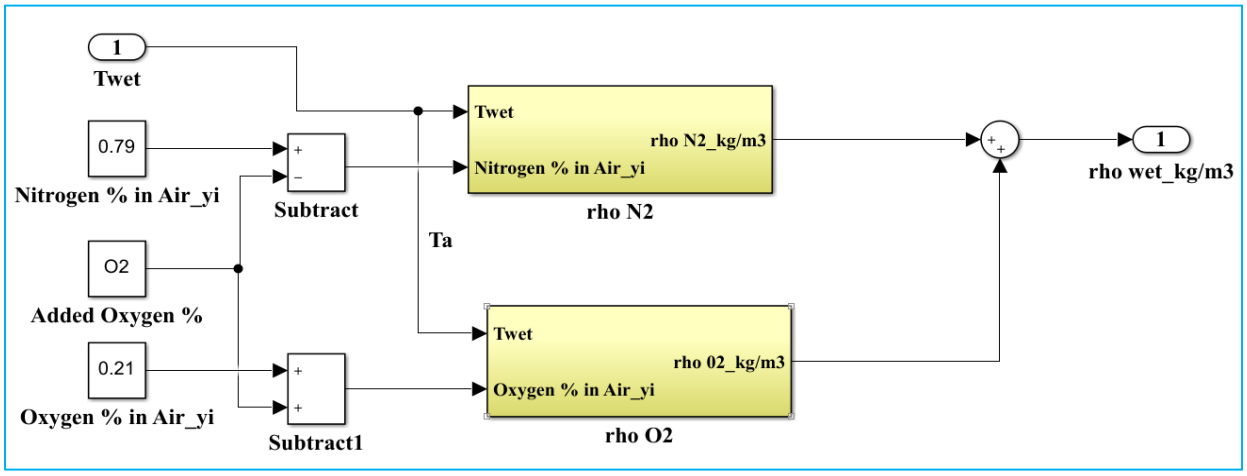

Figure 4. 35 Density of wet air

Figure 4.36 shows heated air water vapour partial pressure, while Figure 4.37 shows wetted air water vapour partial pressure.

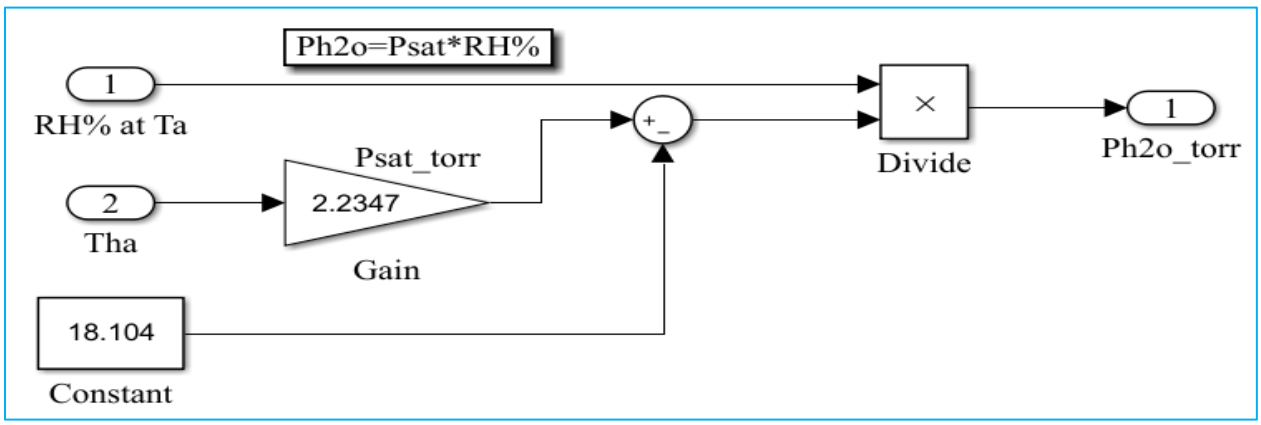

Figure 4. 36 Heated air water vapour partial pressure

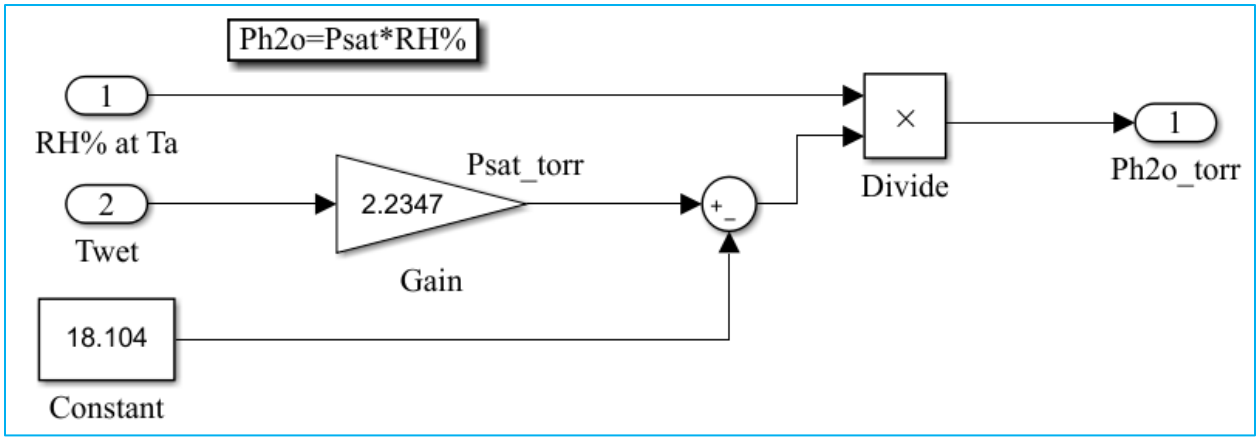

Figure 4. 37 Wetted air water vapour partial pressure

4.2.8.2 Water Mass Humidification Process

Figure 4.38 shows the water mass humidification process and represents in equation (3.91). The output water temperature (T_{wa}) represents how the temperature of the water mass has changed over time.

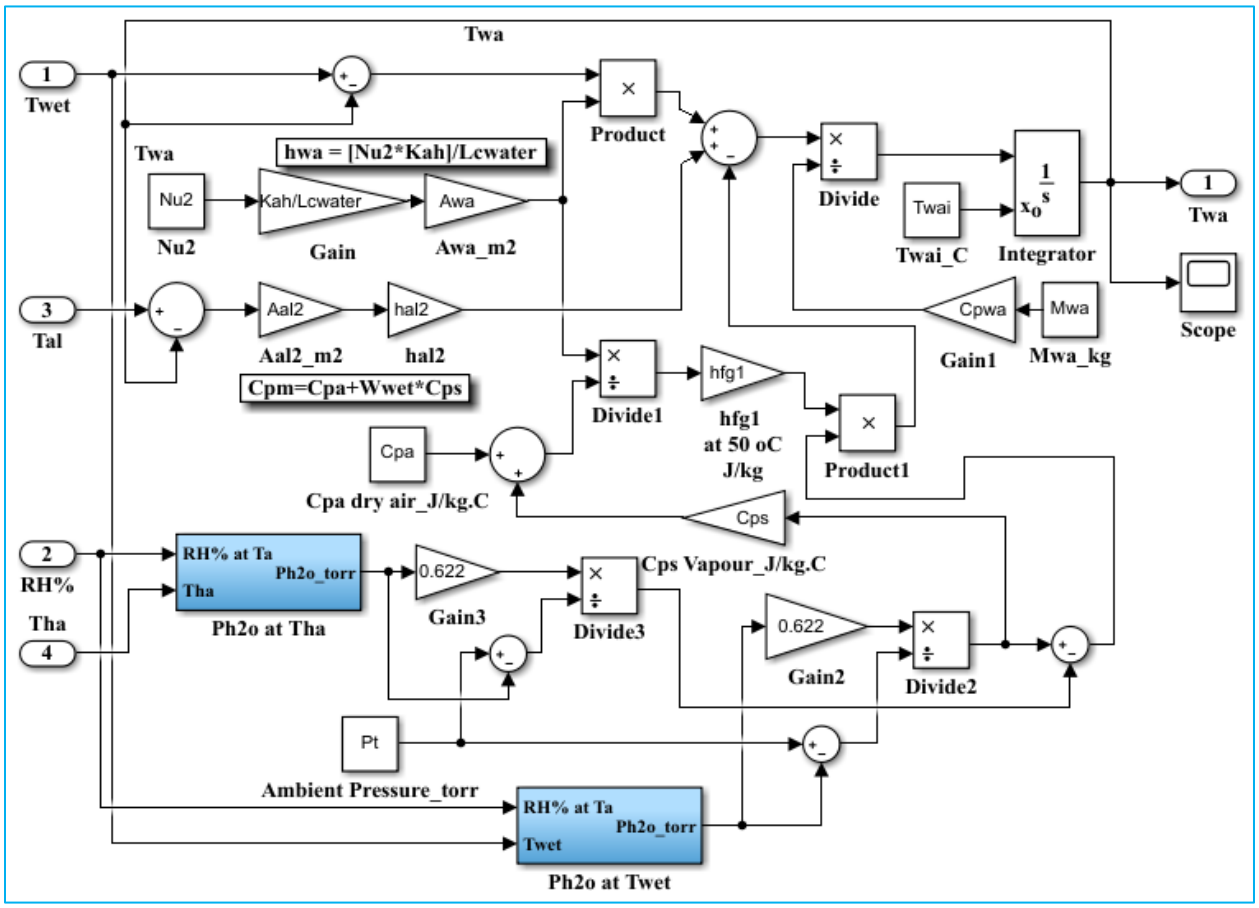

Figure 4. 38 Water mass humidification process

4.2.8.3 Aluminium Block Humidification Process

The components of the water tank are made of aluminium. This section features the Simulink model of the heat exchange, which is represented by equation (3.98), shown in Figure 4.39.

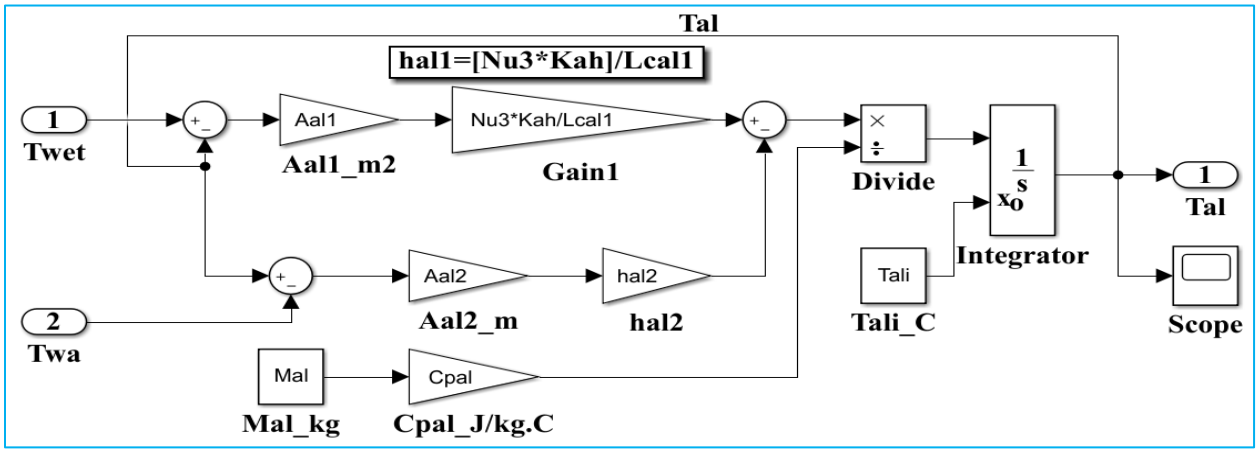

Figure 4. 39 Aluminium block humidification process

4.2.9 Components of Supplied Air Temperature

The supplied air temperature component consists of both wet and heated air temperature mixture interactions. Figure 4.40 shows how this is done and is stated in equation (3.102).

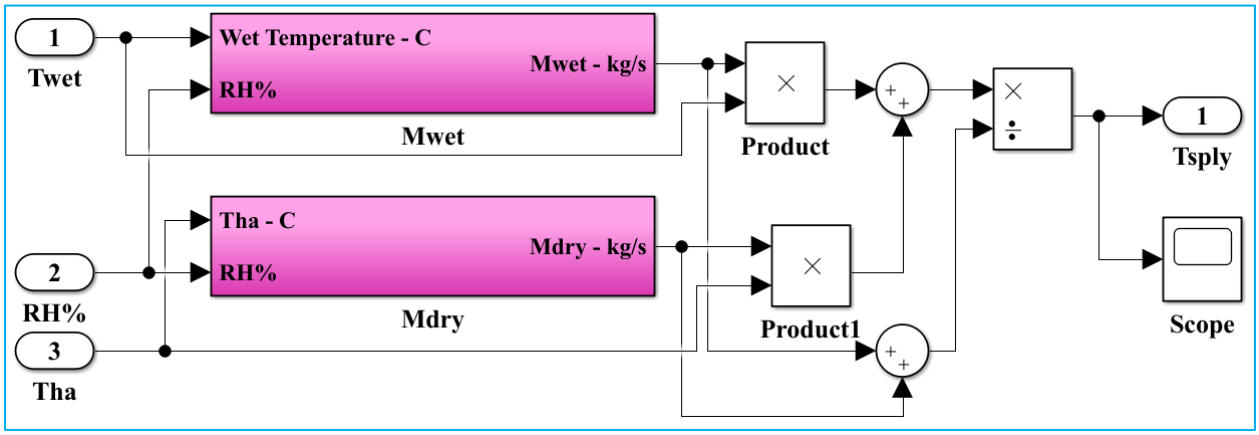

Figure 4. 40 Components of supplied air temperature

4.2.9.1 Mass-Flow Rate of Wet-Air

Figure 4.41 shows the Simulink model for the wet air mass flow rate. It is depicted in equations (3.99) and (3.103).

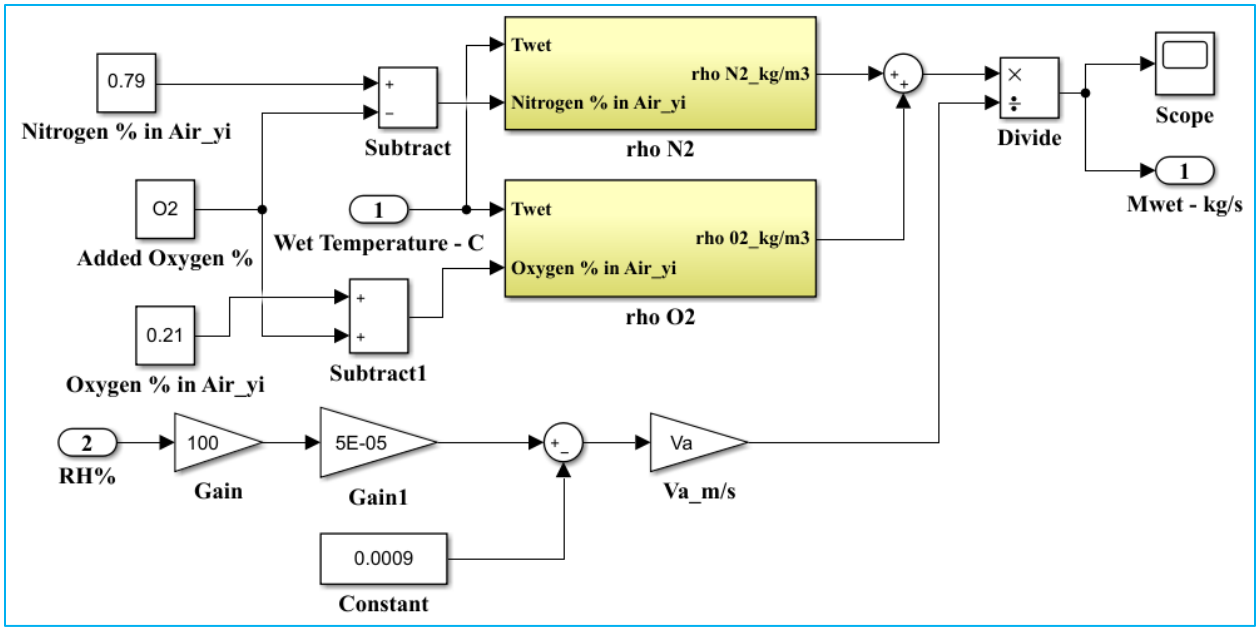

Figure 4. 41 Mass flow rate of wet air

4.2.9.2 Mass Flow Rate of Dry Air

Figure 4.42 shows the Simulink model for mass-flow rate of the dry-air which was stated in equations (3.100) and (3.104).

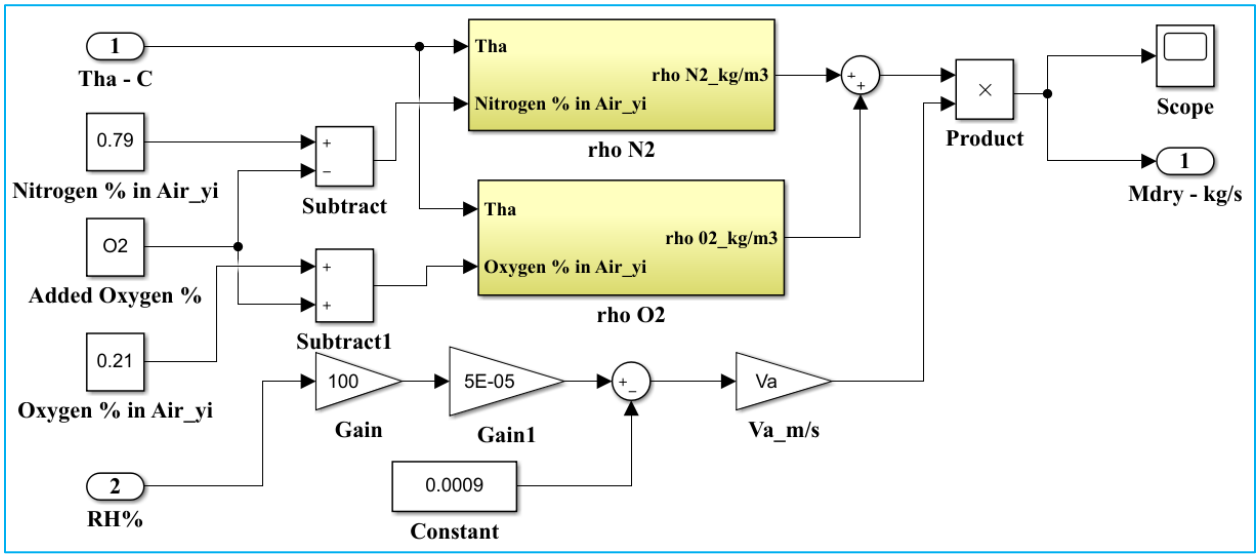

Figure 4. 42 Mass flow rate of dry air

4.2.10 Incubator Relative Humidity

Figure 4.43 shows the approximated relative humidity model for neonatal incubator. From equation (3.105), two commonly used measures of the quantity of moisture in the air are dewpoint

temperature and humidity. To make things simpler, it is assumed that the dew point temperature is 29.046 ^{o}C and that the temperature of air is similar to humidification temperature of water.

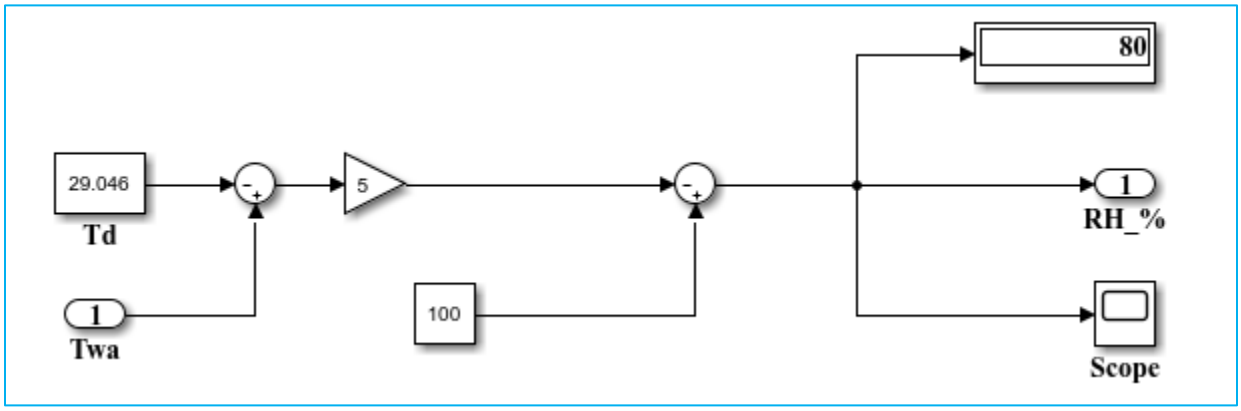

Figure 4. 43 Incubator relative humidity

4.3 Overall System Stability and Multivariable PID Controller Design

The overall system of the neonatal incubator Simulink model is represented in Figure 4.2. The system has both an air mode and a skin mode of operation. The multiport switches control the two modes. by putting in 1 for the skin mode and 2 for air mode operation. There is a heater that has a power range of 0 to 260 watts. Since the heating element has some time delay in real-world functioning, the transport delay of 0.2 second is included in the model.

The stability of the system is checked by applying a step input and observing the response of the system [46], [47]. MATLAB's *controlSystemDesigner* tool is used to verify the overall system stability [48]. Control The design of the controller settings and the analysis and tuning of the control systems are both possible with *controlSystemDesigner*. In this work, the heater power and the external relative humidity are the inputs to the system. The outputs are temperature and relative humidity.

4.3.1 Skin and Air Mode Operation of Neonatal Incubator

4.3.1.1 Checking the Stability of the System and Transfer Function

4.3.1.1.1 Skin Mode

Figure 4.44 shows the open loop system for skin mode. In this mode, the inputs are the external relative humidity and the power from the heater, and the outputs are the temperature of the skin and internal relative humidity.

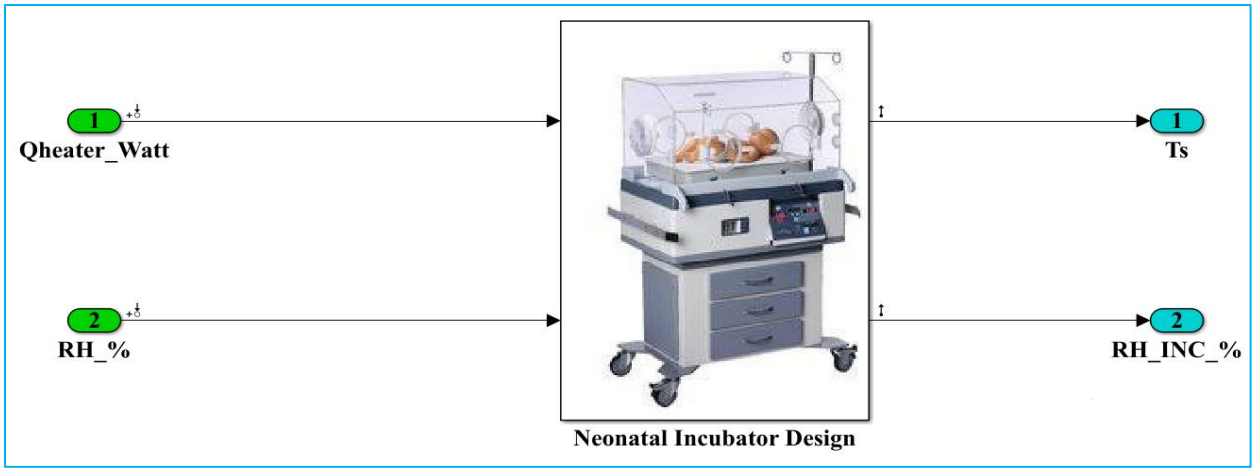

Figure 4. 44 Open loop system for skin mode

The open loop system for the skin mode is a non-linear system. Therefore, this system should be linearized using the MATLAB *Linear Analysis Tool.* The linear analysis tool is applied so as to drive the transfer function of the system. As it is observed from simulation results using the *controlSystemDesigner* tool, the system is stable for skin mode operation.

Figure 4.44 depicts the two inputs and two outputs. These two input/outputs relations lead to the creation of four transfer functions.

The four transfer functions are:

I. From input "Qheater_Watt" to output "Neonatal Incubator Design/1" **($G_{11}(s)$):**

$$\frac{8.66e-14s^6+1.648e-06s^5+1.0428e-07s^4+2.6568e-10s^3+1.537e-13s^2+1.7548e-17s+3.91e-22}{s^8+0.3544\,s^7+0.02884\,s^6+0.0007068\,s^5+2.293e-06\,s^4+1.599e-09\,s^3+2.983e-13\,s^2+1.694e-17s+1.395e-22}$$

II. From input "Qheater_Watt" to output "Neonatal Incubator Design/3" **($G_{21}(s)$):**

$$\frac{-2.448e-05\,s^6-4.903e-06\,s^5-1.758e-07\,s^4-7.746e-10\,s^3-5.798e-13\,s^2-1.112e-16\,s-5.945e-21}{s^8+0.3544\,s^7+0.02884\,s^6+0.0007068\,s^5+2.293e-06\,s^4+1.599e-09\,s^3+2.983e-13\,s^2+1.694e-17\,s+1.395e-22}$$

III. From input "Design_of_NI_New1/RH_%" to output "Neonatal Incubator Design/1" **($G_{12}(s)$):**

$$\frac{0.01829\,s^7+0.005756\,s^6+0.0003087\,s^5+1.694e-06\,s^4+2.867e9\,s^3+1.396e-12\,s^2+1.212e-16\,s+2.268e-22}{s^8+0.3544\,s^7+0.02884\,s^6+0.0007068\,s^5+2.293e-06\,s^4+1.599e-09\,s^3+2.983e-13\,s^2+1.694e-17\,s+1.395e-22}$$

IV. From input "Design_of_NI_New1/RH_%" to output "Neonatal Incubator Design/3"**($G_{22}(s)$):**

$$\frac{0.004116\,s^7 + 0.001297\,s^6 + 8.417e-05\,s^5 + 1.68e-06\,s^4 + 5.063e-09s^3 + 3.32e-12\,s^2 + 5.291e-16\,s + 2.249e-20}{s^8 + 0.3544\,s^7 + 0.02884\,s^6 + 0.0007068\,s^5 + 2.293e-06\,s^4 + 1.599e-09\,s^3 + 2.983e-13\,s^2 + 1.694e-17\,s + 1.395e-22}$$

4.3.1.1.2 Air Mode

Figure 4.45 shows the open loop system for air mode. In this mode, the inputs are the external relative humidity and the power from the heater and the outputs are the temperature of the skin and internal relative humidity.

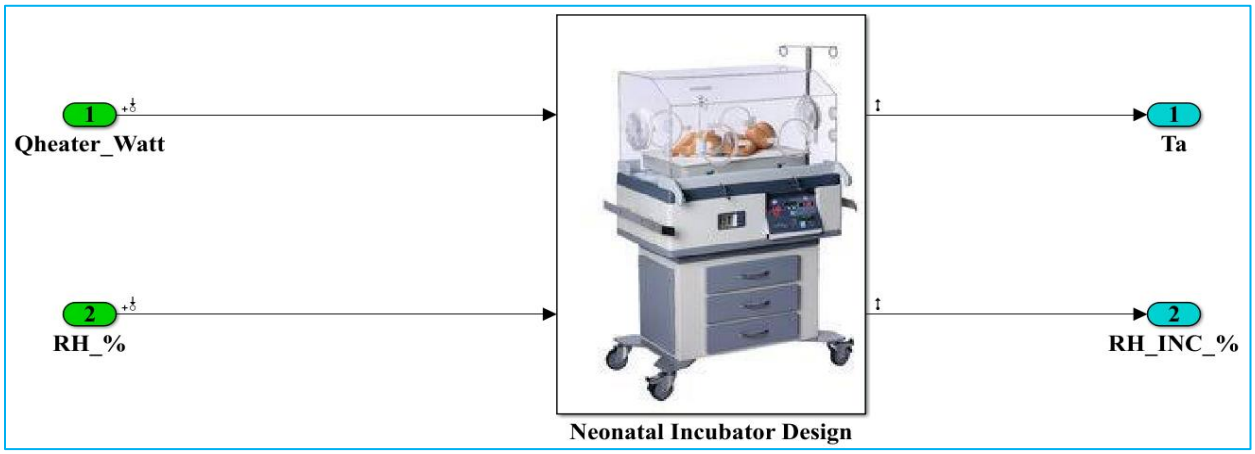

Figure 4. 45 Open loop system for air mode

The open loop system for the air mode is non-linear system. Therefore, this system should be linearized using the MATLAB *Linear Analysis Tool.* The linear analysis tool is applied so as to drive the transfer function of the system. MATLAB uses Taylor series approximation. As it is observed from simulation results using *controlSystemDesigner* tool, the system is stable for air mode operation.

Simulink Control Design linearizes models using a block-by-block approach. This block-by-block approach individually linearizes each block in the Simulink model and combines the results to produce the linearization of the specified system. and also linearize the system using full-model numerical perturbation, where the software computes the linearization of the full model by perturbing the values of the root-level inputs and states. For each input and state, the software perturbs the model by a small amount and computes a linear model based on the model's response to these perturbations.

Figure 4.45 depicts the two inputs and two outputs. These two input/outputs relations lead to the creation of four transfer functions.

The four transfer functions are:

I. From input "Qheater_Watt" to output "Neonatal Incubator Design/2" **($G_{11}(s)$):**

$$\frac{4.261e-11\,s^7 + 0.0008106\,s^6 + 8.217e-05\,s^5 + 2.034e-06\,s^4 + 1.884e-09\,s^3 + 4.574e-13\,s^2 + 3.639e-17\,s + 7.232e-22}{s^8 + 0.3544\,s^7 + 0.02884\,s^6 + 0.0007068\,s^5 + 2.293e-06\,s^4 + 1.599e-09\,s^3 + 2.983e-13\,s^2 + 1.694e-17\,s + 1.395e-22}$$

II. From input "Qheater_Watt" to output "Neonatal Incubator Design/3" **($G_{21}(s)$):**

$$\frac{-2.448e-05\,s^6 - 4.903e-06\,s^5 - 1.758e-07\,s^4 - 7.746e-10\,s^3 - 5.798e-13\,s^2 - 1.112e-16\,s - 5.945e-21}{s^8 + 0.3544\,s^7 + 0.02884\,s^6 + 0.0007068\,s^5 + 2.293e-06\,s^4 + 1.599e-09\,s^3 + 2.983e-13\,s^2 + 1.694e-17\,s + 1.395e-22}$$

III. From input "Design_of_NI_New1/RH_%" to output "Neonatal Incubator Design/2"**($G_{12}(s)$):**

$$\frac{-0.01544\,s^7 - 0.0008572\,s^6 + 3.917e-05\,s^5 + 2.124e-06\,s^4 + 2.633e-09\,s^3 + 9.365e-13\,s^2 + 6.569e-17\,s - 9.011e-22}{s^8 + 0.3544\,s^7 + 0.02884\,s^6 + 0.0007068\,s^5 + 2.293e-06\,s^4 + 1.599e-09\,s^3 + 2.983e-13\,s^2 + 1.694e-17\,s + 1.395e-22}$$

IV. From input "Design_of_NI_New1/RH_%" to output "Neonatal Incubator Design/3"**($G_{22}(s)$):**

$$\frac{0.004116\,s^7 + 0.001297\,s^6 + 8.417e-05\,s^5 + 1.68e-06\,s^4 + 5.063e-09s^3 + 3.32e-12\,s^2 + 5.291e-16\,s + 2.249e-20}{s^8 + 0.3544\,s^7 + 0.02884\,s^6 + 0.0007068\,s^5 + 2.293e-06\,s^4 + 1.599e-09\,s^3 + 2.983e-13\,s^2 + 1.694e-17\,s + 1.395e-22}$$

4.3.1.2 System Design without PID Controller

4.3.1.2.1 Skin Mode

Figure 4.46 shows the skin mode operation of a neonatal incubator without a PID controller in the MATALB model. The set value for skin temperature is 36.5 ^{o}C and the set value for added humidity is 80% [49], [50].

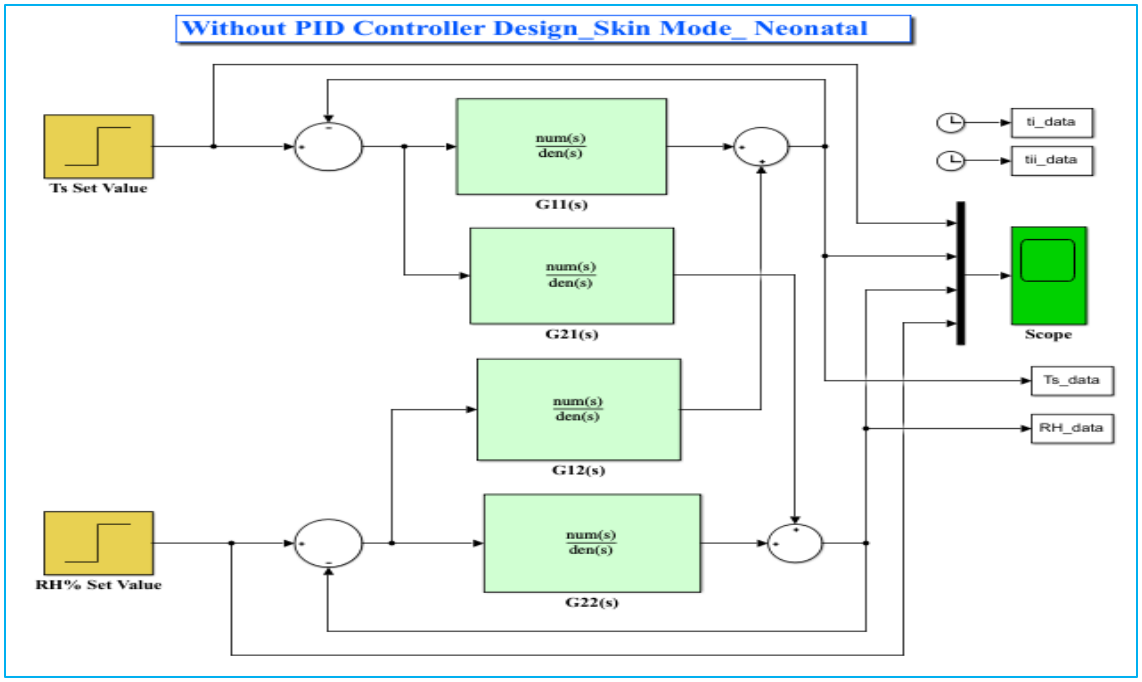

Figure 4. 46 MATALB model for simulation of skin mode operation without PID controller

4.3.1.2.2 Air Mode

Figure 4.47 shows the air mode operation of a neonatal incubator without a PID controller in the MATALB model. The set value for skin temperature is 37 ºC and the set value for added humidity is 80%[49], [50].

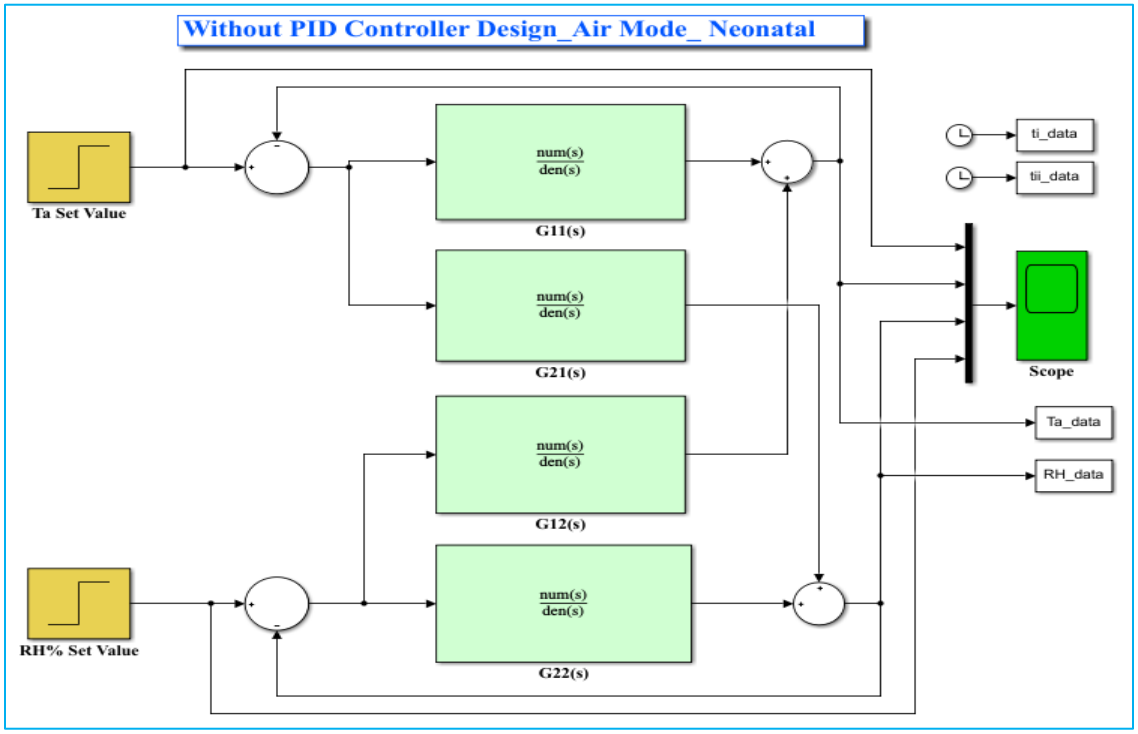

Figure 4. 47 MATALB model for simulation of air mode operation without PID controller

4.3.1.3 System Design with PID Controller

The relative humidity and temperature coupling system is for a system that is based on the strong coupling qualities between temperature and humidity management processes. Without decoupling, each loop in such systems will interfere with the others during operation, making it challenging to get the best possible control effect. As a result, decoupling techniques such as feedforward compensation decoupling, state feedback decoupling, series compensation decoupling, and static decoupling can be used to achieve the decoupling of the relative humidity and temperature coupling systems. The decoupler is compensated and positioned in front of the control object or on the feedback channel in order to entirely eliminate coupling between temperature and relative humidity. For this thesis work, the feedforward compensation decoupling approach, which is based on the feedforward compensation principle, is used. The coupling channel is seen as the disturbance signal of the control object in order to perform the feedforward compensatory decoupling of the disturbance signal [24].

Figure 4.48 describes a system that illustrates the centralized control organization. Between the controller loop and the process, more transfer function blocks (decouplers) can be added. Decoupling's primary goal is to make up for the loop interactions that cross-couplings of the process variables cause [51], [52]. Interactions between the system variables cannot be entirely removed, even if decouplers are used. In this case, the approach of sequential tuning that takes relations into account is used. The fundamental concept is using single loop to analyze a series of several control loops by using decouplers or not. Until all controller parameters have converged, this sequential tuning process can be continued. Keep in mind that the system acts like a single loop for each tuning stage. It follows that any single loop tuning method can be used to tune numerous control loops sequentially and iteratively [51]. The method of feedforward compensation decoupling principle can be stated using the mathematical expression as follows.

$$\frac{Y_2(s)}{U_1(s)} = G_{21}(s) + G_1(s)G_{22}(s) = 0 \tag{4.1}$$

$$\frac{Y_1(s)}{U_2(s)} = G_{12}(s) + G_2(s)G_{11}(s) = 0 \tag{4.2}$$

From the above formula, the feedforward decouplers $G_1(s)$ and $G_2(s)$ can be determined as:

$$G_1(s) = -\frac{G_{21}(s)}{G_{22}(s)} \tag{4.3}$$

$$G_2(s) = -\frac{G_{12}(s)}{G_{11}(s)} \tag{4.4}$$

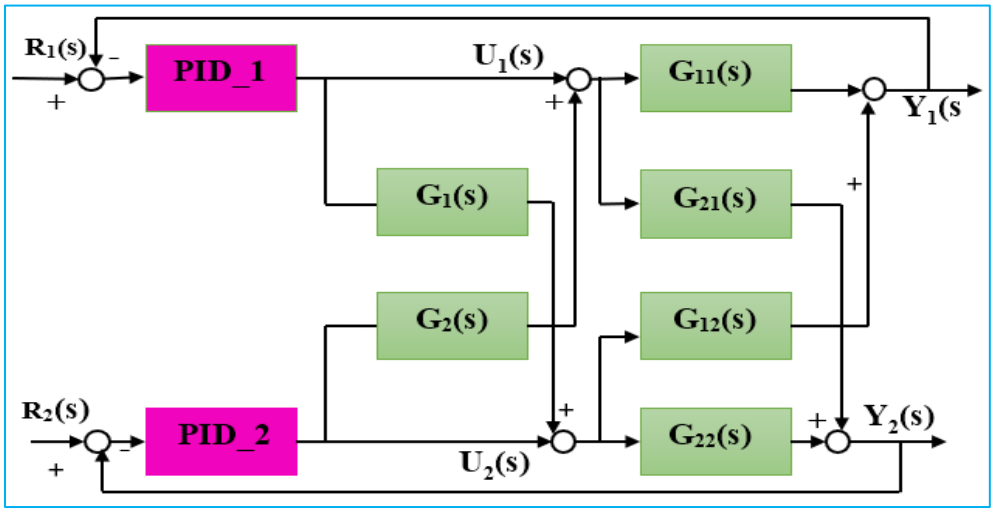

Figure 4. 48 Feedforward decoupling with PID Controller

Figure 4.49 depicts the procedures of the sequential loop closing tuning method using two control loops. As it is shown in Figure 4.49 (a), the tuning process starts at loop 1 by applying a test of closed loop identification. Then, the setting of the controller is fixed. Similar tasks will be continued for loop 2 as described in Figure 4.49 (b). Here, loop 1 should be set in automatic mode considering the previous resultant setting and loop 2 gets the identification test. The identification test will be repeated for loop 1 by making loop 2 closed, as shown in Figure 4.49 (c). The procedure of sequential tuning will be continued till the convergence of all controller parameters is achieved. This procedure will be continued by alternatively using Figure 4.49 (b) and Figure 4.49 (c) and considering the system as a single loop.

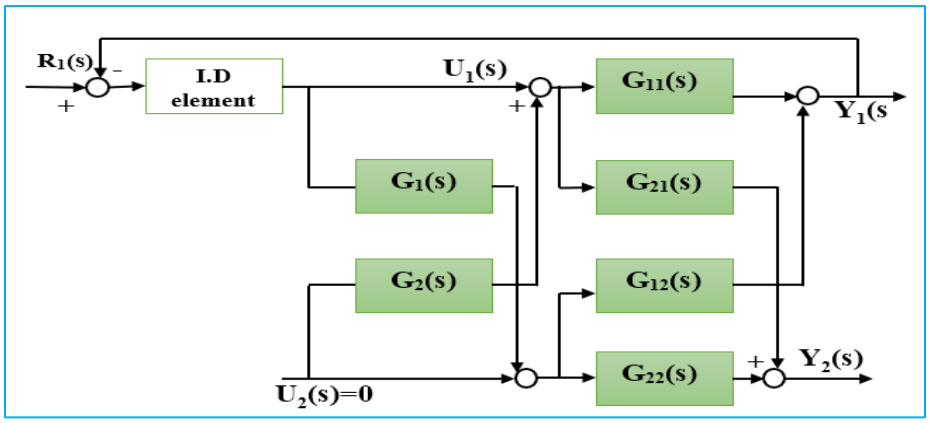

(a)

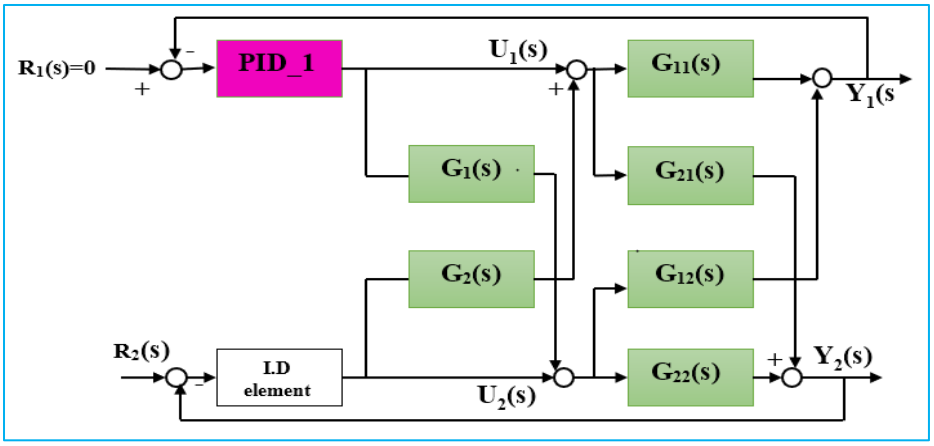

(b)

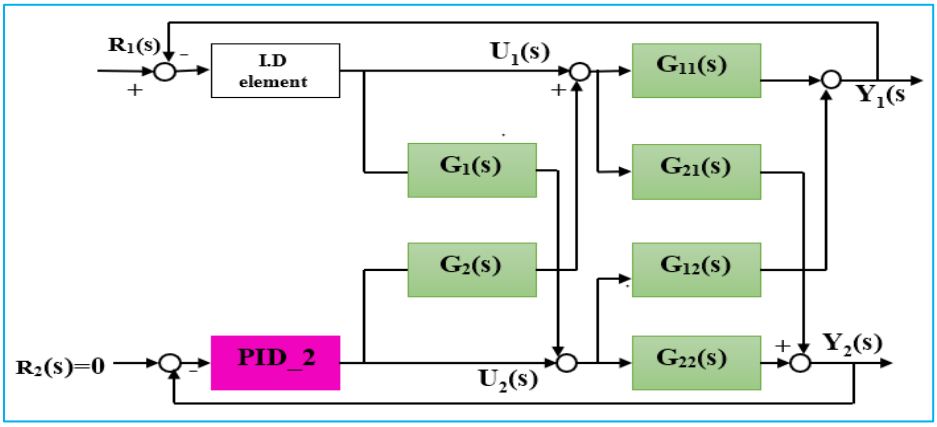

(c)

Figure 4. 49 Procedures of the sequential tuning method for multivariable PID control

Note that the Ziegler-Nichols tuning rule cannot be directly applied in a multiple-input multiple-output system attributable to the fact that the outputs of controllers have a mutual effect on each other. Therefore, the multiple-input multiple-output system should be divided into single-input single-output systems [53], [54].

4.3.1.3.1 Skin Mode

The system without decoupling is shown in Figure 4.50. This system should be decoupled to eliminate interaction between skin temperature and relative humidity using feedforward decoupling method. Therefore, the MATALB model, which simulates the working of a neonatal incubator with a PID controller in skin mode, is shown in Figure 4.51. The skin temperature is set to 36.5 degrees Celsius, with an additional humidity of 80 % [49], [50].

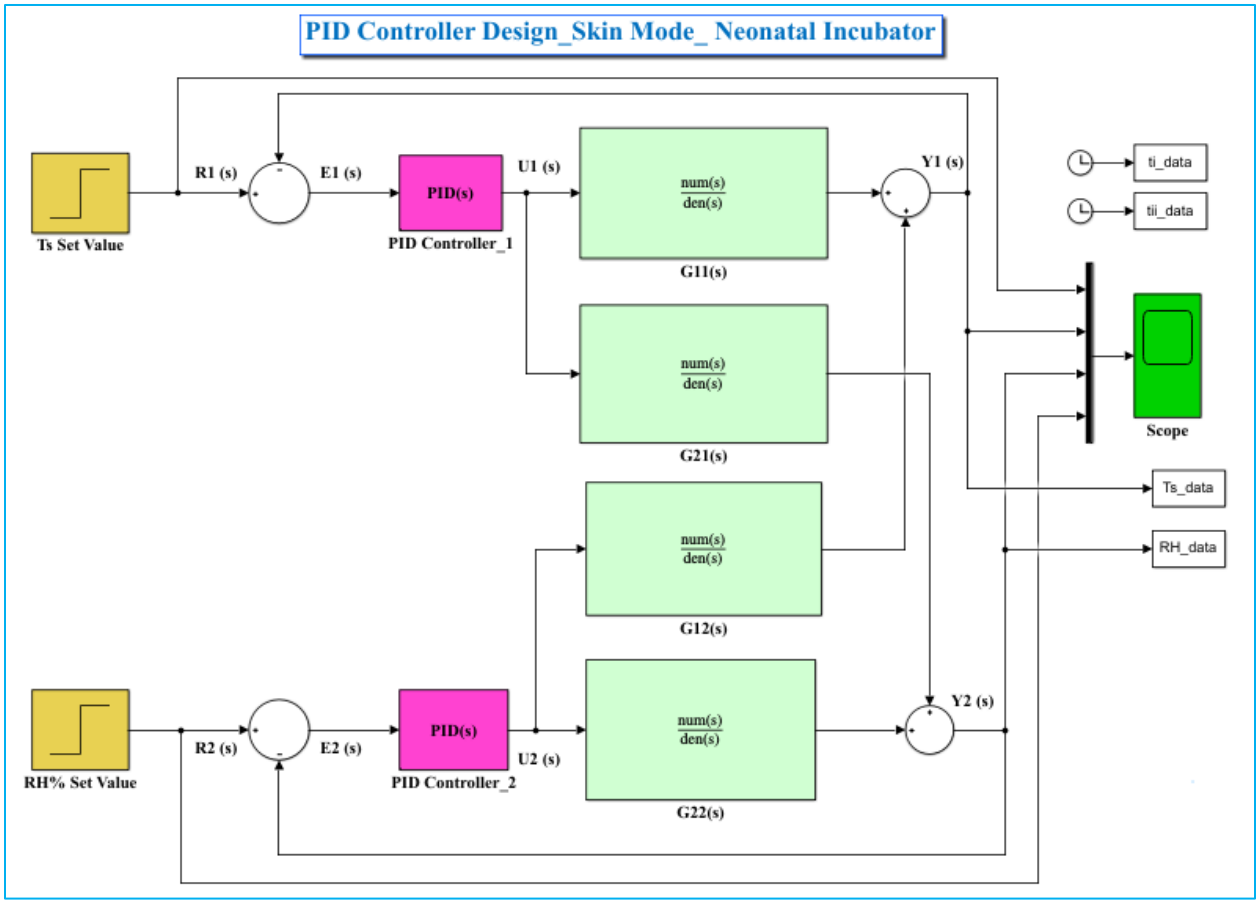

Figure 4. 50 MATALB model for skin mode operation with PID controller

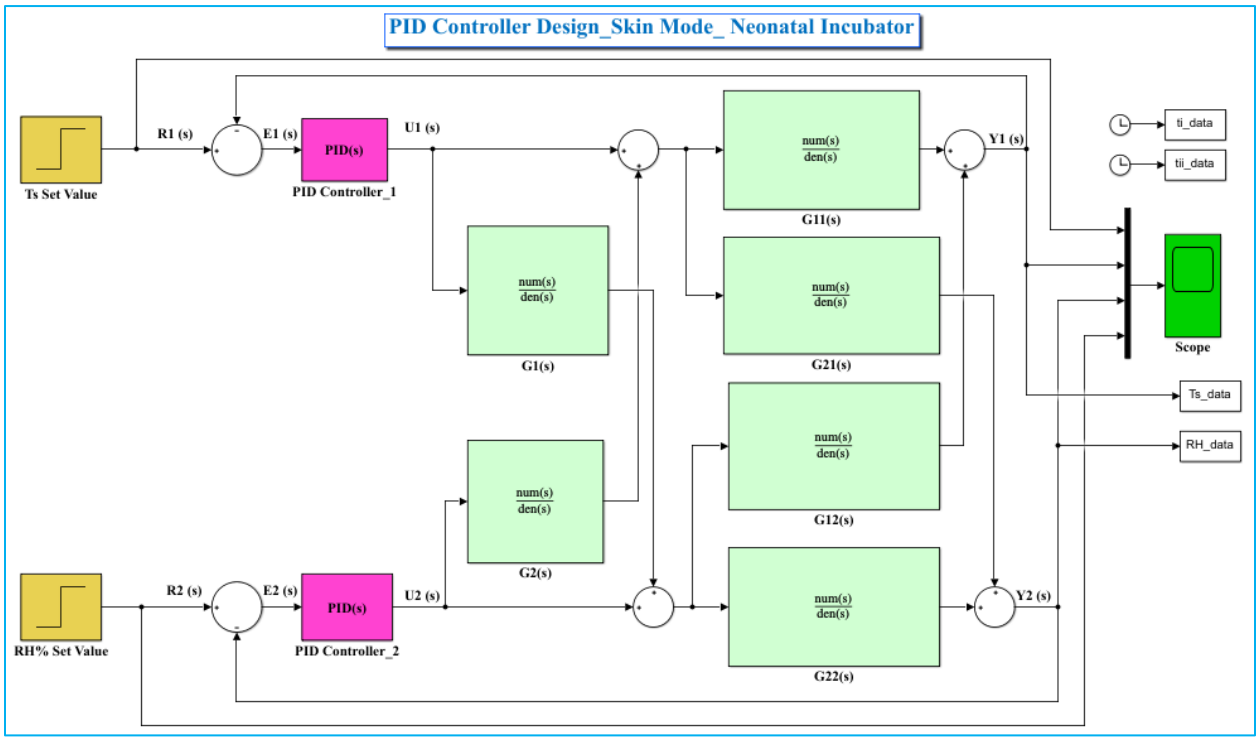

Figure 4. 51 MATALB model for skin mode operation using feedforward decoupling

4.3.1.3.2 Air Mode

Figure 4.52 shows the system without decoupling. This system should be decoupled to eliminate interaction between temperature of air and humidity using the feedforward decoupling method. Therefore, the MATALB model, which simulates the working of a neonatal incubator with a PID controller in air mode, is illustrated in Figure 4.53. The temperature of air is set to 37 degrees Celsius with an additional humidity of 80% [49], [50].

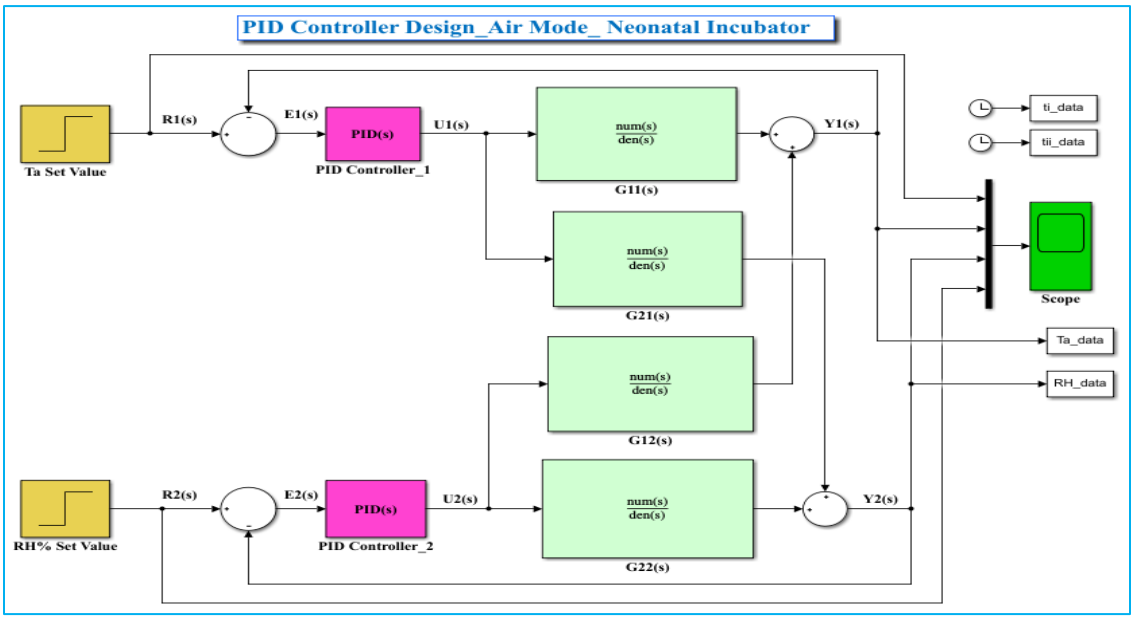

Figure 4. 52 MATALB model for air mode operation with PID controller

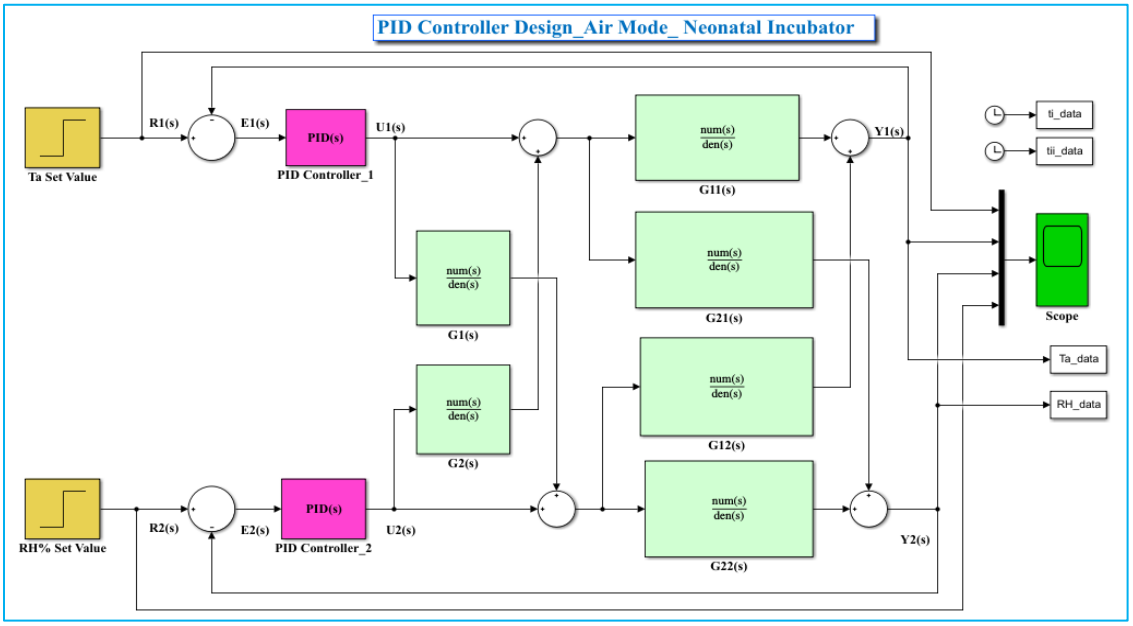

Figure 4. 53 MATALB model for air mode operation using feedforward decoupling

CHAPTER FIVE

5. RESULT AND DISCUSSION

5.1 Introduction

The air and skin mode simulation results are discussed in this chapter. These apply to a baby who was born weighing 900 grams at 28 weeks' gestation on the first day of life. Both types of related initial circumstances and other information are also provided. The neonatal incubator system numerous quantitative results are developed by using the MATLAB/Simulink software, including the ultimate temperatures for each of the 12 components in this work.

5.2 Skin Mode Results

The simulation results for the skin mode operation of the neonatal incubator are obtained for two conditions. The first condition is simulating the system without using a PID controller, and the second condition is using a PID controller. Therefore, the simulation results of all these conditions are discussed in the succeeding sections.

5.2.1 Simulation Results of Neontal Incubator without PID Controller

The MATALB model for simulation of skin mode operation of neontal incubator without PID controller was shown in Figure 4.51. Figure 5.1 indicates the results of the simulation. In this simulation, the performance indicator parameters such as rise time (second), settling time (second), overshoot (%), peak value and peak time (second) are presented in Table 5.1.

Table 5. 1 Performance indicator parameters for skin mode operation without PID controller

S/N	Performance Parameters	Skin Temperature (T_s)	Relative Humidity (RH)
1	Rise time	30.6742	1063.6
2	Settling time	4066.8	2405.9
3	Over shoot	23.1096	0
4	Peak	35.7018	77.6563
5	Peak time	205.4625	3248.7

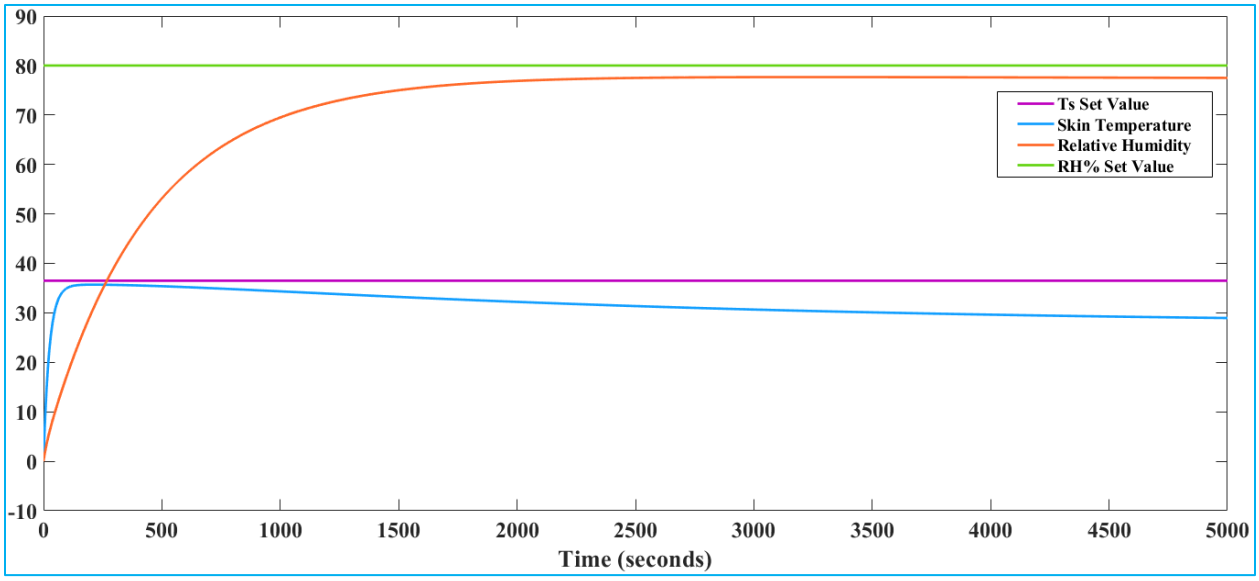

Figure 5. 1 Simulation results skin mode operation of neonatal incubator without PID controller

5.2.2 Simulation Resuls of Neontal Incubator with PID Controller

The MATALB model for simulation of skin mode operation of neontal incubator with PID controller was shown in Figure 4.51. Figure 5.2 indicates the results of the simulation. In this simulation, the performance indicator parameters such as rise time (second), settling time (second), overshoot (%), peak value and peak time (second) are presented in Table 5.2.

Table 5. 2 Performance indicator parameters for skin mode operation with PID controller

S/N	Performance Parameters	Skin Temperature (T_s)	Relative Humidity (RH)
1	Rise time	114.3430	9.8311
2	Settling time	755.7778	85.9114
3	Over shoot	6.1172	8.5586
4	Peak	39.2634	86.8469
5	Peak time	348.4329	31.6578

The performance indicator parameters of the PID controller are Proportional (P), Integral (I) and Derivative (D) for skin mode operation. Therefore, for skin mode operation, for Sin Temperature (T_s), the PID controller parameters: P = 105.061, I = 0.2968 and D = 3712.204. And also, for Relative Humidity (RH), the PID controller parameters: P = 46.945, I = 2.097 and D = 29.678.

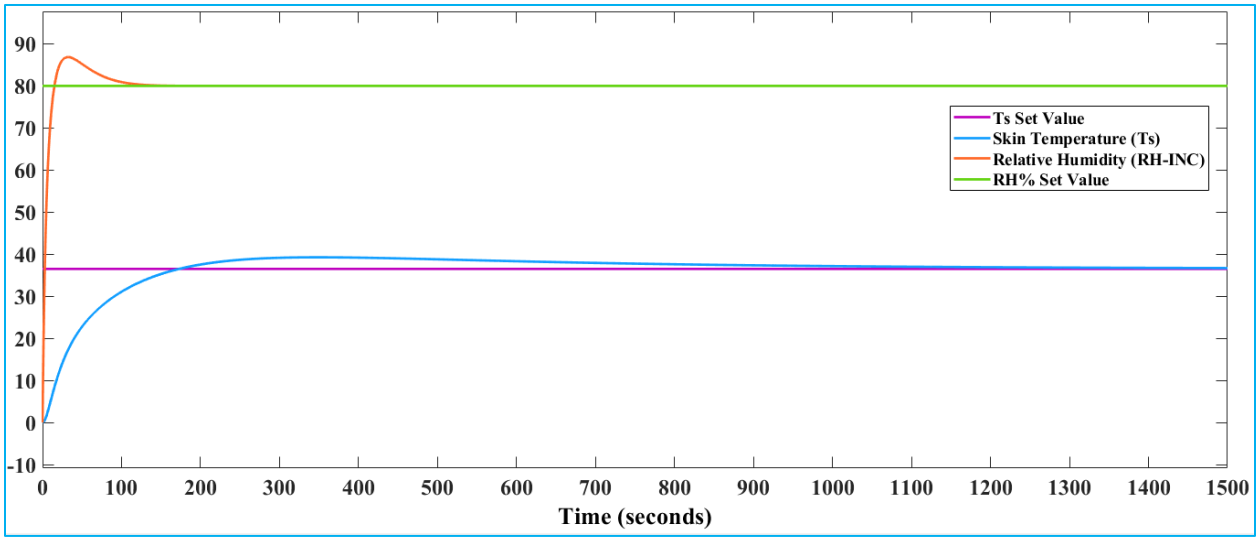

Figure 5. 2 Simulation results skin mode operation of neontal incubator with PID controller

5.3 Air Mode Results

Similar to the simulation of the skin mode operation of neonatal incubator, the simulation resuls for air mode operation of neontal incubator are obtained for two diffferent conditions. The first conditions is simulating the system without using PID controller and the second condition is using PID controller.

5.3.1 Simulation Resuls of Neontal Incubator without PID Controller

The MATALB model for simulation of skin mode operation of neontal incubator without PID controller was shown in Figure 4.52. Figure 5.3 indicates the results of the simulation. In this simulation, the performance indicator parameters such as rise time (second), settling time (second), overshoot (%), peak value and peak time (second) are presented in Table 5.3.

Table 5. 3 Performance indicator parameters for air mode operation without PID controller

S/N	Performance Parameters	Air Temperature (T_a)	Relative Humidity (RH)
1	Rise time	81.3113	983.9486
2	Settling time	2302.1	1962.1
3	Over shoot	59.6521	0
4	Peak	44.7026	77.1609
5	Peak time	376.4795	4353.3

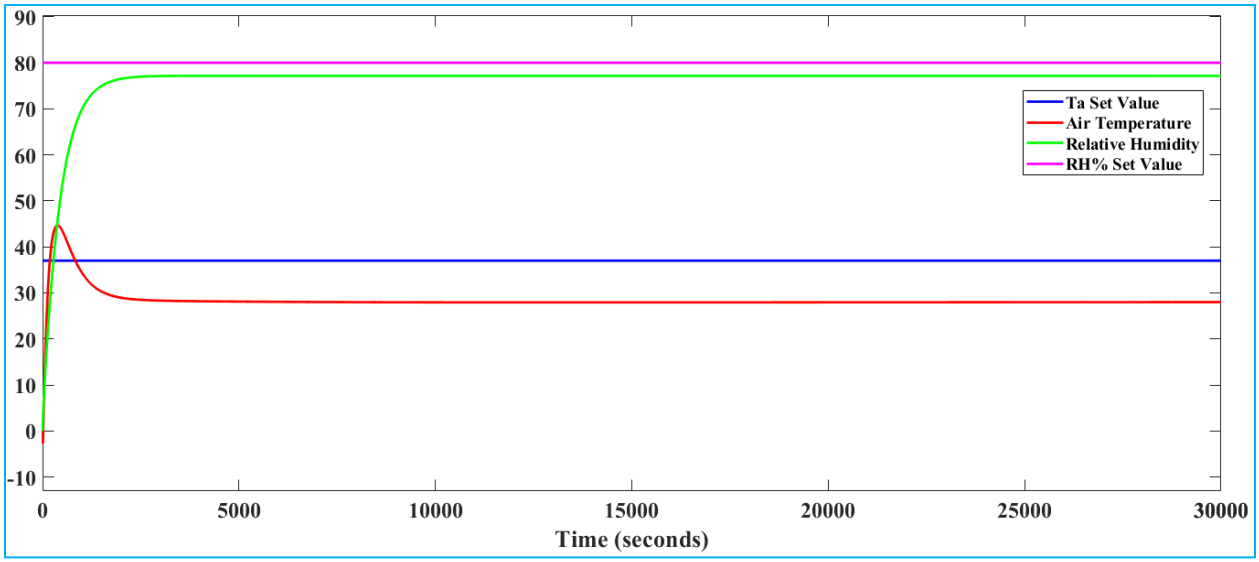

Figure 5. 3 Simulation results air mode operation of neonatal incubator without PID controller

5.3.2 Simulation Resuls of Neontal Incubator with PID Controller

The MATALB model for simulation of skin mode operation of neontal incubator without PID controller was shown in Figure 4.53. Figure 5.4 indicates the results of the simulation. In this simulation, the performance indicator parameters such as rise time (second), settling time (second), overshoot (%), peak value and peak time (second) are presented in Table 5.4.

Table 5. 4 Performance indicator parameters for air mode operation with PID controller

S/N	Performance Parameters	Air Temperature (T_a)	Relative Humidity (RH)
1	Rise time	96.8157	8.6970
2	Settling time	530.4750	69.8222
3	Over shoot	7.2456	9.4301
4	Peak	39.6809	87.5440
5	Peak time	274.2986	26.0676

Similar to skin mode operation, the performance parameters of the PID controller are obtained from the simulation results for air mode operation. The performance indicator parameters of the PID controller are Proportional (P), Integral (I) and Derivative (D) for air mode operation. Therefore, for air mode operation, for Air Temperature (T_a), the PID controller parameters: P = 5.193, I = 0.034 and D = 97.274. And also, for Relative Humidity (RH), the PID controller parameters: P = 52.538, I = 2.946 and D = 31.556.

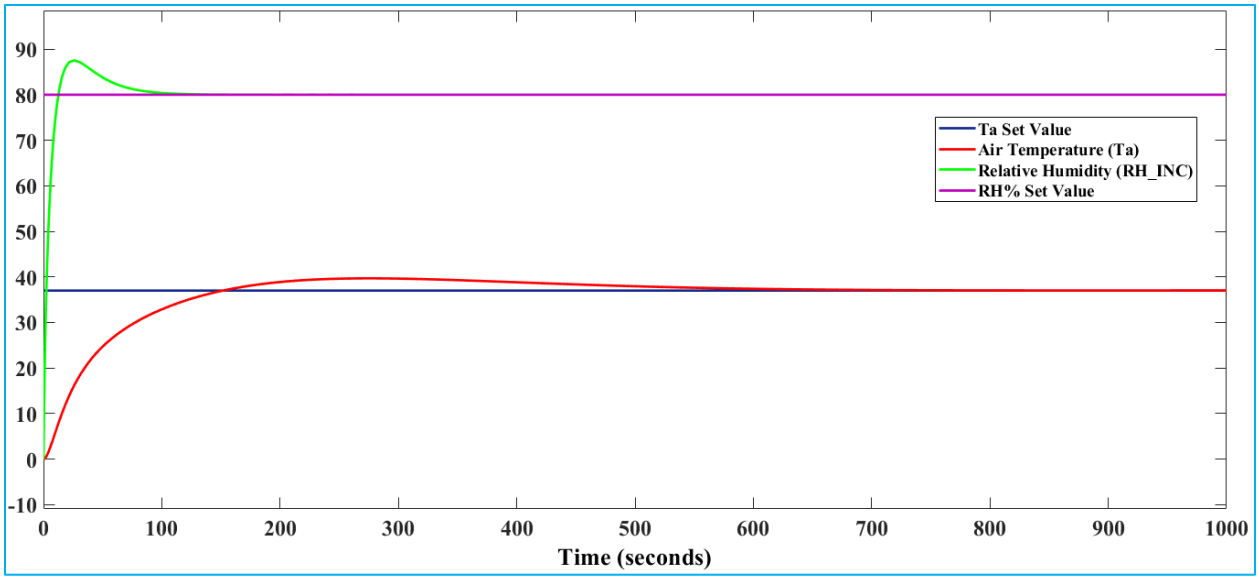

Figure 5. 4 Simulation results air mode operation of neonatal incubator with PID controller

Table 5. 5 Summary of simulation results of neonatal incubator design

S / N	Performance Parameters	Skin Mode				Air Mode			
		Skin Temperature (T_s)		Relative Humidity (RH)		Air Temperature (T_a)		Relative Humidity (RH)	
		Without PID	Decoupling With PID	Without PID	Decoupling With PID	Without PID	Decoupling With PID	Without PID	Decoupling With PID
1	Rise time	30.67	114.3	1063.6	9.8311	81.3113	96.8157	983.949	8.6970
2	Settling time	4066.8	755.8	2405.9	85.91	2302.1	530.48	1962.1	69.82
3	Over shoot	23.1096	6.117	0	8.559	59.65	7.2456	0	9.430
4	Peak	35.7018	39.26	77.6563	86.85	44.7026	39.681	77.1609	87.54
5	Peak time	205.463	348.4	3248.7	31.66	376.48	274.3	4353.3	26.07

The simulation results, which are obtained from the overall system simulation, are summarized in Table 5.5. Therefore, for the skin temperature (T_s), the overshoot is 6.117%, the rise time is 114.3 seconds, and the settling time is 755.8 seconds using the decoupling and sequential loop closing tuning method with PID controller for skin mode operation. However, without a PID controller, the overshoot is 23.1096%, the rise time is 30.67 seconds, and the settling time is 4066.8 seconds. And also, for the incubator relative humidity (RH), the overshoot is 8.559%, the rise time is 9.8311 seconds, and the settling time is 85.91 seconds using a PID controller for skin mode operation. But

without a PID controller, the overshoot is 0, but with a huge settling time (that is, 2405.9 seconds) with a rise time of 1063.6 seconds, as shown in Table 5.5.

On the other hand, using the decoupling and sequential loop closing tuning method with PID controller for air mode operation, the simulation results show that for air temperature (*Ta*), the overshoot is 7.2456%, the rise time is 96.8157 seconds, and the settling time is 530.48 seconds, but without the PID controller, the overshoot is 59.65%, the rise time is 81.3113 seconds, and the settling time is 2302.1 seconds. And also, for the incubator relative humidity (RH), the overshoot is 9.43%, the rise time is 8.697 seconds, and the settling time is 69.82 seconds using a PID controller for air mode operation. But without a PID controller, the overshoot is 0, but with a huge settling time (that is, 1962.1 seconds) with a rise time of 983.949 seconds, as shown in Table 5.5.

As observed from the simulation results, the PID controller improves the overall system performance. The PID controller also makes the system more robust and makes the system faster by reducing the time constant.

CHAPTER SIX

6. CONCLUSION AND FUTURE WORK

6.1 Conclusion

The overall system design of the neonatal incubator is performed using mathematical analysis. The model consists of twelve components. These include the skin, air, core, walls, heater, fan, mattress, water surface air, supplied air temperature, surface of water, heat sink, and relative humidity. The type of neonatal incubator model that was selected in this study is the ATOM V-850.

The overall system is simulated by the MATLAB/Simulink software. The simulation is performed for both air mode and skin mode of operation. The designed system performance is analyzed for each mode of operation. In this thesis work, relative humidity and temperature are the main parameters of neonatal incubator that are monitored. The PID tuner is used to tune the PID parameters automatically There are multiple loops in the overall system. In order to reduce the interaction between loops, the feedforward decoupling method is applied. Also, the sequential loop closing method is used for tuning the PID controller sequentially until it reaches the converged values.

The simulation results show that for the temperature of skin (T_s), the overshoot is reduced from 23.1096% to 6.117% and the settling time is also reduced from 4066.8 seconds to 755.8 seconds using the decoupling and sequential loop closing tuning method with PID controller. On the other side, using the decoupling and sequential loop closing tuning method with PID controller for air mode operation, the simulation results show that for temperature of air (T_a), the overshoot is reduced from 59.65% to 7.2456%, and the settling time is also reduced from 2302.1 seconds to 530.48 seconds. For both skin mode and air mode operation, using the decoupling and sequential loop closing tuning method with a PID controller, the relative humidity has improved settling time with an overshoot of 8.559% and 9.43%, respectively.

In general, the overall system performance is improved by the PID controller, as observed from the simulation results. The PID controller also makes the system to become robust and make the system faster by reducing the time constant.

6.2 Future Work

The most critical metrics that need to be monitored in a neonatal incubator are examined in this thesis work. These are relative humidity and temperature, which were controlled by a multivariable PID controller. Many concepts are thought to exist for more study projects. Some potential directions are as follows:

1. **Controlling oxygen level in a neonatal incubator:**

   The oxygen level in the neonatal incubator should be controlled because unbalanced oxygen for neonates causes breathing difficulties. These include the lung disease caused by a surfactant shortage, hyaline membrane sickness, and respiratory suffering syndrome. An incubator with an oxygen controller can provide the correct oxygen amount for the baby's needs in the incubator, minimize user support, and eliminate the negativity that may arise from user mistakes.

2. **Controlling light in a neonatal incubator:**

   If the light in the neonatal incubator is not controlled, neonatal jaundice may occur. The skin changed to yellow and the eyes were white. This condition can damage the spinal cord and brain, which can be life-threatening. Therefore, the amount of light entering the neonatal incubator should be controlled and it can eliminate the causes of these health problems.

References

[1] T.P.Mote and S.D.Lokhande, "Temperature Control System Using ANFIS," *International Journal of Soft Computing and Engineering (IJSCE),* vol. 2, no. 1, pp. 156-161, March 2012.

[2] Rasha M. Abd El-Aziz and Ahmed I. Taloba, "Real Time Monitoring and Control of Neonatal Incubator using IOT," *International Journal of Grid and Distributed Computing,* vol. 14, no. 1, pp. 2117-2127, 2021.

[3] Shafeek Basheer, Aneesh A. and Austine Cyriac, "Smart Incubator with Real Time Temperature and Humidity Control," *International Research Journal of Engineering and Technology (IRJET),* vol. 6, no. 4, pp. 4357-4362, April 2019.

[4] Lamidi, Abd Kholiq and Muslim Ali, "A Low Cost Baby Incubator Design Equipped with Vital Sign Parameters," *Indonesian Journal of Electronics, Electromedical, and Medical Informatics (IJEEEMI),* vol. 3, no. 2, pp. 55-58, May 2021.

[5] Pallerla Akshay Kumar, Naregalkar Akshay, Thati Anush Kumar, Anusha Sama and Badrinath, "Real Time Monitoring And Control Of Neonatal Incubator Using LabVIEW," *International Journal of Application or Innovation in Engineering and Management (IJAIEM),* vol. 2, no. 2, pp. 375-380, April 2013.

[6] S. Ravi, M. Sudha, and P. A. Balakrishnan, "Design of Intelligent Self-Tuning GA ANFIS Temperature Controller for Plastic Extrusion System," *Hindawi Publishing Corporation,* vol. 2011, pp. 1-8, May 2011.

[7] Hitu Bansal, Dr. Lini Mathew, Ashish Gupta, "Controlling of Temperature and Humidity for an Infant Incubator Using Microcontroller," *International Journal of Advanced Research in Electrical, Electronics and Instrumentation Engineering,* vol. 4, no. 6, pp. 4975-4982, June 2015.

[8] Elyes FEKI, M. Aymen ZERMANI, and Abdelkader MAMI, "Decoupling Control Approach for Neonate Incubator System," *International Journal of Computer Applications,* vol. 47, no. 2, pp. 49-57, June 2012.

[9] Vanda Catur Kirana, Dwi Herry Andayani, Andjar Pudji, Aziza Hannouch, "Effect of Closed and Opened the Door toTemperature on PID-Based Baby Incubator with Kangaroo Mode," *Indonesian Journal of Electronics, Electromedical Engineering, and Medical Informatics (IJEEEMI),* vol. 3, no. 3, pp. 121-127, 2021.

[10] M.Suruthi and S.Suma, "Microcontroller Based Baby Incubator Using Sensors," *International Journal of Innovative Research in Science, Engineering and Technology,* vol. 4, no. 12, pp. 12037-12044, December 2015.

[11] Jose Medeiros, Jose Maria Pires, Alberto Alexandre Moura, Otacılio da Mota Almeida and Fabio Meneghetti Ugulino, "Assessment and Certification of Neonatal Incubator Sensors through an Inferential Neural Network," *sensors,* vol. 13, pp. 15613-15632, 2013.

[12] Sumardi1, Darjat, Enda Wista Sinuraya, and Rahmat Jati Pamungkas, "Design of Temperature Control System for Infant Incubator using Auto Tuning Fuzzy-PI Controller," *International Journal of Engineering and Information Systems (IJEAIS),* vol. 3, no. 1, pp. 33-41, 2019.

[13] K. Ogata, Modern Control Engineering, New Jersey: Prentice Hall, 2010.

[14] N. S. Nise, Control System Engineering, California: John Wiley & Sons, 2015.

[15] W. S. Levine, Control System Funamentals, New York: Taylor and Francis Group, 2011.

[16] Eneh I.I., Onugwu E.O., Eneh P.C. and Okafor P.U., "Improving the Control of Preterm Infant Mass Skin Temperature using Adaptive Neuro Fuzzy Inference System," *International Journal of Research in Engineering & Science*, vol. 3, no. 3, pp. 1-10, 2019.

[17] Osman Yeler and Mehmet Fevzi Koseoglu, "Energy efficiency and transient-steady state performance comparison ofa resistance infant incubator and an improved thermoelectric infant incubator," *Engineering Science and Technology,* vol. 31, pp. 1-13, September 2021.

[18] P. Singhala, D. N. Shah, B. Patel, "Temperature Control using Fuzzy Logic," *International Journal of Instrumentation and Control Systems (IJICS),* vol. 4, no. 1, pp. 1-10, January 2014.

[19] Jing-Nang Lee, Tsung-Min Lin, and Chien-Chih Chen, "Modeling Validation and Control Analysis for Controlled Temperature and Humidity of Air Conditioning System," *Hindawi Publishing Corporation,* vol. 2014, pp. 1-10, 2014.

[20] Felipe C. Freitas, Francisco V. Andrade, Bismark C. Torrico and Jose C. T. Campos, "TEMPERATURE CONTROL OF A NEONATE INTENSIVE CARE UNIT USING KALMAN FILTER," in *23rd International Congress of Mechanical Engineering,* Rio de Jrneiro, RJ, Brazil, December 6-11, 2015.

[21] M. A. Zermani, E. Feki and A. Mami, "Multivariable Control Applied to Temperature and Humidity Case Study: Neonate incubator," in *2012 20th Mediterranean Conference on Control & Automation (MED),* Barcelona, Spain, July 3-6, 2012.

[22] P. Subha Hency Jims, S. Dharmalingam, and G. Jims John Wessley, "AN IMPROVED METHOD TO CONTROL THE CRITICAL PARAMETERS OF A MULTIVARIABLE CONTROL SYSTEM," in *Materials Science and Engineering* , Tamilnadu, India, 2017.

[23] J. El Hadj Ali, and E. Feki, A. Mami, "Dynamic Matrix Control DMC using the Tuning Procedure based on First Order Plus Dead Time forInfant-Incubator," *International Journal of Advanced Computer Science and Applications (IJACSA)* , vol. 10, no. 6, pp. 358-367, 2019.

[24] Liheng Wang and Zhifeng Zhu, "Research on Temperature and Humidity Decoupling Control of Constant Temperature and Humidity Test Chamber," in *International Conference on Optoelectronic Science and Materials*, Wuhan, China, 2019.

[25] Mochamad Sofiyan Mardianto, Anggun Indra Saputra, Candra Sukma, and Anas Nasrulloh, "Infant Incubator Temperature Controlled and Infant Body Temperature Monitor using Arduino Mega2560 and ADS1232," *International Journal of Computer Techniques,* vol. 6, no. 6, pp. 1-5, December 2019.

[26] Tamanna Afrin Tisa, Zinat Ara Nisha and Md. Adnan Kiber, "Design of Enhanced Temperature Control System for Neontal Incubator," *Bangladesh Journal of Medical Physics,* vol. 5, no. 1, pp. 53-62, 2012.

[27] Abdul Latif, Hendro Agus Widodo, Rachmad Andri Atmoko, Thanh Nguyen Phong, and Elsayed T. Helmy, "Temperature and Humidity Controlling System for Baby Incubator," *Journal of Robotics and Control (JRC),* vol. 2, no. 3, pp. 190-193, 2021.

[28] S. A. Pangarkar and S.R. Deshpande, "Artificial Neural Network based Temperature Controllers for Incubators," *International Journal of Electronics Communication and Computer Engineering,* vol. 5, no. 4, pp. 284-286, 2014.

[29] M Alzgool and H Nouri , “PID controller design for a novel multi-input multi-output boost converter hub,” *Jea Jornal of Electrical Engnineering,* vol. 2, no. 1, pp. 10-21, 2018.

[30] Lu Liu, Siyuan Tian, Dingyu Xue, Tao Zhang, YangQuan Chen, and Shuo Zhang, “A Review of Industrial MIMO Decoupling Control,” *International Journal of Control, Automation and Systems,* vol. 17, no. X, pp. 1-9, 2019.

[31] R. Hanuma Naik, D.V. Ashok Kumar, and K.S.R. Anjaneyulu, “Controller for Multivariable Processes Based on Interaction Approach,” *International Journal of Applied Engineering Research,* vol. 7, no. 11, pp. 1203-1213, 2012.

[32] Shabeena Memon and Arbab Nighat Kalhoro , “Design of Multivariable PID Controllers: A Comparative Study,” *International Journal of Computer Science and Network Security,* vol. 21, no. 8, pp. 212-218, 2021.

[33] Daniele Trevisanuto, Ivano Coretti, Nicoletta Doglioni, Angelo Udilano, Francesco Cavallin, and Vincenzo Zanardo , “Effective temperature under radiant infant warmer: Does the device make a difference?,” *SceinceDirect,* vol. 82, pp. 720-723, 2011.

[34] S. Thulasi dharan, K. Kavyarasan and V. Bagyaveereswaran, “Tuning of PID controller using optimization techniques for a MIMO process,” in *IOP Conf. Series: Materials Science and Engineering 263 (2017) 052019,* Tamil Nadu, 2017.

[35] Mehmet Ali Ustuner and Sezai Taskin, “Inverted Decoupling PID Controller Design for a MIMO System,” *igma Journal of Engineering and Natural Sciences,* vol. 37, no. 4, pp. 1139-1151, 2019.

[36] Wameedh Riyadh Abdul-Adheem and Ibraheem Kasim Ibraheem , “Decoupled control scheme for output tracking of a general industrial nonlinear MIMO system using improved active disturbance rejection scheme,” *Alexandria Engineering Journal,* vol. 58, p. 1145–1156, 2019.

[37] J. El Hadj ali , E. Feki , M. A. Zermani, C. de Prada , A. Mami, “Incubator System Identification of Humidity and Temperature: Comparison between two identification environments,” in *The 9th International Renewable Energy Congress (IREC 2018),* Valladolid, 2018.

[38] Y. A. Cengel, Heat Transfer: A Practical Approach, McGraw-Hill, Second Edition.

[39] K. S. N. Raju, Fluid Mechanics, Heat Transfer, and Mass Transfer, New Jersey: John Wiley & Sons, 2011.

[40] Pauline Decima, Erwan Stephan-Blanchard, and Amandine Pelletier, “Assessment of radiant temperature in a closed incubator,” *Eur J Appl Physiol,* vol. 112, p. 2957–2968, 2012.

[41] Zaid H. Al-Sawaff, Yahya Zakariya Yahya and Fatma Kandemirli, “Neonatal Incubator Embedded Temperature Observation and Monitoring Using GSM,” *ournal of Engineering Research and Reports,* vol. 4, no. 1, pp. 1-9, 2019.

[42] S. M. Ghiaasiaan, Convective Heat and Mass Transfer, New York: Cambridge University Press, 2011.

[43] Alejandro Rincon Casado, Mauricio Larrode-Diaz, Francisco Fernandez Zacarias and Ricardo Hernández Molina, “Experimental and Computational Model for a Neonatal Incubator with Thermoelectric Conditioning System,” *Energies,* vol. 14, pp. 1-16, 2021.

[44] M. Bell, 25 April 2020. [Online]. Available: https://iridl.ldeo.columbia.edu/dochelp/QA/Basic/dewpoint.html.. [Accessed 16 May 2022].

[45] P. Singh, 21 June 2018. [Online]. Available: https://www.omnicalculator.com/physics/relativehumidity. [Accessed 16 May 2022].

[46] Liuping Wang, Shan Chai, Dae Yoo, Lu Gan and Ki Ng, PID and Predictive Control of Electrical Drives and Power Converters using MATLAB/Simulink, Singapore: John Wiley & Sons, 2015.

[47] W. S. Levine, Control System Advanced Methods, Maryland: Taylor & Francis Group, 2011.

[48] L. Wang, PID Control System Design and Automatic Tuning using MATLAB/Simulink, Hoboken: 2020 John Wiley & Sons , 2020.

[49] Daniel B. Zimmer, Aaron A. P. Inks, Nathan Clark, and Chokri Sendi, "Design, Control, and Simulation of a Neonatal Incubato," *IEEE,* vol. 8, no. 20, pp. 6018-6023, 2020.

[50] "The Royal Children's Hospital Melbourne," 10 May 2020. [Online]. Available: https://www.rch.au/rch.cpg/hospital_clinical_guideline_index. [Accessed 01 June 2022].

[51] Shing-Jia Shiu and Shyh-Hong Hwang, "Sequential Design Method for Multivariable Decoupling and Multiloop PID Controllers," *Ind. Eng. Chem. Res.*, vol. 37, no. 1, pp. 107-119, 2010.

[52] Sergio Fragoso, Juan Garrido, Francisco Vázquez and Fernando Morilla, "Comparative Analysis of Decoupling Control Methodologies and H∞ Multivariable Robust Control for Variable-Speed, Variable-Pitch Wind Turbines: Application to a Lab-Scale Wind Turbine".

[53] Yun-Hyung Lee, Seok-Kyung Kwon, and Myung-Ok So, "Design of RCGA-based PID controller for two-input two-output system," *Journal of the Korean Society of Marine Engineering*, vol. 39, no. 10, pp. 1031-1036, 2015.

[54] O. M. M. Vall, "Design of Decoupled PI Controllers for Two-Input Two-Output Networked Control Systems with Intrinsic and Network-Induced Time Delays," *Sciendo,* vol. 15, no. 4, pp. 201-208, 27 July 2021.

Appendixes

Appendix-I: M-Files (MATLAB Codes) for Neonatal Incubator Design

```
%% M-Files (MATLAB Codes) for Neonatal Incubator Design
m = 0.900;              % Mass of Neonate (Kg)
M_rst = 24.8;           % Metabolic rate in resting situation (W/m^2)
age = 1;                % Age of Neonate after birth (day)
GA = 28;                % Age for gestational (weeks)
th_s = 0.0005;          % Neonate skin thickness (m)
V_cb = 80*m;            % Blood volume (mL)
bf = 0.0035;            % Flow rate of the Blood (1/sec)
IV = 3.333;             % Inspired minute volume (mL/kg/sec)
A_mat = 0.21045;        % Mattress total area (m^2)
A_wi = 1.3988;          % Incubator walls surface area (m^2)
th_w = 0.006;           % Incubator wall thickness (m)
th_m = 0.0274;          % Thickness of mattress (m)
M_m = 0.258;            % Mass of mattress (kg)
q_air = 0.35;           % Rate of air flow (1/sec)
q_O2 = 0;               % Rate of oxygen flow (1/sec)
V_inc = 0.1413;         % Incubator volume (m^3)
O_2 = 0;                % Added oxygen (%)
A_al1 = 0.0560;         % Finned aluminium block surface area (exposed)
A_al2 = 0.0973;         % Finned aluminium block surface area (submerged)
A_wa = 0.0390;          % Water surface total area (m^2)
M_ah =0.0013;           % Air mass inside the water tank (kg)
M_wa = 1.7018;          % Water mass inside the water tank (kg)
M_al = 0.882;           % Aluminium block mass (kg)
R_u = 8.315;            % Universal gas constant (KJ/Kmol)
G_a = 0.0004;           % The air mass flow (m3/s)
RH_i = 0.5;             % Initial humidity (%)
K_c = 0.51;             % Core thermal conductivity (W/m*°C)
K_mat = 0.04184;        % Mattress thermal conductivity (W/m*°C)
K_a = 0.02625;          % Incubator air space thermal conductivity
ρ_c = 1080;             % Density of the core (kg/m^3)
ρ_s = 1000;             % Density of the skin (kg/m^3)
ρ_a = 1.145*10^-6;      % Density of the air (kg/mL) at 35 °C
```

```
ρw = 1190.24;          % Density of the Plexiglass (kg/m^3)
ρb = 1.06E-3;          % Density of the blood (kg/mL)
ρwater = 0.001;        % Density of the Water (kg/mL)
Pt = 760;              % Ambient pressure (torr) at 35 0c
Awh = 0.3438;          % Horizontal wall surface area (m^2)
g = 9.81;              % Gravitational acceleration (m/sec^2)
β = 3.36*10^-3;        % Coefficient of expansion (1/k)
Lc = 0.2737;           % Horizontal surface characteristic length (m)
μao = 1.87*10^-5;      % Dynamic viscosity
Cpao = 1007;           % Air specific heat at 30 °c
Kao = 0.02588;         % Air thermal conductivity (W/kg*°c) at 30 °c
V = 1.61*10^-5;        % Air kinematic viscosity at 30 °c
Lc1 = 0.420;           % Vertical surface Length (m)
Awv = 0.3583;          % Vertical long side surface area (m^2)
Awv1 = 0.1693;         % Vertical short side surface area (m^2)
hal2 = 443.33;         % Aluminium block natural convection
Tex = 37;              % Air temperature of exhaled (°c)
Te = 25;               % Air temperature of environmental (°c)
RH1 = 1.00;            % Exhaled air relative humidity
hfg = 2419000;         % Water latent heat (J.kg) at 35 °c
hfg1 = 2383000;        % Water latent heat of (J.kg) at 50 °c
Cpa = 1007;            % Air specific heat (J/kg* °c) at 35 °c
CpO2 = 925.2;          % Added oxygen specific heat (J/kg* °c) at 25 °c
CpN2 = 1038.5;         % Nitrogen specific heat (J/kg* °c) at 25 °c
Cpc = 3470;            % Core specific heat (J/kg* °c)
Cpsk = 3766;           % Skin specific heat (J/kg* °c)
Cpm = 1757;            % Mattress specific heat (J/kg* °c)
Cpb = 3840;            % Blood specific heat (J/kg* °c)
Cpw = 1297;            % Plexiglass specific heat (J/kg* °c)
Cps = 1900;            % Vapour specific heat (J/kg* °c) at 53.5 °c
Cpwa = 4180;           % Water specific heat (J/kg* °c)
Cpal = 900;            % Aluminium specific heat (J/kg* °c)
μa = 1.9*10^-5;        % Air dynamic viscosity at 35 °c
μs = 1.9*10^-5;        % Skin Dynamic Viscosity at 36 °c
Va = 0.1;              % Air velocity (m/sec)
Diasph = 0.08;         % Neonate diameter (approximately) (m)
```

```
Pr = 0.7270;            % Prandtel number at 35 °c
Re =483.3773;           % Neonate's reynolds number
Nusph = 12.9675;        % Neonate's nusselt number
Ac = 0.17;              % Incubator area (m^2)
P = 1.6460;             % Incubator perimeter (m)
Dh = 0.4113;            % Incubator hydraulic diameter (m)
f = 0.0119;             % Forced convection friction factor
Re1 = 2.4853x10^3;      % Incubator's reynold number
Nu1 = 1.7724;           % Incubator's nusselt number
ρah = 1.1;              % Air density (kg/m^3) at 50 °c
Lcwater = 0.335;        % Water surface length (m)
μah = 1.963*10^-5;      % Air dynamic viscosity (kg/m*sec) at 50 °c
ReL = 1.8636x10^3       % Air's reynolds number
Cpah = 1007;            % Air specific heat (J/kg* °c) at 50 °c
Kah = 0.02735;          % Air thermal conductivity (W/m* °c) at 50 °c
PrL = 0.7228;           % Air's prandtel number at 50 °c
Nu2 = 25.7240;          % Water nusselt number at 50 °c
Lcal1 = 0.2;            % Finned length (m)
ReL1 = 1.1126x10^3      % Air's reynold number
Nu3 = 19.8761;          % Aluminium block nusselt number at 50 °c
σ = 5.67*10^-8;         % Stephen boltzmann constant(W/m2*k^4)
εskin = 1.00;           % Skin emissivity
εwall = 0.86;           % Plexiglass emissivity
OFF = 0;                % Switch off condition
Tci = 36;               % Core temperature initial value (°c)
Tsi = 36.5;             % Skin temperature initial value (°c)
Tai = 29;               % Air temperature initial value (°c)
Tmi = 29;               % Mattress temperature initial value (°c)
Twi = 25;               % Wall temperature initial value (°c)
TO2 = 25;               % Added oxygen temperature initial value (°c)
Tweti = 46;             % Wetted air temperature initial value (°c)
Twai = 34;              % Water temperature initial value (°c)
Tali = 35;              % Aluminium block temperature initial value (°c)
%% ======================================================================== %%
```

Appendix-II: MATLAB Codes to Check Stability of the System

```
% M-File Codes to Check System Stability for Skin Mode

% Transfer Function I
>> S=tf(linsys01)
>> controlSystemDesigner(S)

% Transfer Function II
>> SS=tf(linsys1)
>> controlSystemDesigner(SS)

% Transfer Function III
>> SR=tf(linsys2)
>> controlSystemDesigner(SR)

% Transfer Function IV
>> SSR=tf(linsys3)
>> controlSystemDesigner(SSR)

% M-File Codes to Check System Stability for Air Mode

% Transfer Function I
>> A0=tf(linsys7)
>> controlSystemDesigner(A0)

% Transfer Function II
>> A1=tf(linsys8)
>> controlSystemDesigner(A1)

% Transfer Function III
>> A2=tf(linsys9)
>> controlSystemDesigner(A2)

% Transfer Function IV
>> A3=tf(linsys10)
>> controlSystemDesigner(A3)
```

Appendix-III: MATLAB Codes to get Step Response Information

```
% Step response information for Skin Mode operation
% Without PID Controller
clc
t=ti_data(:,1);
y=Ts_data(:,1);
stepinfo(y,t,29)
t1=tii_data(:,1);
y1=RH_data(:,1);
stepinfo(y1,t1,79)

% Decoupling and SLC with PID Controller
clc
t=ti_data(:,1);
y=Ts_data(:,1);
stepinfo(y,t,37)
t1=tii_data(:,1);
y1=RH_data(:,1);
stepinfo(y1,t1,80)
```

```
% Step response information for Air Mode operation
% Without PID Controller
clc
t=ti_data(:,1);
y=Ta_data(:,1);
stepinfo(y,t,28)
t1=tii_data(:,1);
y1=RH_data(:,1);
stepinfo(y1,t1,78)

% Decoupling and SLC with PID Controller
clc
t=ti_data(:,1);
y=Ta_data(:,1);
stepinfo(y,t,37)
t1=tii_data(:,1);
y1=RH_data(:,1);
stepinfo(y1,t1,80)
```